



UNIVERSITY OF THE PHILIPPINES

Master of Science in Geomatics Engineering

Michael Andrew G. Manalili

Geosimulation of Riverine Type Mangrove in Palawan, Philippines
Using Cellular Automata

Thesis Adviser:

Ariel C. Blanco, Dr. Eng
Department of Geodetic Engineering
University of the Philippines Diliman

Thesis Co-Adviser

Engr. Edgardo G. Macatulad, MSc
Department of Geodetic Engineering
University of the Philippines Diliman

Date of Submission

June 2018

Thesis Classification

P

This thesis is not available to the public. Please ask the library for assistance.

"I hereby grant the University of the Philippines a non-exclusive, worldwide, royalty-free license to reproduce, publish and publicly distribute copies of this thesis or dissertation in whatever form subject to the provisions of applicable laws, the provisions of the UP IPR policy and any contractual obligations, as well as more specific permission marking on the Title Page."

"Specifically I grant the following rights to the University:

- a) *To upload a copy of the work in the theses database of the college/school/institute/department and in any other databases available on the public internet;*
- b) *To publish the work in the college/school/institute/department journal, both in print and electronic or digital format and online; and*
- c) *To give open access to above-mentioned work, thus allowing "fair use" of the work in accordance with the provisions of the Intellectual Property Code of the Philippines (Republic Act No. 8293), especially for teaching, scholarly and research purposes."*

Student Name over Signature and Date

This thesis, entitled **GEOSIMULATION OF RIVERINE TYPE MANGROVE IN PALAWAN PHILIPPINES USING CELLULAR AUTOMATA**, prepared and submitted by **MICHAEL ANDREW G. MANALILI**, in partial fulfilment of the requirements for the degree of **MASTER OF SCIENCE IN GEOMATICS ENGINEERING** is hereby accepted.

ARIEL C. BLANCO, DR. ENG.
Thesis Adviser

ENGR. EDGARDO G. MACATULAD, MSC
Thesis Co-Adviser

Accepted as partial fulfilment of the requirements for the degree **MASTER OF SCIENCE IN GEOMATICS ENGINEERING**.

RIZALINDA L. DE LEON, PH.D.
Dean

Dedication

To Cecil & Hope for being my inspiration and for the love,

to Mommy, Daddy, RJ, Debbie, Sam and Lola for the support, guidance, trust and hope,

*and to all the people who helped me directly and indirectly to finish this manuscript,
Thank you.*

Acknowledgement

I would like to thank first God for giving me strength, wisdom and perseverance to finish this manuscript.

My heartfelt thanks to my wife, Cecil for all her understanding, care and love and for pushing me to be the best that I can ever be. I could not have done all these without you. You are the only person who can understand all the hard work and sacrifices I have gone through during my MS journey. Thank you for always being there for me. I love you.

To my thesis adviser, boss, mentor and professor, Dr. Ariel Blanco, thank you so much for all the knowledge you have imparted to me. You taught me so much more than what books can offer. Thank you for the experience working for the UP TCAGP and for trusting me. Maraming salamat Sir!

To my thesis Co-Adviser Engr. Edgardo Macatulad, for always supporting me and for all the help you have shared with me from the start of my MS journey up to finishing this manuscript.

To my panel members Dr. Rene Rollon and Dr. Sev Salmo III, thank you so much for all the comments and suggestions for the improvement of this work. I learned a lot from you especially during my thesis defense.

To my friends and colleagues at UP, TCAGP, DGE especially to Engr. Alexis Claridores (my MS batch mate and friend) for being a good friend and for always making the class lively and exciting. To Alvin Baloloy for being a good friend and for trusting me. And to Mr. Russell Albaniel for assisting me in printing this thesis while I am away. Thanks to you all!

To all my classmates during my GmE journey, thanks for all the memories and for sharing with me the challenges of exams, machine problems, lab exercises including enrolment in UP!

To my family Cecil, Mommy, Daddy, RJ, Debbie, Sam and Lola, thank you for all your support and love and for always being my inspiration. This is all for you.

Abstract of Thesis

Mangroves of the Philippines has been in a hotspot due to rapid decrease in the extent as a result of combined environmental, anthropogenic and socio-economic stresses at the local, landscape, and regional levels. Although there had been numerous rehabilitation efforts by the government, still there was a failure in understanding and implementation of site-species suitability for mangrove rehabilitation and majority of mangrove rehabilitation in the Philippines has failed. Palawan province has long been known as the Philippines' biodiversity hotpot for mangroves. The dynamic interactions of man and environment from upland to coast has made it more difficult to implement single solution in addressing coastal issues. Many environmental models have been developed to understand processes that are unique in space and in time. However, information is lost in transition when studying high temporal phenomena and spatial details are generally aggregated. This study focused on identifying geomorphologic and bioclimatic variables that is highly correlated with mangrove area on a regional scale using 183 catchment areas for the mainland Palawan. A statistical random forest regression model revealed that geomorphologic variables (i.e., extent of tidally inundated floodplain, main river channel width, presence of neighbouring mangroves, and main river channel length) correlates to 67% of the variability in mangrove extent. The same model also revealed that longitudinal position of mangrove, precipitation during wettest month, and area of agriculture within the watershed correlates to 50.49% of the regional variability of mangrove decline based

on a 24-year mangrove observations. Geosimulation using Cellular Automata approach was implemented in this study to model spatially explicit interactions of different land uses within the watershed which captured spatial and temporal interactions of six land uses. Event-based Markov chain model was able to simulate temporally dynamic land use transitions as to how the mangroves are affected by land use allocations. Finally, local geosimulation model presented multiple future scenarios and use cases of mangrove mortality and growth which implements spatial and time-dependent parameters that mimics both natural and spatial patterns and processes. The modelled projection for the state of mangrove in Iwahig, Bataraza mangrove is threatened to be more fragmented if no immediate local and holistic interventions are implemented.

Table of Contents

Approval Page

Acknowledgement

Abstract of Thesis

Table of Contents

List of Figures

List of Tables

List of Appendices

1. Introduction

 1.1 Statement of the problem

 1.2 Objectives of the study

 1.3 Scope and limitations of the study

 1.4 Location of the study area

2. Review of Related Literature

 2.1 State of Philippine Mangroves

 2.2 Random forest statistics and variable selection for ecological modelling

 2.3 Geosimulation methods for ecological modelling

3. Methodology

 3.1 Watershed area delineation

 3.2 Clustering analysis for riverine type mangroves

3.3 Regression analysis

3.3.1 Exploratory Data Analysis

3.3.2 Test for Spatial Dependence

3.1.3 Random Forest Regression

3.1.4 Variable importance and variable selection using random forest

3.4 Cellular Automata Model

3.4.1 Cell State

3.4.2 Neighborhood Rules

3.4.3 Transition Rules

3.5 NetLogo programming language for Cellular Automata model

3.6 Mangrove Fragmentation

4. Results and Discussion

4.1 Variable importance and variable selection using Random Forest regression

4.2 Physical processes in a riverine type mangrove

4.3 Geosimulation modelling

4.3.1 Simulation model for Iwahig watershed

4.3.2 Simulation of mangrove mortality

4.3.3 Simulation of Mangrove Gap Closure

4.4 Model Sensitivity

5. Summary and Conclusions

6. Recommendations for future work

References

Appendices

List of Figures

- Figure 1.1 Location of the study area. Inset A refers to the regional scale analysis and Inset B for the local scale modelling
- Figure 2.1 Published mangrove area estimates for the Philippines. Adapted from Long, J.B & Giri, C. (2011). Licensed under Creative Commons.
- Figure 2.2 Mangrove types by hydrologic regime. Adapted from Woodroffe (1992)
- Figure 3.1 General workflow of the study. Right most box (in bold) will answer objective 1, middle box (in bold) will answer objective 2 and left most box (in bold) will answer objective 3.
- Figure 3.2 Delineated watershed areas with at least 1,000 hectares (n=183) for mainland Palawan using the IfSAR 5m Digital Elevation Model (DEM)
- Figure 3.3 Clustering and hot spot analysis of 3km X 3km (left) and 1km X 1km grid neighbourhood for the entire Palawan province.
- Figure 3.4. Correlation plot for 29 explanatory variables and predictor variable for mangrove area. Refer to Table 1 for the variable code and description.
- Figure 3.5 Principal component circle of correlation for component 1 (x-axis) and component 2 (y-axis) containing more than 60% of the variation.
- Figure 3.6 Spatial Regression Decision Tree (Geoda Workbook p. 199)
- Figure 3.7 Regression diagnostics and spatial dependence for watersheds
- Figure 3.8 Regression diagnostics (spatial dependence) for *mangrove_area* parameter
- Figure 3.9 Reference image in true color (RGB) Landsat 5 satellite image acquired in 1993 (left) and initial cell state assignment using the classified land use and land cover of Iwahig watershed (right)
- Figure 3.10 Land use and Land Cover types of Iwahig watershed during 1993 initial state (left) and final state in 2017 (right)
- Figure 3.11 Von Neumann (left) and Moore (right) neighbourhood rules.

Figure 3.12 Hypothetical Moore neighborhood transition rules from left to right: central cell at time 0 (left), initial state using moore neighbor, final state using moore neighbor, and final state using von Neumann neighbor.

Figure 3.13 The Markov chain transition probability model for the six (6) LULC classes. The circle corresponds to different land use and land cover and the number represents transition probabilities ranging from 0 – 1 where probability of 1.0 is called an absorbing state.

Figure 3.14 Land transition models adapted from Clarke, K. 1997. A represent state transition from one class to another. B is the transition of one class in space (spatial) and C is the transition of a class in the context of its immediate neighbors.

Figure 3.15 Temporal mangrove cover classification from 1985 – 2010

Figure 3.16 Sentinel-2 true color composite (left), PCA Composite (PC9-PC8-PC10 - center) and mangrove species grouping used in *NetLogo* simulation (right)

Figure 3.17 Euclidean distances of local mangrove transitions

Figure 3.18 Satellite derived mangrove fragmentation of Iwahig Mangrove observed between 1985 – 2010

Figure 4.1 Variable importance using random forest model (top 15).

Figure 4.2 Variable Selection Using Random Forest (VSURF) VI mean, VI SD, OOB error (nested) and OOB error (predicted) , the explained variation and cross validation results

Figure 4.3 Variable importance of mangrove area decrease using selected variables at regional scale

Figure 4.4A Correlation between mangrove area (x-axis) and river mouth width (y-axis)

Figure 4.4B Correlation between mangrove area (x-axis) and area of tidally inundated flood plain (y-axis)

Figure 4.5 Correlation plot of 29 exploratory variables and response variable. Blue box shows relative clustering of watershed variables, black box shows relative clustering of local geomorphologic variables and yellow-orange box shows relative clustering of bioclimatic variables.

Figure 4.6 Conceptual model of physical processes for a riverine type (R-type) mangrove setting

Figure 4.7 Graphical User Interface of the Iwahig watershed simulation model implemented in NetLogo. The left side tools are the *set-up* functions to read the data and assign cell colors and the *go* function to initialize the model. The *floodplain_dev* and *cultivated_t* are parameters the user can modify. On the right side are report interface for cultivated area and mangrove area. It is given by percentage within the watershed (top right) and total number of pixels (middle right). The bottom is the graphical change in land use based on the actual total number of pixels that has changed.

Figure 4.8 Reference images (A and B) corresponding to two different time periods (1993 and 2017). The resulting dynamic simulation model (C) and the graph (D) of land use and land cover exchange

Figure 4.9 Typical land use and land cover transitions and exchange for major regions of the world (Gibbs *et al.*, 2009).

Figure 4.10 Multiple Markov chain events and corresponding projected *mangrove* class re-allocation with respect to all other classes. Model number corresponds to different Markov chain events used to exaggerate re-allocation probabilities within the watershed. Model 0 is close to 2017 condition while Model 1 to Model 40 are from ideal to worst case scenarios. All percentage values are sum total of the area of the Iwahig watershed.

Figure 4.11 Simulated LULC by modifying *cultivated* class the probability (A1) and resulting class allocation on *built-up* class (A2) and modified *mangrove* class (B1) and resulting *mangrove* area trend (B2)

Figure 4.12 Temporal fragmentation trend of Iwahig mangrove forest from 1986 to 2015 using perimeter area ratio and core area index parameter

Figure 4.13 Actual (A) vs. simulated (B) mangrove fragmentation of different mangrove groups. Core distance influence used is 150 meters

Figure 4.14 High resolution Google Earth images showing existing patches (2018) of preparatory coastal development within fragmented mangrove areas at selected mangrove locations within the study area

Figure 4.15 Simulated mangrove mortality scenarios with varying accessibility and proximity distances to built-up area (A), road network (B), fragmented core area (C) and river network (D).

Figure 4.16 Different phases of mangrove forest light gap and recovery cycle. Adapted from Duke, N. (2009).

Figure 4.17 Hypothetical Field of Neighborhood (FON) model adapted from (Höfener, *et al.*, 2009).

Figure 4.18 Model of mangrove tree competition adapted from Höfener *et al.* (2009) showing ZOI in red where strong plant-to-plant competition exist. Thus, the more suitable site goes from red to blue.

Figure 4.19 Mangrove gap filling models with fixed tree diameter configurations where tree positions are placed randomly. Group A (tree diameter @ 1 pixel), Group B (tree diameter @ 3 pixels) and Group C (tree diameter @ 5 pixels) and three iteration models (Left: 1000 iterations, Center: 2000 iterations, and Right: 3000 iterations). This model typical for an even aged forest (more or less same diameter) or plantation type. However, gap closure is static since the diameter at initial condition does not change or grow at every iteration.

Figure 4.20 Hypothetical natural mangrove setting with mixed diameter setting. Each green dots (small, medium and large) in figure A are individual mangrove trees. Dots that are not completely circle are overlapping in terms of diameter FON. The FON and mangrove diameter changes dynamically at each iterations which mimics the actual mangrove growth cycle. Dynamic FON and tree diameter allows incremental growth and gap closure.

Figure 4.21 Simulated rehabilitated conditions for canopy gap closure using FON influence of 4,8 and 16 neighbors for image B,C and D respectively. Image A is the 2017 actual mangrove condition.

Figure 4.22 Quantity, Shift and Exchange metrics illustration by Pontius & Sta Cruz (2014). Original image from DOI: 10.1080/2150704X.2014.969814 page 7545

Figure 4.23 Quantity, exchange and shift contingency matrix (Pontius *et al.*, 2014) for 1993 LULC and simulated LULC after 24 iterations

Figure 4.24 Overall Quantity, Exchange, and shift pixels from actual and simulated land use and land cover classes

List of Tables

Table 3.1 Variables and parameters used in regression model for riverine type mangroves based on geomorphology, bioclimatic variables and land use/cover

Table 3.2 LULC code and patch color assignment for initial cell states for Iwahig watershed for the year 1993

Table 3.3 Neighborhood rules applied for Land use and land cover transition states

Table 3.4 LULC class transition probability matrix (1993 and 2017)

Table 3.5 Selected species list in Bataraza Palawan adapted and modified from PCSD 2015 and corresponding tidal position of species (Primavera *et al.* 2013)*

Table 4.1 Selected variable explaining the variations in mangrove area based on geomorphologic and bioclimatic variables using random forest

Table 4.2 Variable considers determining factors affecting mangrove change at regional scale

Table 4.3 Variable Selection for mangrove cover change using BioClim and potential decrease variables on a regional scale

Table 4.4 Random forest regression for three (3) watershed size clusters and resulting variance explained and corresponding variable importance.

Table 4.5 Markov chain models and resulting transition probability models for *mangrove* class allocation (in **bold**) versus all other classes within the Iwahig watershed

List of Appendices

Appendix 1 Random Forest Regression

Appendix 2 Land Use and Land Cove Change Comparison

Appendix 3 Species Distribution Modelling (SDM) and Fragmentation Analysis

Appendix 4 Markov Chain Model

Appendix 5A & 5B Iwahig Watershed Landscape Model

Appendix 6A – 6F Mangrove Mortality and Growth Models

Appendix 7A – 7C Mangrove Canopy Gap Growth Model

Appendix 8 Graphical User Interface (GUI) of NetLogo Landscape Simulation Model

Appendix 9 &10 Graphical User Interface (GUI) of NetLogo Mangrove Mortality Model

Appendix 11 Graphical User Interface of Mangrove Canopy Gap Growth Model

Appendix 12 R-codes for Random Forest Regression model

Appendix 13 R-codes for Markov Chain model

Appendix 14 R-codes for Mangrove Fragmentation

1. INTRODUCTION

The world recognizes the ecological, societal and economic importance of mangrove ecosystem. The United Nations Educational, Scientific and Cultural Organization (UNESCO 1990) labelled the island of Palawan as a *Man and Biosphere Reserve* because of high endemism and diversity of fauna and flora (PCSD 2015). Zooming in at a regional level, scientific studies on mangroves suggests that majority of the world's mangrove forests are spread over South and Southeast Asia which accounts to about 42% of the total mangrove area in the world (Spalding *et al.* 1997). In the Philippines, the Department of Environment and Natural Resources (DENR) ranked Palawan province of having the largest area of mangrove among 81 provinces. This was supported by the Palawan Council for Sustainable Development (PCSD) which also found Palawan province as having the most area of mangrove coverage in the country for the last decade (PCSD 2005).

Palawan has also been named as the country's "last ecological frontier" by the UNESCO. During the 2nd ASEAN Mangrove Congress, Samson & Rollon, (2012) enumerated various local and national policies which are significant to mangroves and wetlands in the Philippines. One of which is the Presidential Proclamation 2152 of 1981 which declares the entire island of Palawan and some parcels of mangrove area in the

country as Mangrove Swamp Forest Reserve
(<http://www.gov.ph/1981/12/29/proclamation-no-2152-s-1981>). The Republic Act 7611 or the Strategic Environmental Plan (SEP) for Palawan Act of 1992 under section 20 of the law states the creation of the Palawan Council for Sustainable Development which is the primary mandated agency to manage, protect and conserve the natural resources of Palawan in general.

1.1 Statement of the problem

Numerous studies have recognized the Philippine mangroves (including its neighboring countries) as one of the most diverse in Asia and the world. However, a declining trend of mangrove area extent and failures in mangrove rehabilitation were found by several studies to be caused by diverse anthropogenic disturbances, often ignored site-species suitability, increased issuance of fisheries license agreement (FLA), urbanization and combination thereof (Primavera, 2000; Garcia *et al.*, 2014; Hamilton & Casey, 2016; Walters 2005; Spalding *et al.*, 1997; Long *et al.*, 2013; Primavera & Esteban 2008; Polidoro *et al.*, 2010).

A recent survey by Gonzales *et al.* (2017) in the Municipality of Bataraza (south of Palawan) suggests that majority of the community see mangroves as building materials for construction of houses (22.2 %), fuel wood (38.4%) and for charcoal production (39.0 %) based on 600 respondents. The frequency of the mangrove tree resource utilization accounts for 10.9% on a weekly basis, 21% once a month and 14.8% twice a month.

The continuing deterioration and degradation of mangrove ecosystem in multiple reasons and scales in Palawan have been the motivation of the study. Studies suggest that policies and conservation measures in place does not always translate conservation measures to protect mangrove ecosystem because of the complexity of environmental, societal, human and behavioural interplay that influences human behaviour and its response and perception of mangrove as a resource. This study examined selected regional environmental, bioclimatic and watershed configurations as explanatory variables and how are they correlated to the mangrove area and extent Palawan. More specifically, a local model was also developed to see how the development of simple rules would mimic mangrove dynamics in space and time.

1.2 Objectives of the study

The general objective of the study is to find correlations between geomorphologic, bioclimatic and local variables on a riverine type mangrove ecosystem at three spatial scales (i.e., regional, watershed, and mangrove) and simulate scenarios of possible change dynamics. Specifically, the study aims to;

- 1) Identify correlations between mangrove area extent and the environmental, bioclimatic and catchment geomorphologic variables on riverine type mangrove;
- 1) Design a conceptual diagram of landscape processes in a riverine type mangrove ecosystem; and
- 2) Simulate multiple mangrove conditions at watershed and local scales to describe possible future mangrove trends using a combination of spatial and temporal approaches.

1.3 Scope and limitations of the study

This research will focus on the analysis of mangrove at three (3) different spatial scales at one (1) hydrologic zonation. Geomorphologic and bioclimatic factors were examined for the main island mass of Palawan province with watershed areas greater than or equal to 1,000 hectares (10 km^2) where the main channel drains to a mangrove.

Thus, the smallest spatial unit for regional analysis is at watershed level. Fringing and basin mangroves were not considered in the study for simplicity and because of the limited information on high resolution bathymetry, calibrated and localized wave and tide data / models for the entire Palawan.

Iwahig watershed in the Municipality of Bataraza was selected for landscape analysis because of the presence of large patch of riverine mangrove within the tidally inundated plain of the watershed draining to the coast. And because Bataraza is a mining, fishing, and agricultural municipality, time series land use and land cover analysis could reveal spatial and temporal patterns which could impact downstream coastal environment. This alterations of natural resources within the watershed and coastal environment is one of the interest of this research to identify possible correlations of mangrove area change to different watershed processes. No primary data were collected in field for this study due to limitations in funding by the researcher.

For the geosimulation exercise, the growth and mortality models were performed to the mangrove tidal groupings (landward, midstream, and seaward) because species level model is more complicated and there is no field data and calibration is made. The time component in the geosimulation does not translate to real world time, instead, time

abstraction in the model is based on one round of cell neighbourhood computation which is affected by the computing “time” of the researcher’s machine (computer).

1.4 Location of the study area

The research was performed at three (3) different spatial scales: regional, watershed, and mangrove scale. The regional geographical study extends at 117.209, 8.3931 (minimum latitude and longitude) and 119.707, 11.4045 (maximum latitude and longitude) respectively which is about 3 degrees in latitude and 2 degrees longitude (Inset A in Figure 1.1). This scale is sufficient to detect variations in bioclimatic variations in the region. The watershed geographical extent has 117.374, 8.56898 (minimum latitude and longitude) and 117.533, 8.73465 (maximum latitude and longitude) respectively covering five (5) barangays: Bulalacao, Tarus-an, Iwahig, Igang-igang, and Sarong in Municipality of Bataraza south of Palawan (Inset B in Figure 1.1).

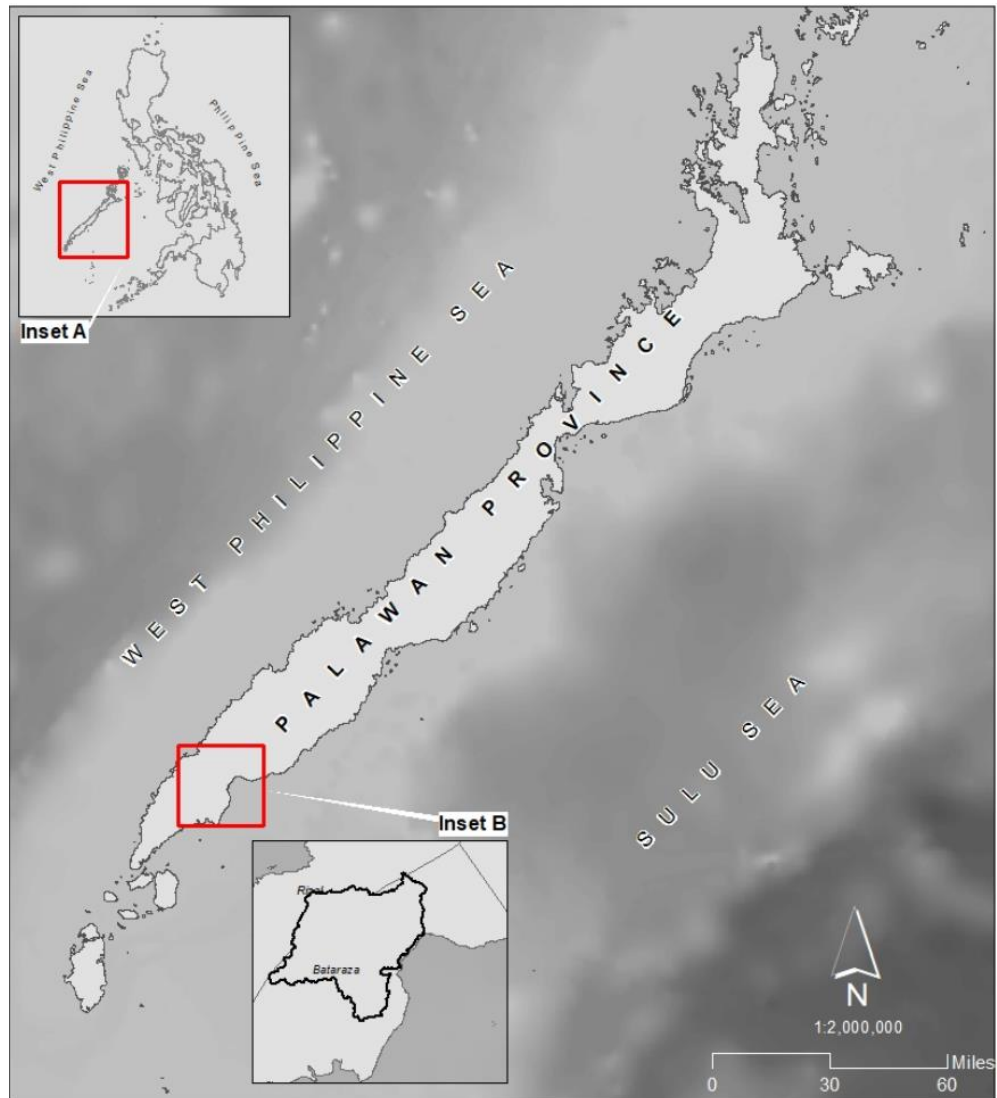


Figure 1.1 Location of the study area. Inset A refers to the regional scale analysis and Inset B for the local scale modelling

2. REVIEW OF RELATED LITERATURE

2.1 State of Philippine Mangroves

Mangrove area estimates for the Philippines have been well documented by previous studies as presented by Long, J.B & Giri, C. (2011) in Figure 2.1. Numbers do not tally mainly because the methods implemented during estimation is not standard and can be also due to the different scales at which the estimate was based. (Primavera & Esteban 2008). However, deviations of estimates from recent years (2000 – 2003) have less deviation due to improvements in technology and space based natural resources monitoring (e.g., Satellite Remote Sensing).

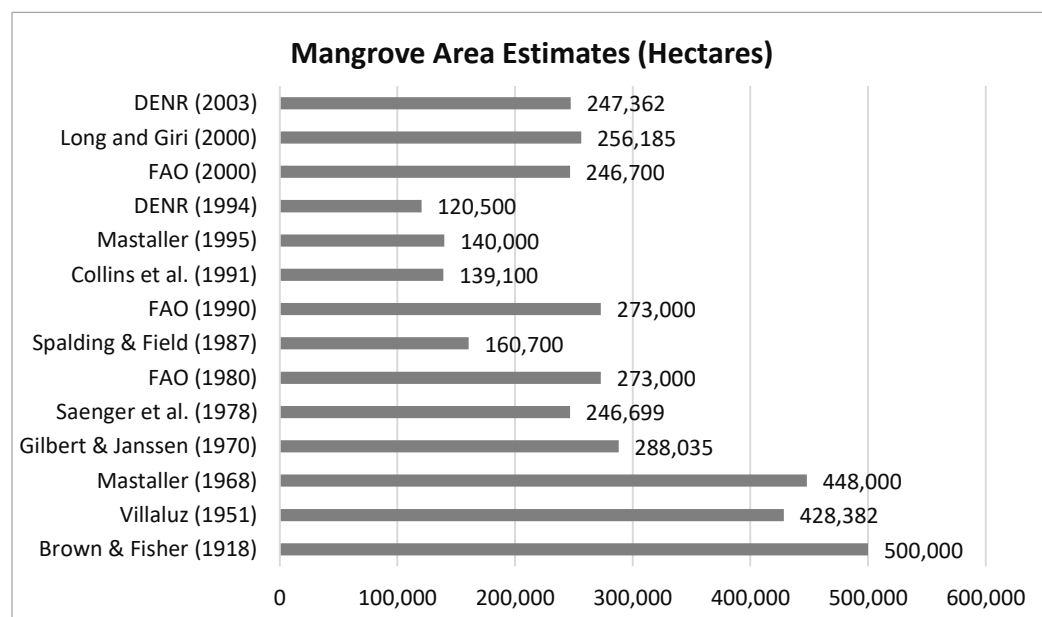


Figure 2.1 Published mangrove area estimates for the Philippines. Adapted from Long, J.B & Giri, C. (2011). Licensed under Creative Commons.

2.2 Mangrove types by hydrologic regime

Mangroves are assemblage of trees that grows and is uniquely adapted within the intertidal regions (Duke 1992, Hogarth 1999, FAO 2007, Saenger 2002). There were originally five (5) classification of mangroves as described by Snedaker *et al.* in 1995: Riverine type, Hammock, Overwash, Fringe and Basin (as cited by Mazda *et al.* 2007). These are further re-grouped into three (3) types based on geomorphology or landform: Riverine type, Fringe and Basin by Cintron *et al.* (1984) (Figure 2.2). The first two (Riverine type and Fringing) are the most common type of mangroves found in the Philippines (Primavera *et al.* 2013). Mazda (2007) described riverine mangrove (R-type) as a forest within a tidally inundated plain in proximity to a meandering river, drainage or creek that is inundated during high tides and is dry at low tides.

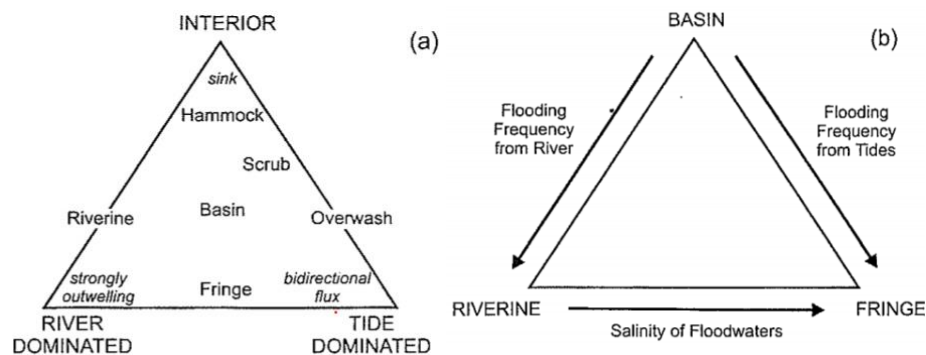


Figure 2.2 Mangrove types by hydrologic regime. Adapted from Woodroffe (1992)

This study focused on the study of a riverine type mangrove ecosystem. According to Pool *et al.* (1977), riverine type mangroves are the most productive type from all types of mangrove. The functional role of river in a riverine type mangrove is very important as found by Siemerink (2011). His study revealed the importance of supply of sediment from upstream in order to sustain riverine type mangrove ecosystem.

2.3 Random forest statistics and variable selection for ecological modelling

Various statistical techniques can be considered in finding correlations of response variables to a set of multiple predictor variables. However, these always come with assumptions like normality of the distribution of data, homogeneity, and independence of the observed variables to name a few (Breiman, 2001). High dimensionality of data and violation of independence are common in spatial science because of spatial autocorrelation. Thus, traditional linear models are often not applicable in ecological research (Cutler *et al.*, 2007 as cited in De'ath & Fabricus, 2000).

Liaw & Weiner 2002 described random forest as a type ensemble learning which generates several classifiers that aggregates the result by boosting (Shapire *et al.*, 1998) and bagging (1996). Random forest technique is attractive in ecological research because

it can be used both for regression and classification (Liaw *et al.*, 2002); can deal with high dimensionality of the data (Nguyen *et al.*, 2015); can handle multicollinearity which is common in spatial data (Santibanez *et al.*, 2015); has a novelty method of variable importance for selecting the most important predictor and relatively high classification accuracy (Breiman, 2001). There are two methods in random forest: Regression and Classification. *Regression* is predicting the values of the response from a set of predictors and *Classification* is separation of multi-dimensional data into two or more known classes in a feature space based on similarity or common characteristics to determine new observations to the class employing multiple numerical and categorical x variables (Breiman 1994 & Breiman 2001, Cutler *et al.* 2007).

A study by Evans *et al.* (2011) used random forest in modelling the possible potential future distributions (Prasad *et al.* 2006; Rehfeldt *et al.* 2006) of specific plant species: *A. lasiocarpa* (Subalpine fir) and *Pseudotsuga menziesii* (Douglas fir) in the US. The study used variable importance and concluded that elevation, mean annual temperature and mean annual precipitation are among the most important variables or strongest predictors to explain variations in species distribution. Another research done by Hollings *et al.* (2017) presented a work on species distribution modelling for disease epidemics using twenty-two (22) predictor variables. The study tested different machine learning algorithms including random forest. Result show that random forest outperforms other algorithms despite the ‘noisy’ data. Finally, a research by Record *et al.* (2013) used

random forest to project global mangrove species and community distributions under climate change. Twenty-one (21) climatic, hydrological and geomorphological variables were considered. The researchers concluded that various climatic variables are attributed to the variations in the distribution of different mangrove species as suggested by the variable importance ranking in random forest. The details of the random forest algorithm and variable selection were discussed in more detail on the methodology section.

2.3 Geosimulation methods for ecological modelling

Geosimulation, by definition, is an adequate representation of geospatial entities. It should capture attributes of objects which associate its interactions and behaviour. Model should be done to capture both spatial and temporal scales where simulations should observe patterns which are close to reality (Marceau & Benenson, 2011). It has been widely used extensively by previous studies to model urban expansion (Kamusoko & Gamba 2015, Akin & Berberoğlu 2015, Alkherer *et al.* 2006, Arsanjani *et al.* 2013, Barredo *et al.* 2003, Chen *et al.* 2002, Clarke & Gaydos 1998, Couclelis 1997, Deep 2014, He *et al.* 2008, Liu & Phinn 2003, Mubea *et al.* 2014, and Yeh & Li 2002), and in forest studies (Adhikari 2012, Bone & Roberts 2006, and Karafyllidis 1997). Previous works (Al-sharif & Pradhan 2014, Arsanjani *et al.* 2011, De Almeida *et al.* 2003, Gong *et al.* 2015, Guan *et al.* 2011, Halmy *et al.* 2015, Huang *et al.*, 2015, Memarian *et al.*

2012, Nadoushan *et al.* 2015, Pan *et al.* 2010, and Yang *et al.* 2014) have already implemented geosimulation to model land use and land cover using cellular automata and markov chain models.

In the Philippines, there are very few studies on the use of simulation models implemented for on mangrove. One of which is done by Salmo & Juanico (2015) where individual based model for *Rhizophora (Rhizophora mucronata)* plantation was simulated to model long term forest growth under varying physiological variables. Agent based model of post disaster regrowth of mangrove forest were studied by Ang *et al.* (2016) which adapted Salmo & Juanico's work on individual based mangrove plantation growth simulation. Claridores *et al.* (2017) have use 3D simulation and modelling of mangrove visualization using various platforms. This research is the first attempt to use cellular automata approach for geosimulation in a riverine type mangrove in Palawan province and in the Philippines.

3. METHODOLOGY

The research involves three major workflows which include: (1) regression analysis of geomorphological and bioclimatic factors affecting mangrove, (2) conceptualization of relationships of riverine type mangrove dynamics and (3) use of cellular automata to model spatially explicit interactions of different land uses at watershed scale and mangrove zonation level. These major workflows are highlighted in Figure 3.1, where each bold solid boxes will answer the three main objectives of the study.

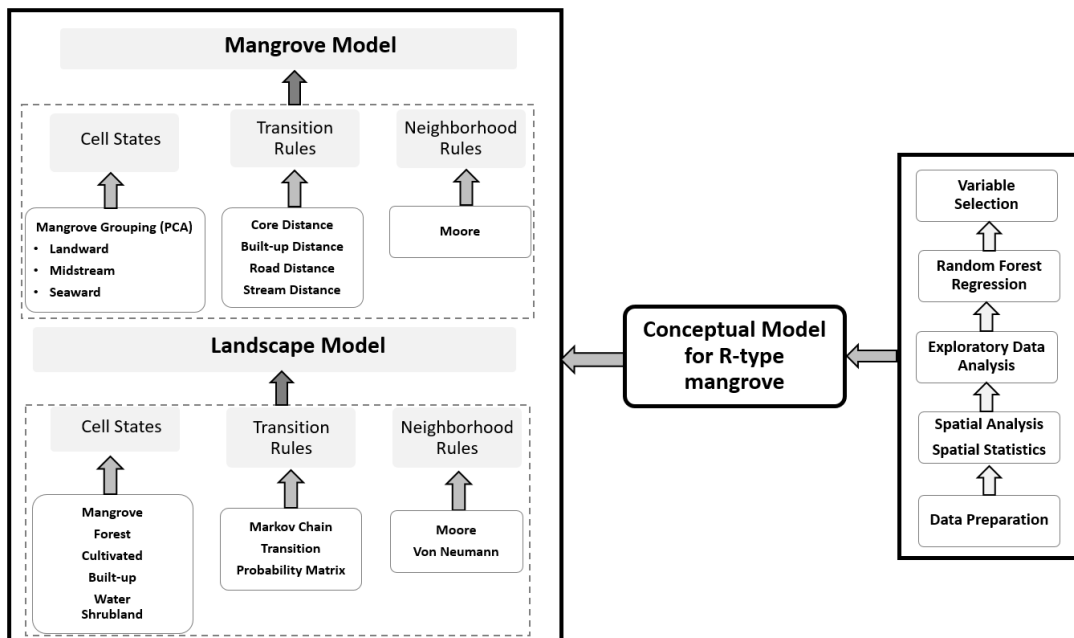


Figure 3.1 General workflow of the study. Right most box (in bold) will answer objective 1, middle box (in bold) will answer objective 2 and left most box (in bold) will answer objective 3.

3.1 Watershed area delineation

The watersheds were delineated using a 5 x 5 meter resolution Digital Elevation Model (DEM) single pass X-band Interferometric Synthetic Aperture Radar (IfSAR) acquired by STAR-3i mission operated by Intermap Technologies in 2014. The data was requested from the National Mapping and Resource Information Authority (NAMRIA) through the Philippine Hydrologic Dataset project of the Training Centre for Applied Geodesy and Photogrammetry (TCAGP). Watershed boundaries were delineated using the modified *Watershed Delineation Tool* in ArcMap where the minimum area is 1,000 hectares (Figure 3.2). The primary information that were extracted are: Watershed boundaries, stream network and stream drainage points with a total of 183.



Figure 3.2 Delineated watershed areas with at least 1,000 hectares (n=183) for mainland Palawan using the IfSAR 5m Digital Elevation Model (DEM)

3.2 Clustering analysis for riverine type mangroves

Clustering was done to identify hot spot areas of riverine type mangroves for the mainland Palawan. Figure 3.3 shows two different clustering information using a 3km by 3km (Figure 3.3-left) and 1km by 1km (Figure 3.3-right) gridded vector neighborhood search. The analysis performed was based on the Getis-Ord Gi* statistics of every feature in the dataset. The statistic (Gi*) uses the Z score which tells us where values of high and low cluster spatially. Hot spot means a high z-value should be surrounded by other

high values in its neighbourhood where the neighbourhood can be assigned arbitrarily as a parameter. Same goes for the coldspot where the low z-values as the basis.

Cluster analysis show that majority of the mangroves with watershed areas having at least 1,000 kilometer in size cluster within the main island of Palawan with 95% - 99% statistical confidence value based on the Getis Ord Gi* z value. This means that for each 1 kilometer and 3 kilometer grid neighbourhood, riverine type mangroves with catchment area of at least 1000 hectares cluster together. Thus, there is 90-95% confidence that the mainland Palawan has riverine type mangrove.

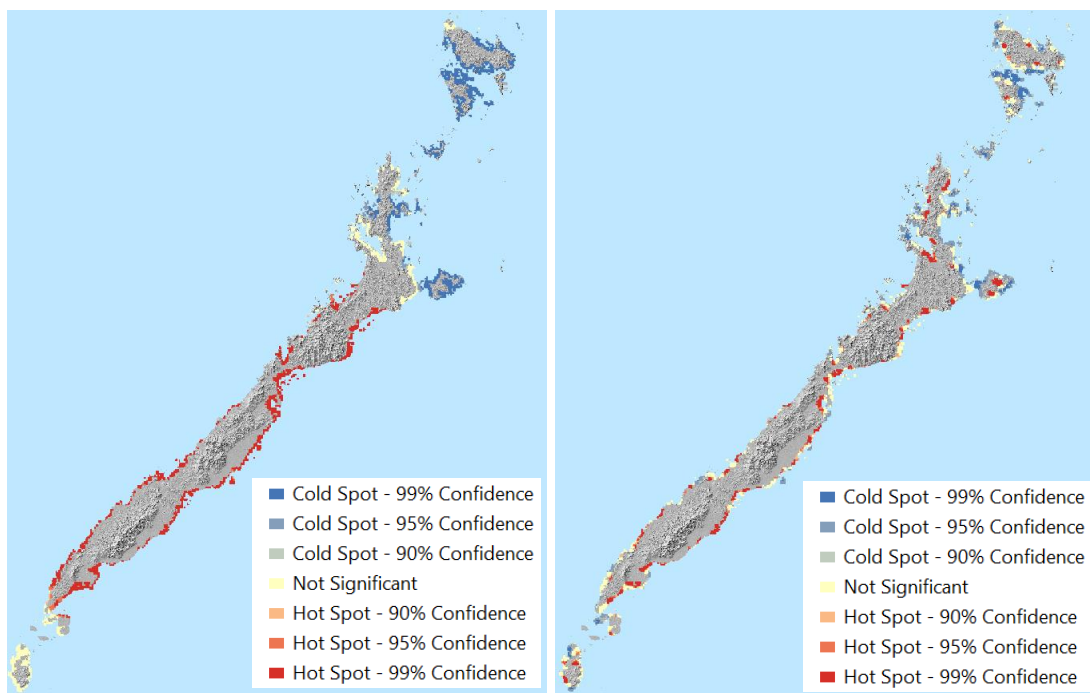


Figure 3.3 Clustering and hot spot analysis of 3km X 3km (left) and 1km X 1km grid neighbourhood for the entire Palawan province.

3.3 Regression analysis

This section will discuss the random forest regression model used for the assessment of 183 watersheds of a riverine type mangrove using all predictor variables listed in 3.1. The *R* programming language - a free and open source statistical modelling software with support for multiple geospatial analysis and functions was used in this research. Details of the script including the libraries are illustrated in Appendix 1 of the report.

A total of 30 predictor variables (Table 3.1) were used to model the best combination which will yield the highest correlation with response variable mangrove area (*mg_Area*). Mangrove extent were extracted from Landsat data for the whole Palawan provided by the Philippine Corals and Mangrove Remote Sensing (PhilCoMaRS) and Corals Vulnerability Assessment CorVA (CorVA) projects of the Training Center for Applied Geodesy and Photogrammetry (TCAGP) & the Marine Science Institute (MSI) of the University of the Philippines Diliman. Pixel based classification of mangroves were done for multi-temporal composite of Landsat 4, 5, 7, and 8 data from the United States Geological Survey (USGS) using a Support Vector Machine (SVM) algorithm. The reported accuracy of the classification is 72% for the entire Palawan Island with Kappa coefficient of 0.76.

Table 3.1 Variables and parameters used in regression model for riverine type mangroves based on geomorphology, bioclimatic variables and land use/cover

| Variable Name | Code | Description |
|-----------------------|-----------------|--|
| Mangrove Area | <i>Mg_Area</i> | The area of the mangrove within the watershed measured in hectares. <i>This is also the Y-variable</i> |
| Watershed Area | <i>CA</i> | Area of the Watershed with at least 1,000 hectares |
| Frequency of Stream | <i>FS</i> | The number of streams (permanent and intermittent) within the watershed |
| Length of Stream | <i>Ls</i> | The total length of stream within the watershed in kilometres |
| Mean Slope | <i>MSl</i> | Mean slope within the watershed expressed in % |
| Area of Flood Plain | <i>AFP</i> | The area of the flood plain within the watershed in hectares |
| River Sinuosity | <i>RS</i> | The measure of meander of the main channel within the watershed |
| Mean Elevation | <i>Mel</i> | The mean elevation of the watershed measured in meters |
| Percent Tree Cover | <i>pTC</i> | The percentage of tree cover within the watershed |
| Fishpond | <i>FP</i> | Presence or absence of fishpond within the watershed. Boolean Yes or No |
| Area of Forest | <i>aFor</i> | Extent of forest cover (open and closed) within the watershed in hectares |
| Area of Agriculture | <i>aAg</i> | Extent of cultivated area within the watershed (in hectares) |
| Area of Built-up | <i>aBU</i> | Extent of built-up area within the watershed (in hectares) |
| Elongation Ratio | <i>ERatio</i> | Ratio of the diameter of a circle having same area as the watershed to the maximum watershed length |
| Coastal Exposure | <i>expC</i> | Land to water ratio at 2.5 kilometer radius from the river mouth |
| River mouth Width | <i>rmW</i> | The width of river mouth (in meters) at the watershed outlet |
| Main Channel depth | <i>cdep</i> | Depth of the main channel in meters |
| Main Channel Length | <i>mainCL</i> | Length of the main channel from mouth to the first branch |
| Main Channel Slope | <i>mainCS</i> | The slope of the main channel in (%) |
| Coast Length | <i>CoastLen</i> | The length of the coast based on a 2.5 km radius of the river mouth |
| Longitude | <i>long</i> | Longitude of the center point of the largest mangrove patch |
| Latitude | <i>lat</i> | Latitude of the center point of the largest mangrove patch |
| Mangrove neighborhood | <i>Mg_NBHd</i> | The number of mangrove neighbourhood patch counted clock wise |

| | | |
|---------------------|---------------|---|
| Average tree height | <i>TH_ave</i> | The average mangrove tree height within the watershed derived from the nDSM |
| SD of tree height | <i>TH_std</i> | The standard deviation of mangrove tree height within the watershed derived from nDSM |
| Bioclim 3 | <i>bio3</i> | Isothermality (Bio2/Bio7) (*100) |
| Bioclim 5 | <i>bio5</i> | Max Temperature of Warmest Month |
| Bioclim 13 | <i>bio13</i> | Precipitation of Wettest Month |
| Temperature 4 | <i>tmax4</i> | Maximum Temperature during April |
| Temperature 5 | <i>tmax5</i> | Maximum Temperature during May |

Bioclimatic parameters were utilized for the regional study aggregated at each watershed unit. The *WorldClim* data is a gridded 1 km x 1 km climate statistics raster for the entire globe based from 9,000 to 60,000 weather stations. These include information on average monthly temperature and precipitation data, solar radiation, vapor pressure and wind speed between over a 30-year period (1895 – 2009). Information on satellite data (evapotranspiration, Land Surface Temperature (LST) from MODIS Terra and Aqua satellites), elevation, and distance to coast including cloud cover were included in the model (Fick S, & Hijmans R., 2017). These data were downloaded from *WorldClim* website (www.worldclim.org) using the latest available version 2.0.

3.3.1 Exploratory Data Analysis

It is necessary to perform exploratory data analysis prior to analysis to ensure that researchers do not violate the underlying assumptions when selecting proper statistical methods and tools especially for ecological research. Correlation of all predictor (including the response) variables were plotted and is illustrated in Figure 3.4. Blue colour represents positive correlation and red if otherwise. The size of the circle represents the degree of correlation ranging from -1 to 1 and variables that are highly correlated with mangrove area (*Mg_Area*) is highlighted in the black box in Figure 3.4. This correlation plot was implemented in *R* programming language using the *corrplot* library.

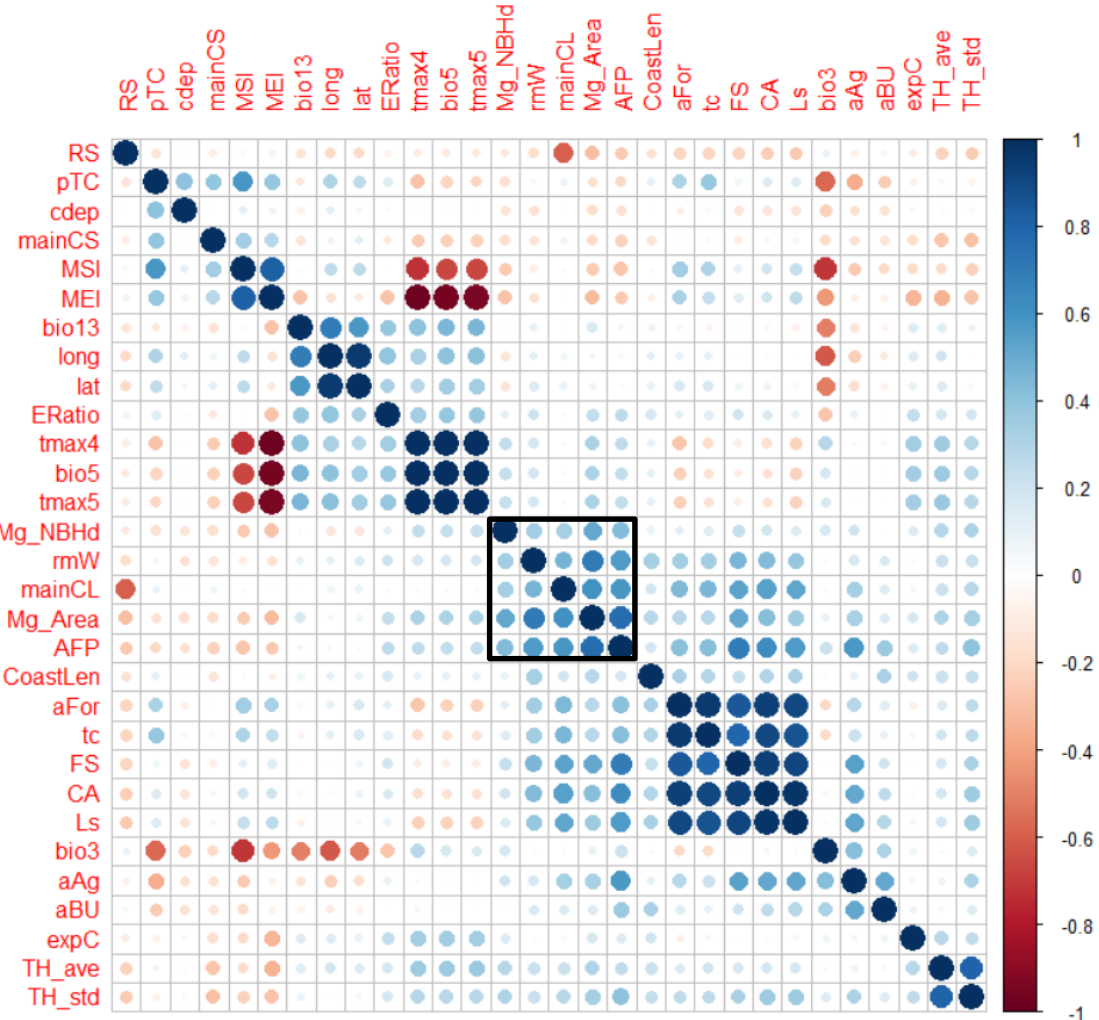


Figure 3.4. Correlation plot for 29 explanatory variables and predictor variable for mangrove area. Refer to Table 3.1 for the variable code and description.

The Principal Component - Partial Least Squares regression in R provides a good tool to visualize highly correlated variables as seen in Figure 3.5. It can be observed that there are clustering of variables close to mangrove area variable (*Mg_Area*) along with other correlated variables. These variables were based on the principal components 1 & 2

where majority of the variation (more than 50%) in mangrove area is observed. The illustration was generated using the partial least squares (*pls*) package in *R*.

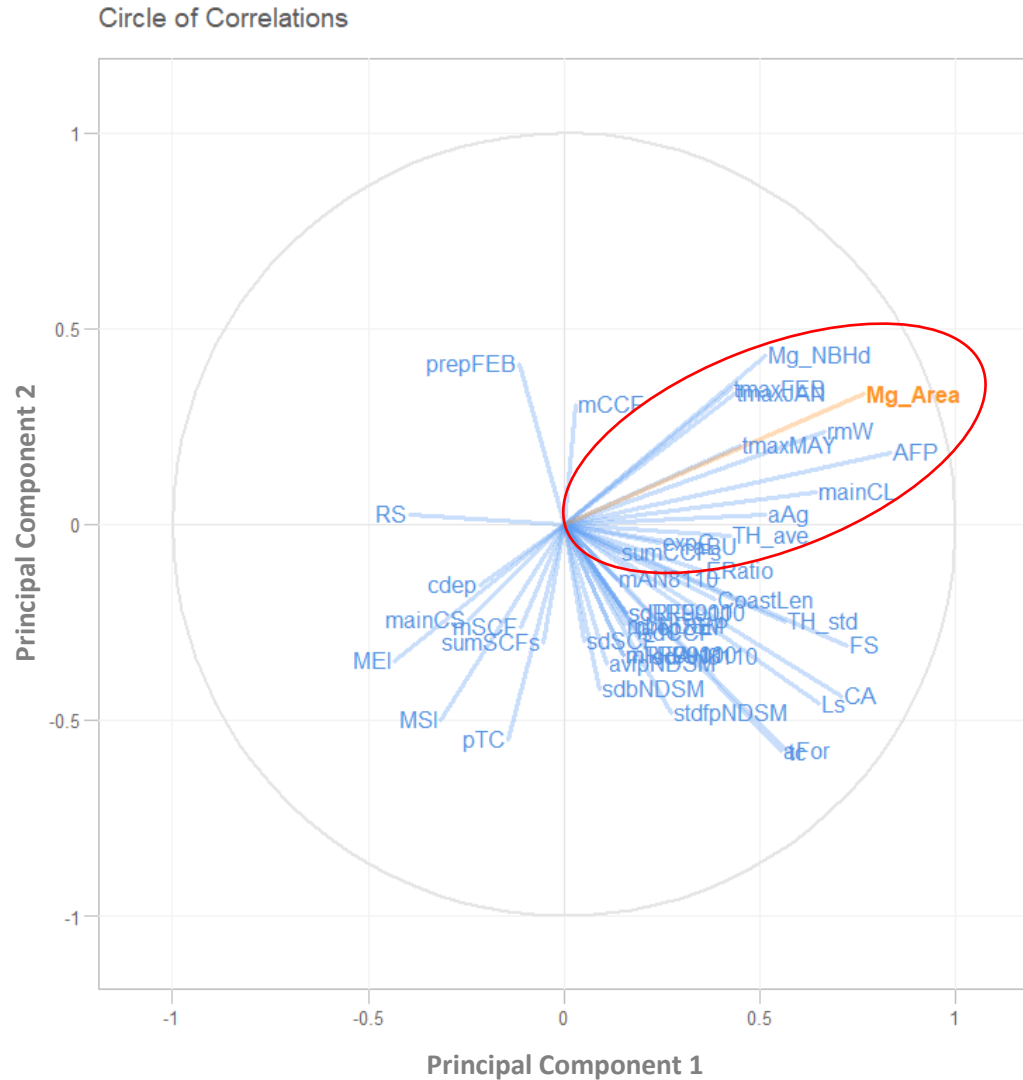


Figure 3.5 Principal component circle of correlation for component 1 (x-axis) and component 2 (y-axis) containing more than 60% of the variation.

3.3.2 Test for Spatial Dependence

The study performed a test for spatial dependence to check if there's any violation of spatial autocorrelation of the error term or if spatial lag effect is present. Several statistical diagnostics were used following the diagram in Figure 3.6.

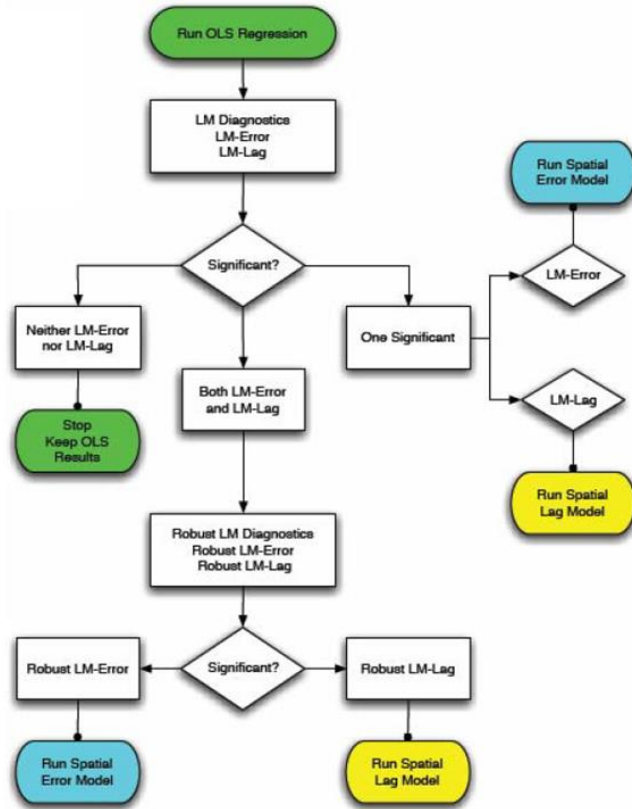


Figure 3.6 Spatial Regression Decision Tree (Geoda Workbook p. 199)

Results showed (as illustrated in Figure 3.7) that the Lagrange Multiplier (LM) for lag and error are not significant (very high probability of rejection) for watershed area. Therefore, there is no statistical evidence to prove that there is spatial dependence on watershed areas draining to each mangrove. This maybe because watersheds are independent or “self-contained” spatial unit and thus cross-boundary spatial effects are negligible or is controlled by the physical boundary (e.g., ridge, elevation and slope). Thus, individual watersheds have very little to no effect with respect to its neighbouring watersheds. However, since the water that drains into each watershed eventually meet at the mixing zone in the ocean or bay, another hypothesis is that mangrove area (as a parameter) might have spatial dependence. To rule this out, same test was applied to mangrove areas.

| REGRESSION DIAGNOSTICS | | | |
|---|--------|----------|---------|
| MULTICOLLINEARITY CONDITION NUMBER | | | |
| TEST ON NORMALITY OF ERRORS | | | |
| TEST | DF | VALUE | PROB |
| Jarque-Bera | 2 | 121.7526 | 0.00000 |
| DIAGNOSTICS FOR HETROSKEDEASTICITY | | | |
| RANDOM COEFFICIENTS | | | |
| TEST | DF | VALUE | PROB |
| Breusch-Pagan test | 12 | 217.0798 | 0.00000 |
| Koenker-Bassett test | 12 | 74.1645 | 0.00000 |
| DIAGNOSTICS FOR SPATIAL DEPENDENCE | | | |
| FOR WEIGHT MATRIX : Rtype (row-standardized weights) | | | |
| TEST | MI/DF | VALUE | PROB |
| Moran's I (error) | 0.0319 | 0.7248 | 0.46857 |
| Lagrange Multiplier (lag) | 1 | 0.1802 | 0.67124 |
| Robust LM (lag) | 1 | 0.0448 | 0.83229 |
| Lagrange Multiplier (error) | 1 | 0.1895 | 0.66334 |
| Robust LM (error) | 1 | 0.0542 | 0.81593 |
| Lagrange Multiplier (SARMA) | 2 | 0.2343 | 0.88943 |
| ===== END OF REPORT ===== | | | |

Figure 3.7 Regression diagnostics and spatial dependence for watersheds

```

REGRESSION DIAGNOSTICS
MULTICOLLINEARITY CONDITION NUMBER   6343864.546053
TEST ON NORMALITY OF ERRORS
TEST          DF      VALUE      PROB
Jarque-Bera    2     116.7205    0.00000

DIAGNOSTICS FOR HETROSKEDEASTICITY
RANDOM COEFFICIENTS
TEST          DF      VALUE      PROB
Breusch-Pagan test  26     629.6950    0.00000
Koenker-Bassett test  26     365.9735    0.00000

DIAGNOSTICS FOR SPATIAL DEPENDENCE
FOR WEIGHT MATRIX : MG_sample_reg_5
  (row-standardized weights)
TEST          MI/DF      VALUE      PROB
Moran's I (error)  0.4225    21.9755    0.00000
Lagrange Multiplier (lag)  1     80.2394    0.00000
Robust LM (lag)    1     2.0886    0.14840
Lagrange Multiplier (error)  1     455.0800    0.00000
Robust LM (error)   1     376.9292    0.00000
Lagrange Multiplier (SARMA)  2     457.1686    0.00000
===== END OF REPORT =====

```

Figure 3.8 Regression diagnostics (spatial dependence) for *mangrove_area* parameter

Figures 3.7 & 3.8 showed that both LM lag and LM error are significant for mangrove area and therefore there is spatial dependence between mangrove and its neighbors. Since LM error is more significant than LM lag, statistics show that error term in mangrove areas have spatial dependence. This observation needs further investigation which is beyond the scope of this research. Even though the cause of spatial dependence of error term is not known and cannot be attributed to any variable in this thesis, mangrove area as a variable will be treated with caution by not using the mangrove area as a spatial unit but instead, all data will be aggregated to watershed areas which will serve as the spatial unit for the regression modelling.

3.3.3 Random Forest regression model

Ho (1995) defined random forest as an “ensemble classifier” consisting of many decision trees (inside a forest) which outputs the mode of the class by individual trees. Breiman (2001) later added the boosting and aggregation method in the random selection of feature. There are three major procedures in the random forest regression model. Evans *et al.* (2011) simplified the steps as (1) construction of bootstrap sample of 36% of the total data, (2) grows the tree (unpruned) to become a forest where trees to be grown are selected randomly, choose the best split among all predictors, choose a random sample of predictors to find best split among all the variables and (3) predict the “new” data by getting the average of the aggregates. The formula of random forest is described in equations 1 and 2.

Output ensemble of random-forest trees

$$\{T_b\}_1^B \quad \text{Equation (1)}$$

Regression

$$\hat{f}_{rf}^B(x) = \frac{1}{B} \sum_{b=1}^B T_b(x) \quad \text{Equation (2)}$$

OOB error rate (Mean Squared Error)

$$\text{MSE}_{\text{OOB}} = n^{-1} \sum_1^n \{y_i - \hat{y}_i^{\text{OOB}}\}^2$$
Equation (3)

Where: **Tb** is the random forest tree

B is bootstraps sample

Tb is the random tree

Z is the population to draw bootstrap sample from

M is the independent variable where m is the variable at each node

With each training in random forest, one third (1/3) of the entire data is left out (which is why it's called out-of-bag or OOB). The prediction is iteratively done at each samples of the trees for the entire forest that is left out. The measure of the accuracy is done by averaging OOB error predictions (mean squared error at each split) and is often called the OOB rate or the pseudo R² (Adkins, 2014). The formula for the OOB rate estimation is described in equation 3.

3.3.2 Variable importance and variable selection using random forest

One unique characteristics of random forest is that the model can output variable importance rankings. Developed by Breiman (2001 & 2002) cited by Louppe, G. *et al.* (2013), it is computed by evaluation of “the importance of a variable X_m for predicting Y by adding up the weighted impurity decreases $p(t)\Delta i(s_t, t)$ for all

nodes t where X_m is used, averaged over all N_T trees in the forest.” (p2). This is presented in equation 4 below.

$$Imp(X_m) = \frac{1}{N_T} \sum_T \sum_{t \in T: v(s_t) = X_m} p(t) \Delta i(s_t, t)$$
Equation (4)

Variable importance is unique in random forest (for both regression and classification) because it gives information on the relative explanatory power of each variables to the response. However, variable importance is not yet a strong basis for variable selection because it only ranks all variables from the most importance to the least and not actually selecting the most important variable. In order to do variable selection, Variable Selection Using Random Forest (VSURF) was implemented by cross validation and permutation.

3.4 Cellular Automata Model

Spatial simulation or geosimulation general has two (2) types – Cellular Automata (CA) and Agent Based Modelling (ABM). Cellular Automata is a type of geosimulation which uses finite number of cells (or grid) that change its state based on transition rules and its neighbouring cells in a simultaneous fashion. This process is iterative until a cell reaches the modelled cell state or condition (Kari, 2005). Cellular Automata (CA) was conceptualized by Stanislaw Ulam during the 1940s but it was John Von Neumann’s work that operationalized the concept in the 1950s by continuously studying a “self-replicating” system (Clarke, 2014). Cellular Automata as defined by Miller (2009) as a “discrete spatio-temporal dynamics system based on local rules” pg 1220. When simulating land use and land cover in which the smallest mapping unit is a regularly spaced grid of cells with fixed dimension, cellular automata models is commonly used (Clarke, 2014 & Miller, 2009). Cellular automata has been used widely by previous studies especially in urban dynamics simulation (Hegde *et al.*, 2017, Kamusoko & Gamba 2015) forest studies (Bendicenti *et al.*, 2002), and land use and land cover analysis (Yang *et al.*, 2012).

$$S_{xy}^{T_{i+1}} = f(S_{xy}^{Ti}, N_{xy}^{Ti}) \quad (\text{Equation 5})$$

Equation 5 presented the general equation for cellular automata where S_{xy}^{Ti} and S_{xy}^{Ti+1} are cell states at position x,y at any given Ti and $Ti + 1$, N_{xy}^{Ti} represents the surrounding neighbours at each cell in time Ti at location (x,y) which represent the transition rule function of the cell after time $Ti + 1$. In simple terms, Cellular automata generally has three (3) main elements: (i) the cell state, (ii) neighbourhood rules, and (iii) transition rules (Clarke 2014, Miller 2009, Kari 2005) and is simplified in equation 6.

$$\text{Cell state}_{t=0} = f(\text{neighborhood})_{t=1} \quad (\text{Equation 6})$$

Where: $t = \text{transition period}$

3.4.1 Cell State

The assigned *cell state* model used a classified land use and land cover (LULC) Landsat data using pixel based method. Analysis ready data (atmospherically corrected Level 2 product) were used. The correction parameter uses the Landsat Ecosystem Disturbance Adaptive Processing System (LEDAPS) surface reflectance Level-2 product ordered from USGS website earth explorer website (www.earthexplorer.com) for scene number 117/054. This satellite image tile covers the enntire south of Palawan and data were acquired for 1993 (Landsat 5) and 2017 (Landsat 8). Supervised

classification was done using a Support Vector Machine (SVM) algorithm. There were six (6) main land use and land cover types classified as illustrated in Figure 3.9 (right) with an accuracy of 82 % and kappa coefficient of 0.80. The classified image for 1993 is assigned as the *initial cell state*.

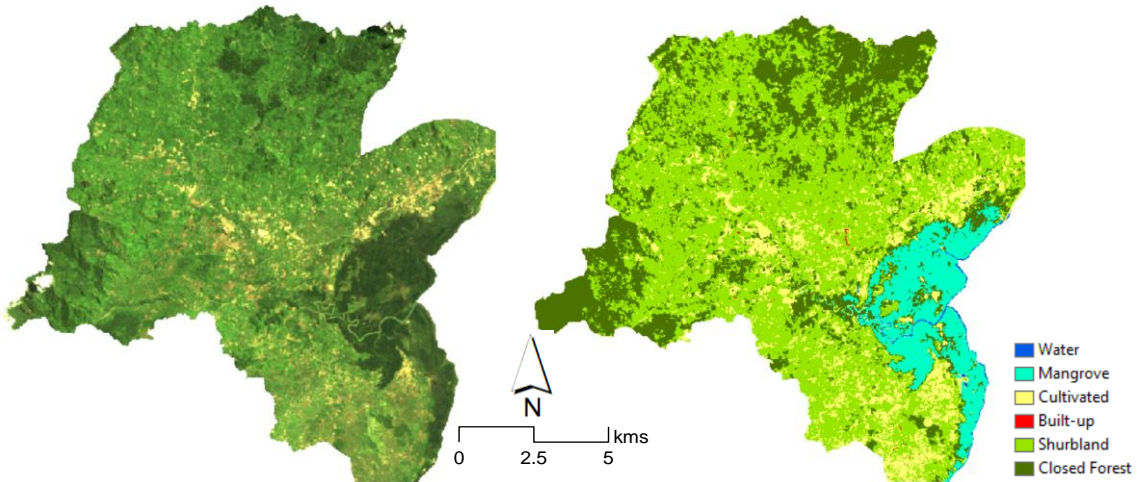


Figure 3.9 Reference image in true color (RGB) Landsat 5 satellite image acquired in 1993 (left) and initial cell state assignment using the classified land use and land cover of Iwahig watershed (right)

Land use and land cover classes (LULC) were derived using pixel-based satellite image classification. Six (6) major land use and land cover classes were identified which was then assigned class codes and class colors as listed in Table 3.2. The patch codes and colors were used as reference in the programming and coding exercise in the simulation. The details of the code is described in Appendix 5A. A function *load_i* in

Appendix 8 calls the initialization and set-up of the simulation environment for the Iwahig watershed landscape model.

Table 3.2 LULC code and patch color assignment for initial cell states for Iwahig watershed for the year 1993

| Land Use Land Cover | Code | Patch Color | Cell Size (meters) |
|--------------------------------|-------------|---|-------------------------------|
| Water | W |  | |
| Mangrove | M |  | |
| Cultivated | C |  | |
| Built-up | BU |  | 30 |
| Shrubland | S |  | |
| Forest | F |  | |

The geosimulation was designed and implemented using *NetLogo* software developed by Uri Wilensky in 2005. Time parameter which controls the temporal transition of cell automaton model is controlled by the *ticks* command in NetLogo. This *ticks* function does not translate to real world time but instead, a single *tick* means one cycle of cell transition in the entire modelling environment. The time it takes for a sing *tick* to complete depends on a number of variables (e.g. size and resolution of data, number of neighborhood influence set by the modeller, computing capacity of the machine use, and algorithms applied on how the cell should transition). There variables were set in Netlogo programming language manually and are described in the Appendix section.

Initial modeling environments were set up prior to the actual simulation. The initial *cell states* (Figure 3.10 - left) were assigned based on the classified Landsat image acquired in 1993. *Cell states* of each land classes were hard coded using the *gis* extension in NetLogo together with the numerical class transition probabilities that were assigned to each classes. Neighborhood rules were assigned on each class which computes neighborhood influence with respect to its six (von Neumann) and eight (Moore) neighbors before the central cell transitions into a new state. The process is done iteratively with respect to the model ‘time’ or period.

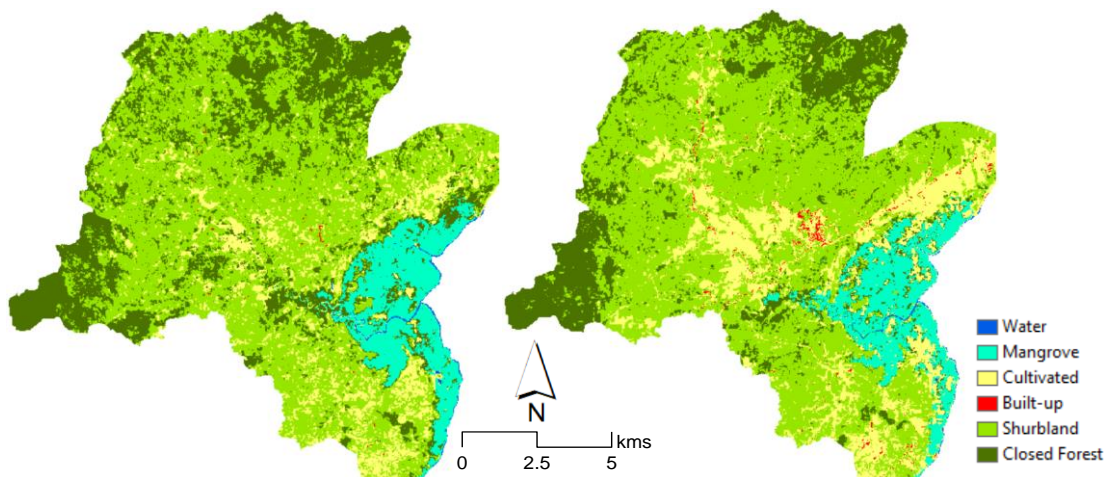
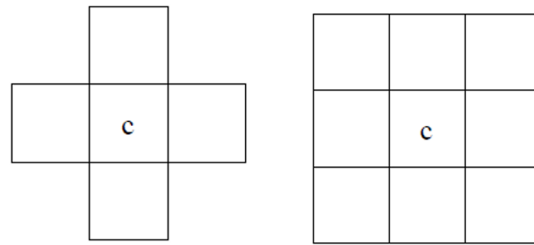


Figure 3.10 Land use and Land Cover types of Iwahig watershed during 1993 initial state (left) and final state in 2017 (right)

3.4.2 Neighbourhood Rules

Neighborhood rules controls the local spatial interaction of classes in a cellular automata. There are two popular types of neighborhood rules. First is the Von Neumann type wherein the central cell considers its immediate neighbors at the four cardinal directions (North, South, East and West) and the model decides how and what would be the final class (Figure 3.10 – Left). On the other hand, Moore neighbourhood considers the eight immediate cells surrounding the central cell (North, North East, East, South East, South, South West, West, North West, and North) as illustrated in Figure 3.10 - Right. Neighborhood rules controls the local spatial attraction of cells with respect to each classes. Cells grow and die as a function of its neighbors and the probability of each class to remain to its original state or transition in another state (or class) (Ghosh *et al.* 2017).



$$N = \{\{0, -1\}, \{-1, 0\}, \{0, 0\}, \{+1, 0\}, \{0, +1\}\}$$

$$N = \{\{-1, -1\}, \{0, -1\}, \{1, -1\}, \{-1, 0\}, \{0, 0\}, \{+1, 0\}, \{-1, +1\}, \{0, +1\}, \{1, +1\}\}$$

Figure 3.11 Von Neumann (left) and Moore (right) neighbourhood rules.

If we take a single class as an example in Figure 3.12, the initial state for that particular class at time 0 is shrubland. Using the Moore neighborhood (Figure 3.11), eight (8) neighbors were considered and the final state for time 1 becomes cultivated. The same class was identified using von Neumann neighborhood. This is because shrubland has 0.46 % probability to transition to cultivated class.

| A | B | C | D |
|-------|--|--|------|
| | M M C | M M C | M |
| S | 0.17 0.17 0.46 0.15 0.15 0.46 0.41 0.00 0.46 | 0.17 0.17 0.46 0.15 0.46 0.46 0.41 0.00 0.46 | 0.17 |
| F B C | | F B C | B |

Figure 3.12 Hypothetical Moore neighborhood transition rules from left to right: central cell at time 0 (left), initial state using moore neighbor, final state using moore neighbor, and final state using von Neumann neighbor.

The choice of neighborhood rules depends on the actual spatial abstraction of different land use and land cover types. Built up areas and water features (river) were assigned a Von Neumann rule because the boundaries in the real world are more discrete. Forest, shrubland, and cultivated meanwhile were assigned Moore neighborhood because the boundary is continuous. Figure 3.12 describes the Moore neighborhood effect by getting the weighted average probabilities of its neighbors including itself (central cell) to determine the new state (Figure 3.12D).

Table 3.3 Neighborhood rules applied for Land use and land cover transition states

| Land Use Land Cover | Code | Neighborhood Rule | Number of Neighbors | Netlogo Function |
|---------------------------|------|----------------------|------------------------|---------------------|
| Water | W | Von Neumann | 4 | <i>neighbors4</i> |
| Mangrove | M | Moore | 8 | <i>neighbors</i> |
| Cultivated | C | Moore | 8 | <i>neighbors</i> |
| Built-up | BU | Von Neumann | 4 | <i>neighbors4</i> |
| Shrubland | S | Moore | 8 | <i>neighbors</i> |
| Forest | F | Moore | 8 | <i>neighbors</i> |

3.4.3 Transition Rules

The 1993 classified satellite image is used as the initial state in the simulation at time zero (t_0) and the classified image for 2017 as the final state or time N (t_n). These were used as inputs to generate the transition probability matrix. Markov chain is a probabilistic modelling technique widely used to predict probability of transition at

initial time that is dependent on its preceding previous state (DelSole, 1999). The procedure is implemented as iterative process (depending on the temporal range in consideration) forming a chain of multiple dynamic system of events and thus called Markov Chain (DelSole, 1999, Ghosh *et al.* 2017, Thomas & Laurence, 2006).

Qualitative cross tabulation is performed between two raster datasets which represents the classified image at two different time events. Assumptions for the cross tabulation are: (i) equal number of classes, (ii) pixel dimension, and (3) same number of rows and columns. The rows and columns (i and j respectively) are arbitrarily assigned in the formula (1) where P_{ij} is the transition probability from one land use (m_x) to another land use (m_y) were values ranges from 0-1 where 1 having the highest probability and is given below (Vazquez-Quintero *et al.* 2016 pp. 5).

Table 3.4 LULC class transition probability matrix (1993 and 2017)

| | Final State (LULC 2017) | | | | | |
|---------------------------|-------------------------|---------------|---------------|---------------|---------------|---------------|
| Initial State (LULC 1993) | Water | Mangrove | Cultivated | Built-Up | Shrubland | Forest |
| Water | 0.5483 | 0.1408 | <u>0.2311</u> | 0.0000 | 0.0000 | 0.0798 |
| Mangrove | 0.0008 | 0.7373 | <u>0.1691</u> | 0.0000 | 0.0036 | 0.0891 |
| Cultivated | 0.0005 | 0.0124 | 0.4779 | 0.0117 | <u>0.4637</u> | 0.0337 |
| Built-Up | 0.0000 | 0.0000 | 0.0000 | 1.0000 | 0.0000 | 0.0000 |
| Shrubland | 0.0000 | 0.0016 | <u>0.1548</u> | 0.0080 | 0.7439 | 0.0917 |
| Forest | 0.0000 | 0.0475 | 0.0682 | 0.0005 | <u>0.4115</u> | 0.4723 |

Markov chain is a probabilistic modelling technique widely used to predict transition probabilities from two reference images taken at different time or event (Arsanjani *et al.* 2011). Markov chain directly utilizes cross tabulated matrix of two raster images representing land use and cover classification image at two different times or events. The assumptions for the cross tabulation is that there should be (i) equal number of classes, (ii) pixel (or cell) sizes are the same, and (3) the dimension of the rows and columns should be the same. The rows and columns can be assigned as i and j respectively as reference for the matrix operation. The probability is then cross reference and is given in equations (7a and 7b).

$$\sum_{I=1}^m P_{ij} = 1 \quad i = 1, 2, \dots, m$$
Equation (7a)

$$P = (P_{ij}) = \begin{matrix} P_{11} & P_{12} & \dots & P_{1m} \\ P_{21} & P_{12} & & P_{2m} \\ P_{m1} & P_{n2} & & P_{mm} \end{matrix}$$
Equation (7b)

Where: P_{ij} = the probability of transition from one land use/cover to another where values ranges from 0–1
 m = land use / land cover type

Previous work has demonstrated the use of Cellular Automata and Markov chain model to model land use and land cover change where Markov chain was used to extract model transition probabilities from two set of conditions in consideration (Cabral &

Zamyatin 2009). A study by Vazquez-Quintero *et al.* (2016) have used CA-Markov model to detect changes in temperate forest condition and found that simulation at year 2028, the reduction of pine forest would continue.

Thus, CA-Markov method is applicable to this study since one of the objectives is to simulate possible future conditions based on what has happened in the locality previously. Spatial and temporal interactions do not only change its state based on its previous condition but is also affected by the state/condition of its immediate neighbourhood (Clarke & Gaydos 1998).

Cellular neighbourhood transitions probabilities were coded in NetLogo (Wilensky 1999) and were assigned transition probabilities for each land use and land cover (LULC) classes. The strongest transition probabilities within and among classes are underlined in Table 3.4. For example, mangrove has more than 16% probability to change into cultivated area and has a 73% probability to remain as mangrove. The cross tabulated transition probabilities were used as a transition functions for each classes. Transition probabilities do not make this model spatially explicit as these probabilities are applied for every class, however, transition probabilities outputted by markov chain controls the temporal transition of each class. Cell neighbourhood transition rules as discussed previously are the ones that make cellular automata a spatially explicit. The

markov chain model was implemented in R using the markov chain package. Figure 3.13 illustrates the transition probabilities of each classes with respect to other class. The markov chain model reported that *built-up* class is a closed and recurrent class while *water*, *mangrove*, *cultivated*, *shrubland* and *forest* are transitory classes. Built-up also is the absorbing state meaning once it becomes built-up, it remains as built-up.

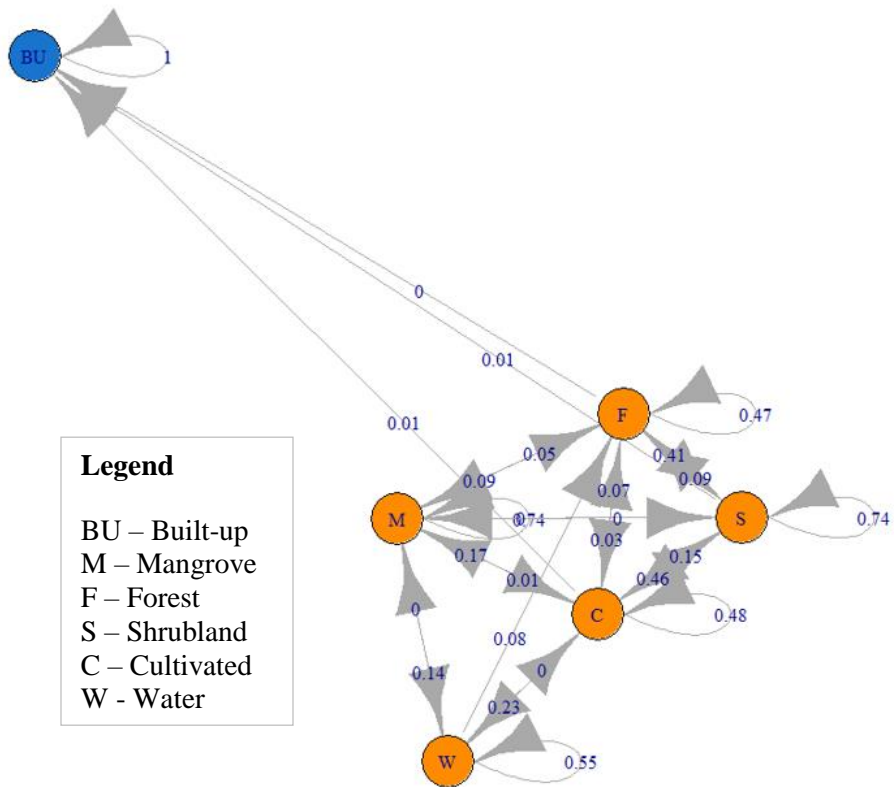


Figure 3.13 The Markov chain transition probability model for the six (6) LULC classes. The circle corresponds to different land use and land cover and the number represents transition probabilities ranging from 0 – 1 where probability of 1.0 is called an absorbing state.

Six different land use and land cover types were assigned at the initial state as discussed in the cell state section. These classes will have varying transition probabilities depending on the weighted sum of its neighbors. The combination of CA and Markov chain makes CA geosimulation a spatially explicit model of LULC change. One limitation of Markov chain model is that it cannot predict LULC changes beyond the initial and final states especially when a new class (that is not in the initial and final state) evolved during the predicted state (Arsanjani, *et al.* 2011, Camacho *et al.* 2015, Yang *et al.* 2015).

Landscape Transition Models

The cell in a cellular automata can only have two general states. One is to remain alive and another is to be dead or change to another state as a new born cell which represents the live-death-rebirth cycle as a natural process (Clarke 1997). This simulation exercise demonstrated diffent land use and land cover transitions patterns which focuses on mangroves. However, understanding other land use and land cover is equally important and vital as the transition of mangrove class to other class will highly depend on its neighboring class and the time factor during transition. The conceptual diagram developed in this research served as a guide in understanding how different land use and land cover classes respond to external facors (climate, sedimentation, rainfall) and other physical processes that directly and indirectly affect the land transition within the the

waterhsed and coastal environment. Clarke (1997) presented a simplified land transition models which can come from land transition to other class (Figure 3.14-A), land transition in space (Figure 3.14B), and the transition of land in the context of its immediate neighbors (Figure 3.14C).

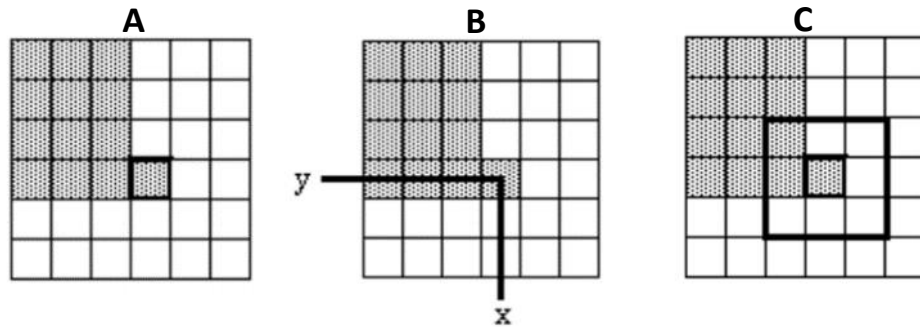


Figure 3.14 Land transition models adapted from Clarke, K. 1997. A represent state transition from one class to another. B is the transition of one class in space (spatial) and C is the transition of a class in the context of its immediate neighbors.

Land transition models follows a number of assumptions based Clarke's Deltatron Model (1997). First, transition matrix accurately estimates land use state transition probabilities. Second, external model can be used to change the state of the dominant or driving class. Third, there is considerable spatial autocorrelation in land transitions. Fourth, there is temporal correlation between land transitions. Fifth, specific land transitions are influenced by context. Finally, land transitions happen to some degree at random (i.e., independent from the driving force). The cellular automata

models generated in this study agree with all these assumptions of Clarke (1997) which is why the statistical regression and conceptual models implemented in this study are directly linked to the geosimulation exercise as they provide context as well as direct and indirect relationships.

For the purpose of this research, mangrove ‘decrease’ refers to any reduction in area as a result of decrease in spatial coverage. The context of decrease refers to the unnatural decrease of mangrove extent as a result of human activity (e.g., clearing for land preparation, mangrove harvesting of any forms and coastal developments). The parameters involved in the perceived potential decrease in area as discussed in the methodology section are: road, built-up area, stream, and fragmented area center point (core). Proximity-based (Euclidean distance) transition model was implemented for the Iwahig mangrove patch in lieu of Markov transition probability model. This is with the assumption that mangrove vulnerability to extraction and disturbance increases with increased proximity to access and manmade structures. Since the data for first three parameters are easily obtainable as a GIS ready data, the fragmentation data will be elaborated further to support the discussion.

3.5 NetLogo programming language for Cellular Automata model

There are several applications available to conduct cellular automata models. Specific simulation platforms are either designed to do Agent Based Models (ABM) or Cellular Automata (CA) only. However, there are software (NetLogo, GAMA, AnyLogic) which can support both Cellular Automata and Agent based modelling. This study used NetLogo multi-agent programmable modelling environment developed by Uri Wilensky under the Center for Connected Learning. Netlogo is a free and open source and licensed under the General Public License (GPL) version 2 (<https://ccl.northwestern.edu/netlogo/>).

Netlogo handles spatial data (real world geographic coordinates) in both 2D and 3D using the *gis* extension. This extension enables reading a geotiff raster file (*.ascii*) and vector data (*.shp*) formats including its geographic projection information (*.prj*). This feature allows the software to do raster to raster, vector to vector and raster to vector overlay assuming the all use the same projection. The only limitation is that the only projection that the program accepts is geographic coordinate system: WGS 1984 EPSG: 4326 (Wilensky 1999, Wilensky & Stroup 1999).

3.6 Mangrove Fragmentation

Temporal mangrove area extents were extracted from multiple Landsat 5 satellite data with scene ID 117 054. A five (5) year interval were used for image analysis to identify patch changes at 30x30 meter resolution using Landsat satellite data. The classifications were performed using Google Earth Engine which is a cloud-based repository of analysis ready historical and recent imageries acquired by multiple earth observation satellites including Landsat (Gorelick *et al.* 2017). The method used for classification is ISODATA (Iterative Self Organizing Data Analysis) which implements a clustering for classification based on spectral similarity. Figure 3.15 illustrates the classified mangrove areas for five (5) year interval from 1985 – 2010. The classified patch of mangrove has an estimated area of 1,600 hectares based on 1985 classified Landsat data.

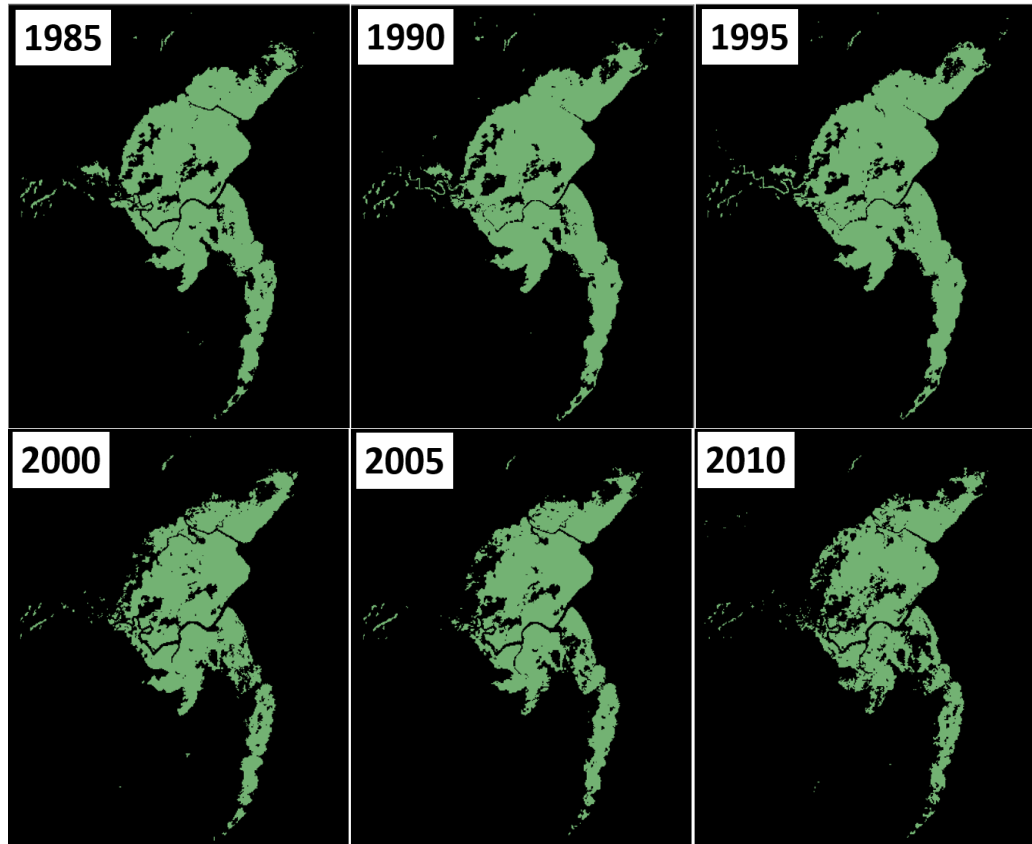


Figure 3.15 Temporal mangrove cover classification from 1985 - 2010

Since no field data was collected for this research, species level classification was not possible due to the absence of training data. To estimate and quantify the mangroves to be affected by the simulation scenarios, unsupervised mangrove classification was performed to estimate mangrove species grouping. A combination of Iterative Self Organizing Data Analysis (ISODATA) and Principal Component Analysis (PCA) technique was implemented on a medium resolution Sentinel 2 satellite image to generate representations on the type and grouping of mangrove classes based on tidal

position using spectral similarity. Sentinel 2A were pre-processed using *sen2cor* atmospheric correction prior to transformation. A forward principal component rotation using the 10 reflective band statistics of the Sentinel-2 data for the covariance matrix computation. Figure 3.16 (center) shows the resulting PCA rotation of the spectrally transformed bands which contains 94.4% of the spectral information. The method shows three unique grouping of mangroves as specified by the color grouping: seaward – green, midstream – yellow and landward – maroon as illustrated in Figure 3.16 (right).

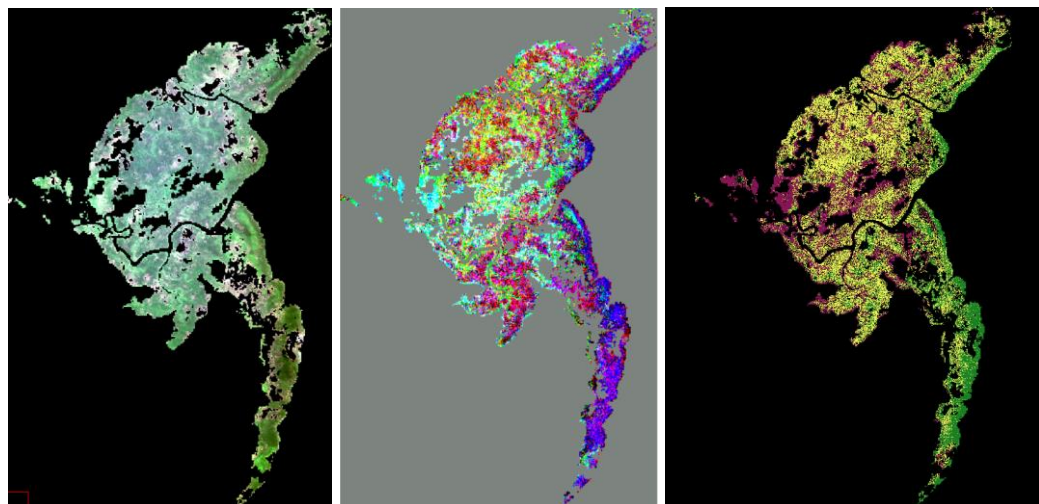


Figure 3.16 Sentinel-2 true color composite (left), PCA Composite (PC9-PC8-PC10 - center) and mangrove species grouping used in *NetLogo* simulation (right)

Mangrove groupings were assigned based on species listed in Table 3.5 since species level assignment is not possible because no field data is collected or available for the Iwahig mangrove forest. Groupings assignment also referred to the tidal position of each

species as identified by Primavera *et al.* 2013. Pixels with different colors were grouped based on the unique species ‘grouping’ in the seaward, midstream and landward zone using the Principal Component Analysis clustering (Figure 3.16-right). Mangrove fragmentation is mainly attributed to human activity and these complex patterns of fragmentation might be due to preferential or selective cutting of species and is thus dependent on the spatial distribution of preferred species. A study by Gonzales in 2005 on impacts of mangroves utilization in southern Palawan showed that mangrove cutting in Bataraza municipality was preferential to *Rhizophora species* which is used mainly for construction material to build houses.

Table 3.5 Selected species list in Bataraza Palawan adapted and modified from PCSD 2015 and corresponding tidal position of species (Primavera *et al.* 2013)*

| Mangrove group | Genus | species | Common Name | Tidal position* |
|----------------|-------------------|--------------------|----------------|-----------------|
| Seaward | <i>Avicennia</i> | <i>marina</i> | Bungalon | Front liner |
| Seaward | <i>Sonneratia</i> | <i>alba</i> | Pagatpat | Front liner |
| Landward | <i>Ceriops</i> | <i>decandra</i> | Malatangal | Inland |
| Landward | <i>Rhizophora</i> | <i>stylosa</i> | Bakawan-bato | Inland |
| Landward | <i>Heritiera</i> | <i>littoralis</i> | Dungon-late | Inland |
| Midstream | <i>Rhizophora</i> | <i>apiculata</i> | Bakawan-lalaki | Tidal creek |
| Midstream | <i>Rhizophora</i> | <i>mucronata</i> | Bakawan-babae | Tidal creek |
| Midstream | <i>Bruguiera</i> | <i>cylindrica</i> | Pototan-lalaki | Tidal creek |
| Midstream | <i>Xylocarpus</i> | <i>granatum</i> | Tabigi | Midstream |
| Midstream | <i>Xylocarpus</i> | <i>moluccensis</i> | Piagau | Midstream |

The mangrove geosimulation model utilized the distance functions as a method for cell transition rules to represent spatial processes of movement to and from the mangrove area (Zhao, 2007). The proximity parameter (relative to the mangrove area/patch) used in this research are: Road (primary, secondary and footpath), River (and tributaries), Mangrove Fragmentation (center point), and built up areas (residential). Distances of each proximity parameters were generated using Euclidean distances resampled to 10 meters which is the same spatial resolution of the Sentinel 2 classified data for mangrove and thus, the unit of the distance rasters are in meters. The initial state assigned in this model was the 1995 mangrove cover classification. Final state was not applicable in this method because the model will try to simulate different scenarios using variable distance parameters: (i) distance to core, (ii) distance to built-up areas, (iii) distance to stream, and (iv) distance to road as illustrated in Figure 3.17.

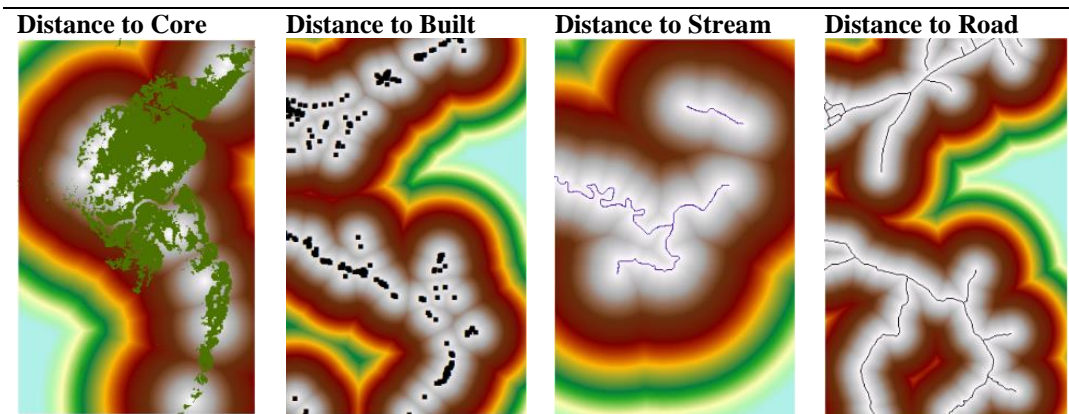


Figure 3.17 Euclidean distances of local mangrove transitions

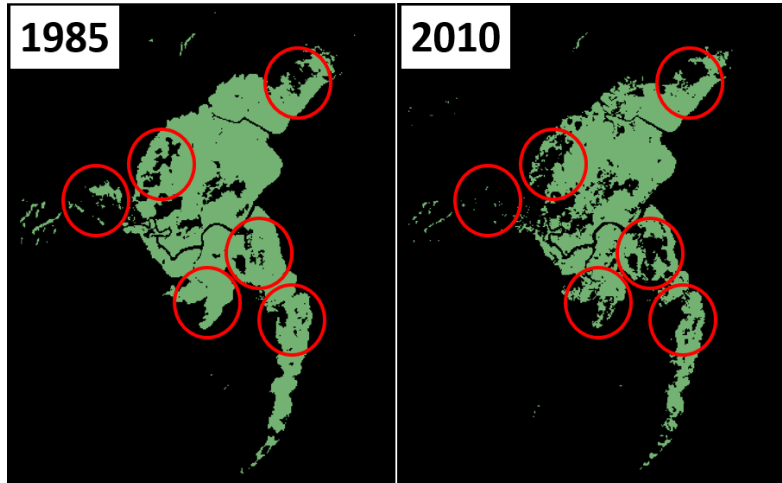


Figure 3.18 Satellite derived mangrove fragmentation of Iwahig mangrove observed between 1985 – 2010

Transition rules for the mangrove model were derived from the distance functions in Figure 3.17. The basis of this research in selecting these parameters are suggestions and finding of related studies that proximity to built-up (Allen 2001, Walters 2005), proximity to road (Ambastha, 2010, Blanco-Libreros 2015), mangrove fragmentation (Blanco-Libreros *et al.* 2015, Allen 2001, Tran 2017, Seto *et al.* 2007), and river network as direct means to access mangrove areas and a combination of these have caused different scales of mangrove mortalities. Patterns or cutting preference specific to mangrove species has also been found to affect fragmentation of mangrove forest in the study due to selective or preferential cutting of *Rhizophora* species (Gonzales *et al.* 2017). Since there have been no major typhoon (100 year return period) in Bataraza Palawan within the period covered by the study (1985 – 2017), no natural perturbations were considered in the model for this study. Thus, only anthropogenic drivers of

mangrove change were considered. Typhoon Yolanda has affected the northern part of Palawan but there was little to no effect in terms of typhoon related damage to mangrove recorded to Southern Palawan based on Yolanda typhoon track.

4. RESULTS AND DISCUSSION

4.1 Variable importance and variable selection using Random Forest regression

Random forest regression in this study revealed that geomorphologic variables outweigh bioclimatic variables in observed variations in R-type mangrove extent. This points out that the condition within the mangrove locality (and its watershed) is very important for the mangroves to thrive. However, climatic variables are not being discounted in this study as previous studies found that local variables affect mangrove directly while watershed processes affect mangrove during dry condition (Eslami-Andargoli *et al.* 2010). The role of watershed in a riverine type mangrove is vital and this study has contributed to the findings of Selvam & Karunagaran 2017, Duarte *et al.* 1998 and Truong *et al.* 2017 that mouth condition and river channel as significant factors in understanding riverine type mangrove ecosystem. The length of the main channel within the watershed of a riverine type mangrove also plays a role in sustaining a rich mangrove ecosystem as this partly controls the out-welling of freshwater from the upstream to the coast (Truong 2017). Figure 4.1 lists the top 15 variables correlated with variations in mangrove area. This is as a result of robust random forest regression for 183 watersheds and 30 explanatory variables.

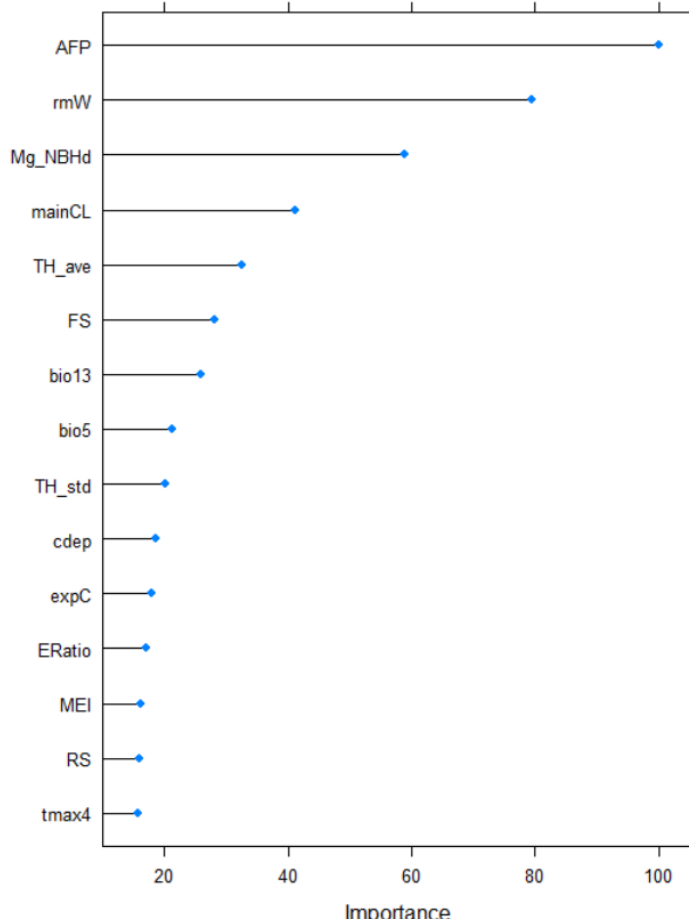


Figure 4.1 The variable importance using random forest model (top 15).

Figure 4.2 graphs the Variable Importance (VI) mean, VI standard deviation, and VI for the nested and predicted models. The variables ranked according to importance are:

- (1) Area of the flood plain within the watershed, (2) river mouth width of the main channel, (3) presence of neighbouring mangrove community and (4) is the length of the main channel which accounts for 67% of the variation in riverine type mangrove areas ($n = 183$) in Palawan island as listed in Table 3.2.

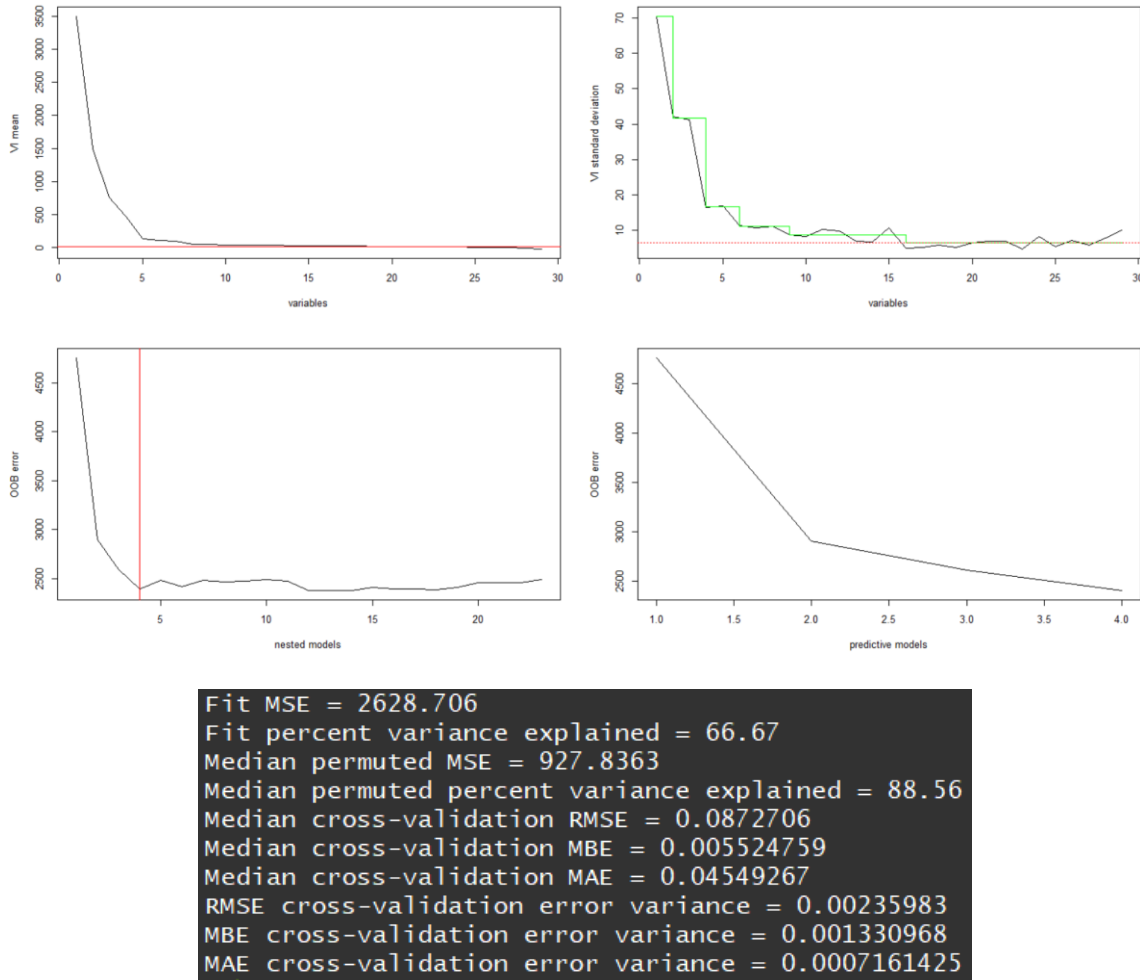


Figure 4.2 Variable Selection Using Random Forest (VSURF) VI mean, VI SD, OOB error (nested) and OOB error (predicted) , the explained variation and cross validation results

Table 4.1 The selected variable explaining the variations in mangrove area based on geomorphologic and bioclimatic variables using random forest

| Parameter | Code | Published Literature | Variable Importance Ranking (this study) |
|--------------------------------------|-------------|--|---|
| Area/extent of floodplain | AFP | Primavera <i>et al.</i> (2013), GIZ | 1 |
| River mouth width | rMW | Selvam V., & Karunagaran VM., (2017) | 2 |
| Main Channel Length | mainCL | Truong <i>et al.</i> (2015) | 3 |
| Presence of Neighboring Mangroves | mgNBHD | Duke <i>et al.</i> (1998) | 4 |

Regression model and variable selection for mangrove area change

A random forest model was tested to identify variables that are correlated to the observed decrease in mangrove area extent at regional scale using bioclimatic variables and other probable factors listed in Table 3.1. A total of fifteen (15) predictor variables were regressed over a mangrove area change per watershed area ($n = 183$). The mangrove area change were derived from the differences in area of two composite satellite acquisition years from 1990 – 2017. This was the same dataset provided by the PhilCoMaRS and CorVA project of UP TCAGP and UP MSI of the Biodiversity Management Bureau of the Department of Environment and Natural Resources (BMB-DENR).

Table 4.2 Variable considers determining factors affecting mangrove change at regional scale

| Variable Name | Code | Description |
|----------------------------|-------------|--|
| Change | change | The area extent change of mangrove from 1970 to 2017. <i>This is also the Y-variable</i> |
| Tree cover | tc | Tree cover area within the watershed |
| Percent of Tree cover | pTC | Percentage of tree cover within the watershed |
| Fishpond | FP | Presence / Absence of fish ponds (Boolean) |
| Area of Forest | aFor | Area of forest cover within the watershed |
| Area of Agriculture | aAg | Area of agriculture within the watershed |
| Area of Built-up | aBU | Area of built-up within the watershed |
| Tree height average | TH_ave | Mean tree height of mangrove |
| Tree height Std. Deviation | TH_std | Standard deviation of mangrove tree height |
| Temperature | bio5 | Maximum temperature of warmest month |
| Precipitation | bio13 | Mean precipitation at wettest month |
| Longitude | long | Longitude of the mangrove center |
| Latitude | lat | Latitude at the mangrove center |
| Mangrove neighbors | Mg_NBHd | Number of mangrove neighbors |
| Max Temperature in April | tmax4 | Maximum Temperature in April (celcius) |
| Max Temperature in May | tmax5 | Maximum Temperature in May (celcius) |
| Population in 2015 | Pop15 | Population within the watershed in 2015 |
| Change in Population | ch_pop | Change in population within the watershed from 2010 - 2015 |

Results of variable selection for mangrove area decrease showed that longitudinal distribution, precipitation of wettest month, and area of agriculture within the watershed are the variables that contribute to 50.49 % of the variation in the observed decrease in mangrove extent (Figure 4.3 and Table 4.2). Results from this exercise were used as guide in the simulation of Iwahig watershed particularly the changes in cultivated or agriculture area within the landscape.

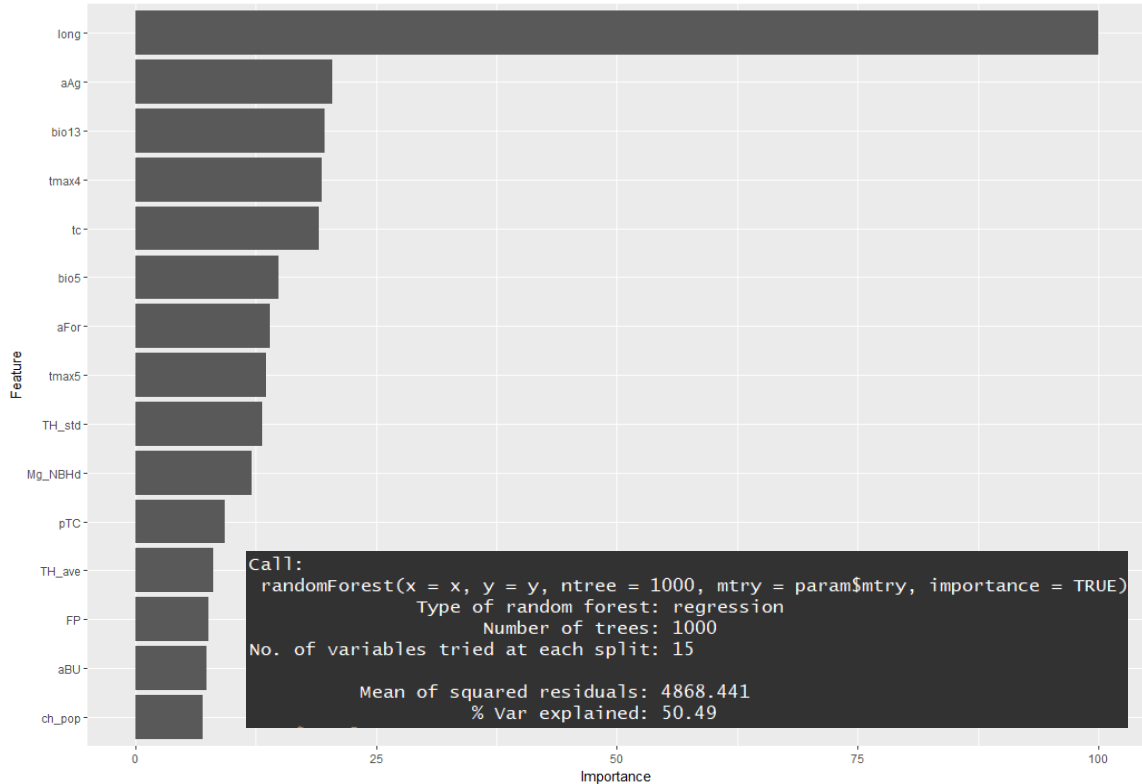


Figure 4.3 Variable importance of mangrove area decrease using selected variables at regional scale

Table 4.3 Variable Selection for mangrove cover change using BioClim and potential decrease variables on a regional scale

| Parameter | Code | Reference | Variable Importance Ranking (this study) |
|--|-------|--------------------------|--|
| Longitude | long | | 1 |
| Area of Agriculture within the watershed | aAg | Enslami-Andargoli (2010) | 2 |
| Precipitation of wettest month | Bio13 | Enslami-Andargoli (2010) | 3 |
| Maximum Temperature in April | Tmax4 | | 4 |

4.2 Physical processes in a riverine type mangrove

Duke *et al.* (1998) did a comprehensive study on factors affecting the distributional gradients of mangrove. There are many scales (spatial) that can be used to study mangrove habitat dynamics by analysing environmental, physical and geomorphological characteristics. The study suggested that there are no simple assessment that can be done to explain the complex distribution of mangrove habitats. Thus, it is also impossible to have few variables to have great explanatory power in the study of these variables. However, this study focused only on one type of mangrove compared with the comprehensive assessment of Duke (1998) where all types of mangroves were considered.

A study by GIZ in 2017 pointed out the importance of coastal floodplain habitats for ecological restoration of mangrove. Primavera *et al.* (2013) found that these flood plain areas are the most ecologically suitable areas for mangrove planting. Since most of the tidally inundated floodplains (weather within a watershed or not) within proximity of populated areas are being developed for aquaculture, Salmo *et al.* (2007) has recommended several management practices for mangrove rehabilitation. One is that mangroves should be planted on abandoned fishponds and unproductive aquaculture ponds among others as supported by Dunca *et al.* (2016). This research has contributed

to the findings of various studies that tidally inundated floodplains as important ecological variable in a mangrove ecosystem especially for riverine type setting. Any activity that encroaches the natural coastal floodplain due to either activities in the upstream of the watershed or stress factors from the coastal ecosystem directly impacts these mangrove habitat. Enslami-Andargoli *et al.* (2010) in their study of watershed and mangrove suggested that human activities are found to impact mangrove directly if the flood plain areas are converted into different land use and/or land cover other than swamp or mangrove.

The relationship of mangrove extent with rainfall and watershed size has been largely studied in Australia and found that mangrove diversity is higher in large watershed areas, long channel and high precipitation (Bunt *et al.* 1982, Duke 1992, Smith *et al.* 1987). This was supported by the finding of Duarte *et al.* (1998) that there is a strong correlation with the size of watershed area, sediment composition and mangrove growth. Duarte *et al.* (1998) concluded that mangroves adjacent to rivers with watershed area greater than 10 km² are the most suitable area for mangrove growth (especially for *Rhizophora apiculata* species). The result of the regression model for 183 riverine type mangroves studied in this research has partially contributed to the findings of Truong *et al.* (2017), Bunt *et al.* (1982), Duke (1992), Smith *et al.* (1987) that river mouth width, channel length & condition, and floodplain condition are important geomorphological variables

in maintaining a healthy riverine type mangrove ecosystem. Linear relationship of mangrove area versus river mouth width show R^2 of 0.493 with p-value of 0.0002 and area of floodplain within the watershed with R^2 of 0.58 and p-value of 2.59e-10 as illustrated in Figures 4.4-A and 4.4-B respectively.

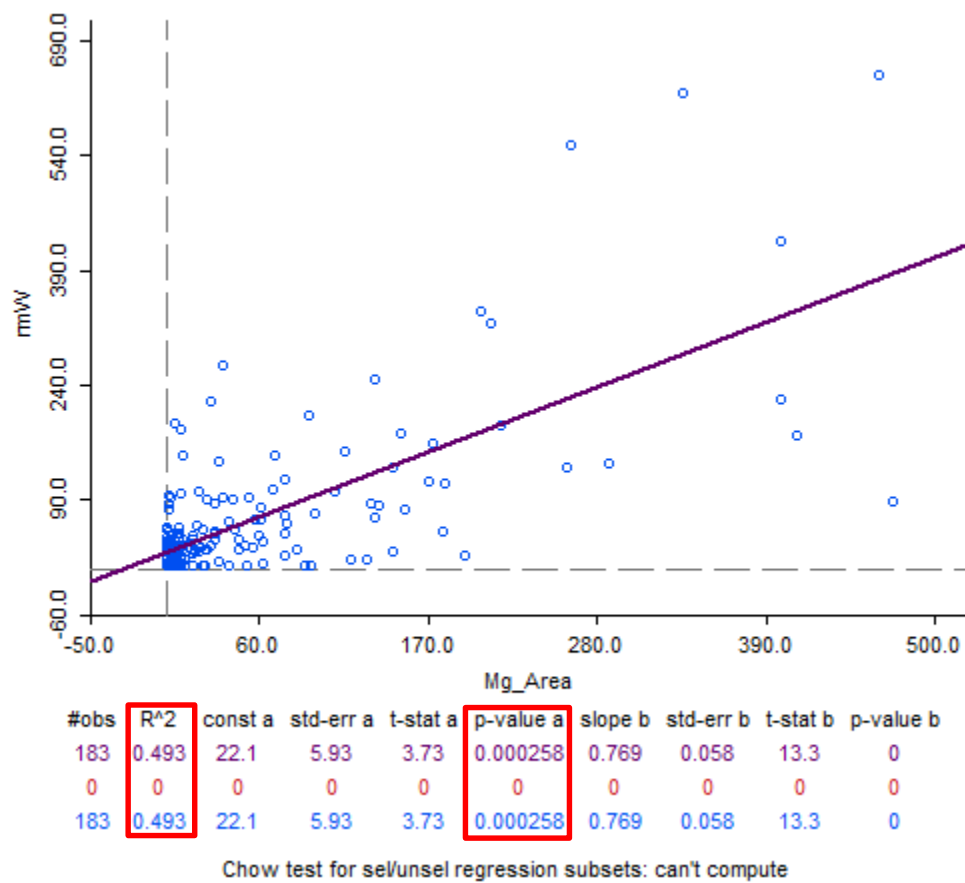


Figure 4.4A Correlation between mangrove area (x-axis) and river mouth width (y-axis)

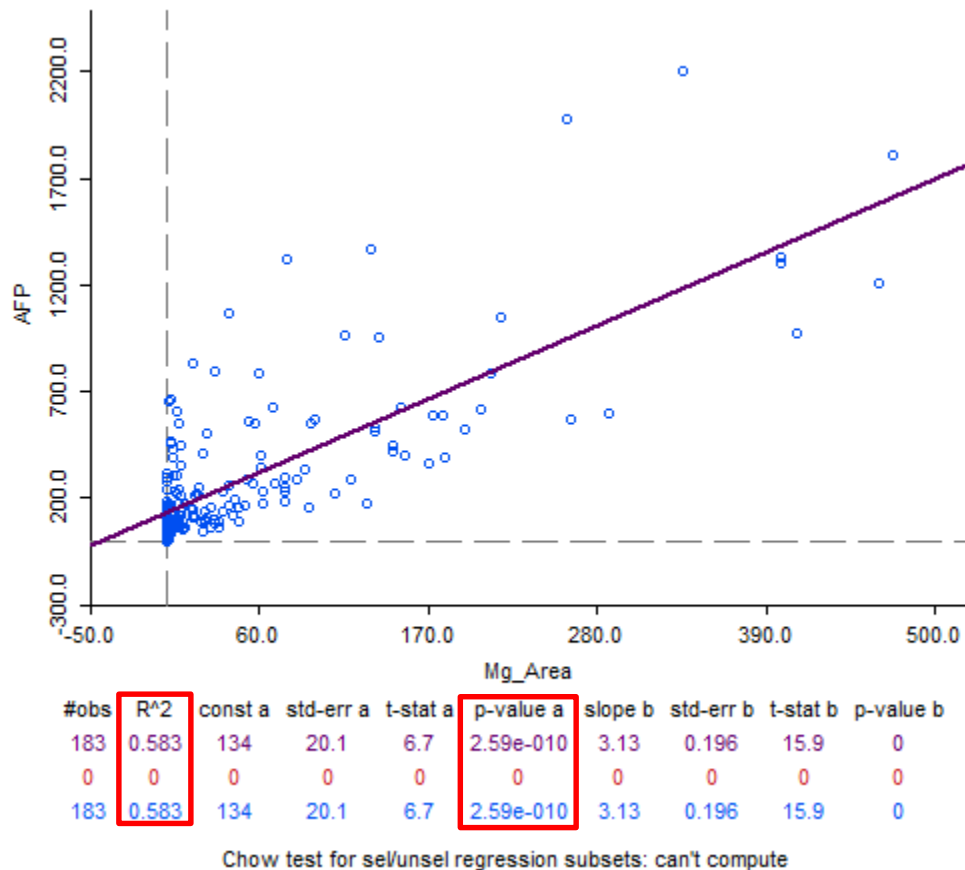


Figure 4.4B Correlation between mangrove area (x-axis) and area of tidally inundated flood plain (y-axis)

The random forest variable selection identified four explanatory variables that are highly correlated with the variations in a riverine type mangrove. These are: area of floodplain within the watershed, river mouth width, length of the main channel and presence of neighboring mangroves. These variables contribute to more than 60 percent of the variations in observed riverine mangrove area.

A conceptual model was developed considering the physical processes in a riverine type mangrove. For the purpose of this study, the conceptual model considered only the geomorphologic, land use and land cover, and bioclimatic factors for mainland Palawan. Bio-climate (e.g., precipitation) plays a significant role in the transport and deposition of sediment within the watershed. The amount of cultivated area, type of soil, the erosive force of runoff during rainfall events and slope of the watershed might dictate intensity and direction of sedimentation which eventually are deposited downstream in the coastal area in long term. This relationship can be observed in Figure 4.5 which shows correlation plot of highly correlated variable, which can actually be grouped into three major groups. First was the clustering of watershed variables (Figure 4.5-blue box), next is the clustering of local geomorphological settings within the watershed (Figure 4.5-black box), and the last is the clustering of bioclimatic parameters (Figure 4.5-orange box).

Vegetative cover (permanent and semi-permanent) and cultivated area within the watershed also contribute in the control of sedimentation process downstream. These watershed properties are significant in finding correlations between upland processes and coastal sedimentation and downstream channel evolution.

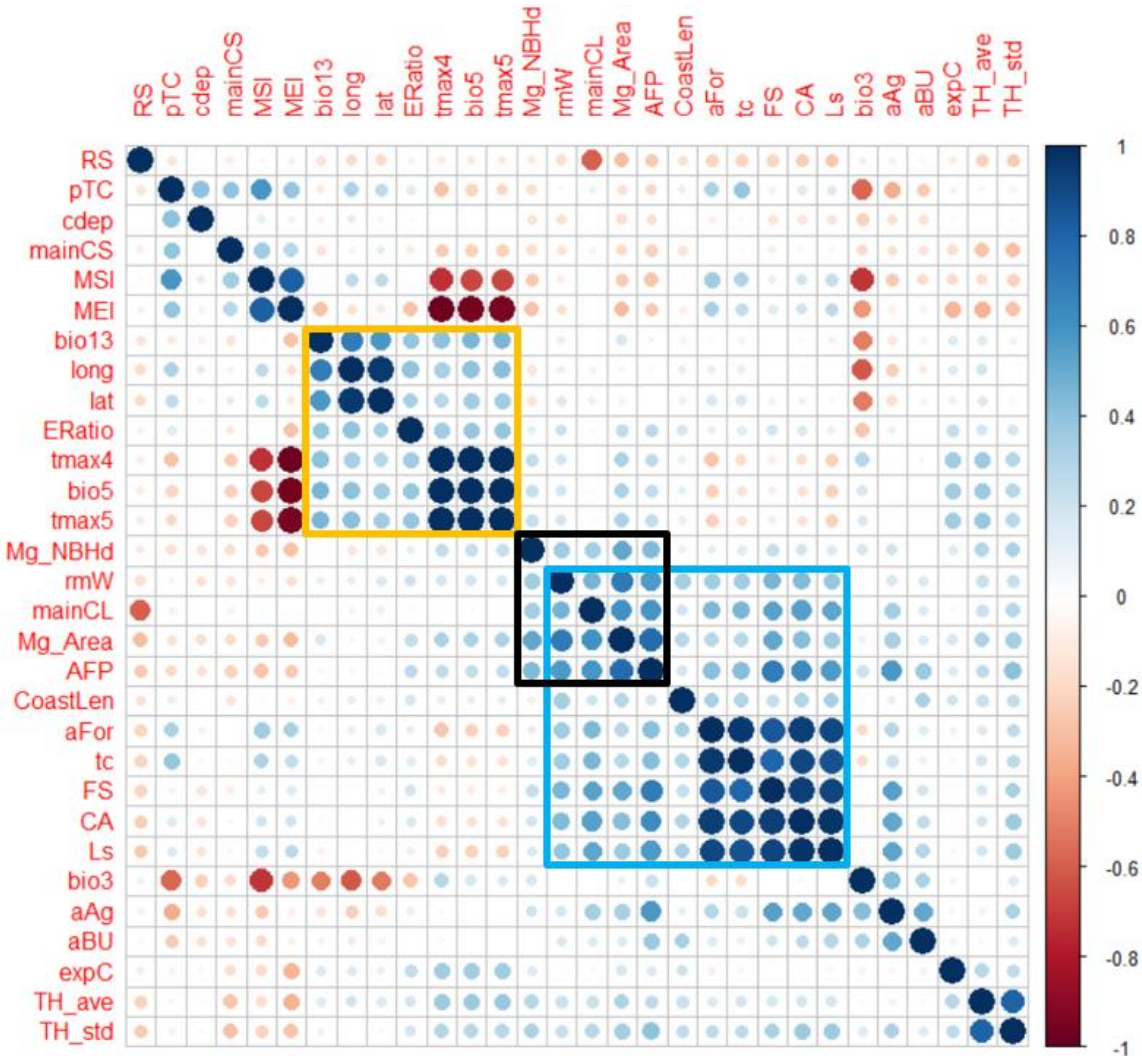


Figure 4.5 Correlation plot of 29 exploratory variables and response variable. Blue box shows relative clustering of watershed variables, black box shows relative clustering of local geomorphologic variables and yellow-orange box shows relative clustering of bioclimatic variables.

Several studies have found direct and indirect links between spatial and temporal watershed to coastal dynamics (Valiela *et al.* 2014, Richmond *et al.* 2007, Eslami-Andargoli *et al.*, 2010, Yimnang *et al.* 2011). Watershed mean elevation, slope and local

coastal geomorphology on the other hand contributes to river mouth and channel alteration (Truong *et al.* 2017). Thus, the mouth condition is largely influenced by upland sedimentation, overland flow, river run-off that partly determines available area for mangrove colonization (Duarte 1992, Woodroffe 1992, Opperman 2005, Walsh 2017). The conceptual model developed in this study (Figure 4.6) will guide the land use and land cover transition during the Cellular Automata simulation exercise for Iwahig watershed.

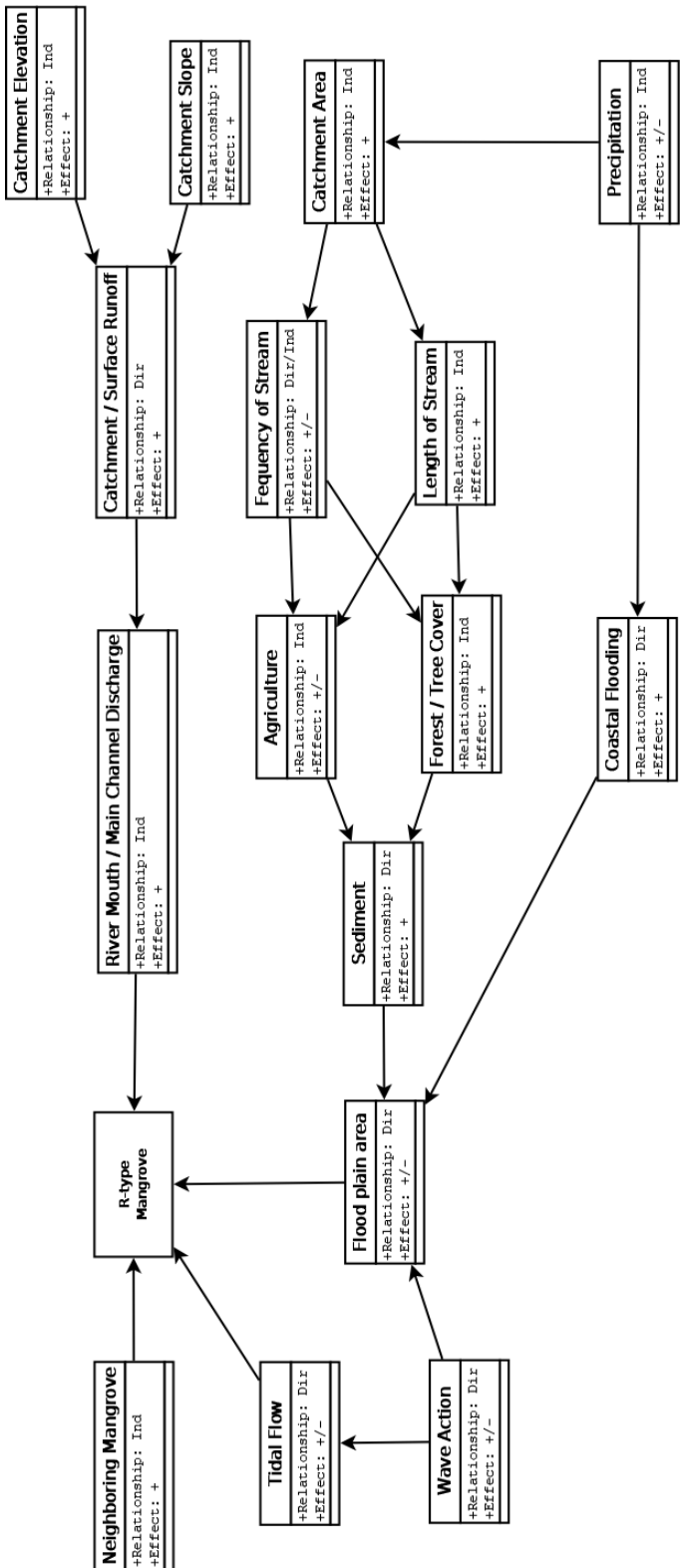


Figure 4.6 Conceptual model of physical processes for a riverine type (R-type) mangrove setting

Although processes will vary depending on the size of watershed, Opperman *et al.* (2005) and Strayer *et al.* (2003) identified that larger watersheds are able to explain downstream ecosystem better than smaller watersheds through dynamics of land use and land cover. This study implemented a random forest model wherein watersheds were grouped into small (1,000 – 5,000 hectares), moderate ($> 5,000 – 10,000$ hectares) and large ($>10,000$ hectares) with $n = 132$, $n = 29$, and $n = 22$, respectively using the same variables for random forest regression used when no grouping is applied. Table 4.4 lists the resulting top important variables and their corresponding explained variance in the model. Since small watershed has more observations than moderate and large watersheds, high explained variance was expected. And because the sample sizes largely differs between small, moderate, and large watersheds, no substantive conclusions can be derived on the variable importance measures and explained variance with mangrove area.

Table 4.4 Random forest regression for three (3) watershed size clusters and resulting variance explained and corresponding variable importance.

| Watershed Size | Top 5 variables | % Variance explained | Sample size |
|--------------------------|--|-----------------------------|--------------------|
| small (1000 - 5000 ha) | Area of Flood Plain River mouth width Average tree height Neighboring mangrove Tree height SD | 67 | 132 |
| medium (5000 - 10000 ha) | Main channel slope Tree cover within the watershed Max temp warmest month Frequency of stream Latitude | 17 | 29 |
| large (> 10,000 ha) | Main channel slope River mouth width Tree height average Precipitation of wettest month Percent tree cover | 38 | 22 |

4.3 Geosimulation modelling

This section describes the three simulation models for this study. The first is the landscape approach for the entire Iwahig watershed where results of the random forest regression is linked. The second and third models are the mangrove models where mortality and growth were considered. The mortality model used distance-based proximity rules as transition functions to model several event-based scenarios of mangrove loss. The final model is a mangrove growth model which modified an existing model to generate multiple neighbourhood influences for mangrove canopy or gap closure.

4.3.1 Simulation model for Iwahig watershed

Coastal development on tidally inundated plain will have potential direct and/or indirect impacts on local geomorphology and river channel morphology. Resource extractive and destructive activities not only impacts the area available for mangroves to grow, floodplain development also alters hydrodynamics and local coastal geomorphology (Truong *et al.* 2017). The study area in Iwahig watershed has experienced dramatic increase in population which results to massive land conversion from to support growing population by boosting local economy. However, the number of households below poverty threshold is still 69.7% in 2015 according to DENR, and

has not change significantly during the time of the study. Bataraza is one of the most populated municipalities in Palawan due to in-migration for employment opportunities in the mine site (Gonzales *et al.* 2005). This could be a long term effect of social and economic developments in Bataraza municipality because of the Rio Tuba Nickel Mining Corporation which has been in operation since the 1980s. The mining company is reported to consume an estimated 92.2 tons of mangrove charcoal per month to power its operation (Gonzales *et al.* 2005). Local economy and population have both increased as a direct and indirect effect of the mining area at the expense of its upland, coastal and marine resources. Drastic change in landscape was modelled in this study using time series analysis (1993 – 2017) at the watershed landscape scale.

Several simulations were performed in this study to visualize and quantify spatial and temporal interactions of six major (6) land use and land cover types classified within the Iwahig watershed. The study followed the land cover classification implemented by the Integrated Natural Resource Management Plan of the DENR for the entire Palawan. Based on the report, the major land use and land cover identified were: forest, shrubland/woodland, wetland, buildup and cultivated (DENR INRMP 2015).

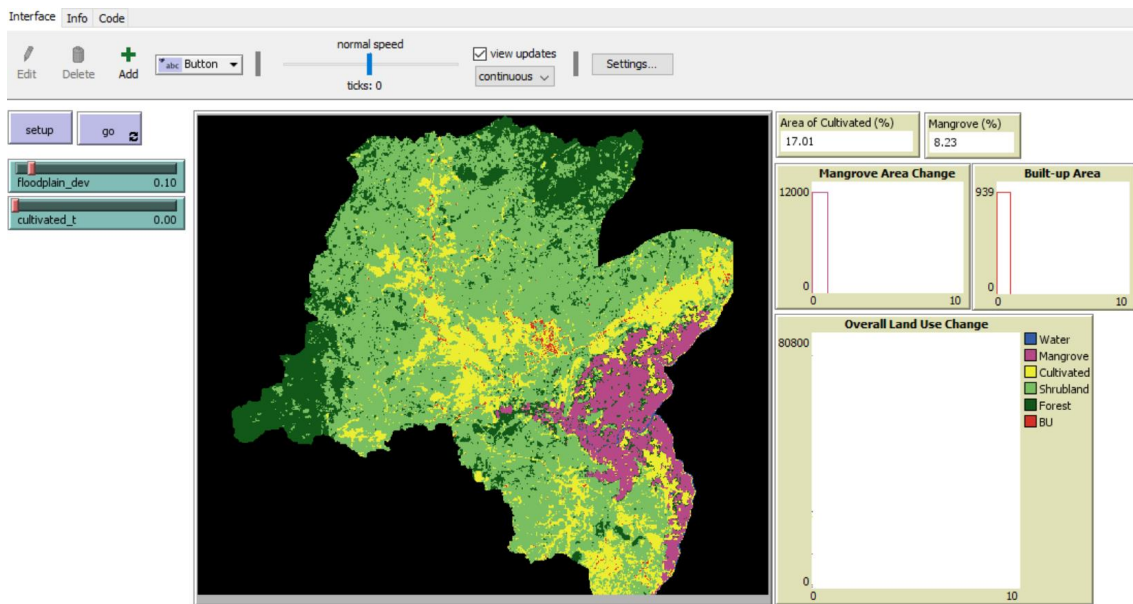


Figure 4.7 Graphical User Interface of the Iwahig watershed simulation model implemented in Netlogo. The left side tools are the *set-up* functions to read the data and assign cell colors and the *go* function to initialize the model. The *floodplain_dev* and *cultivated_t* are parameters the user can modify. On the right side are report interface for cultivated area and mangrove area. It is given by percentage within the watershed (top right) and total number of pixels (middle right). The bottom is the graphical change in land use based on the actual total number of pixels that has changed.

Simulation environment were set up prior to simulation exercise. Class states from the 1993 Iwahig watershed LULC and corresponding transition probabilities from markov chain model were hard coded in the NetLogo platform. Figure 4.7 illustrates the modeling environment (user interface) for the Iwahig watershed model. The *setup* button was used to import the matrix file which represent the land use and cover classes. The *go* button is used to initiaize the simulation. Two modifiable parameters (*cultivated_t* and *floodplain_dev*) were designed to give the modeller the control of the change

probabilities multiplier by raising the markov probability to a desired value. A monitoring interface was designed to visualize and quantify land use and land cover change allocation within the watershed based on the total number of pixels that has changed within the watershed.

The initial model was simulated without changing any parameter to observe how classes will transition using the default markov event. Results showed that the LULC exchanges were abrupt between simulation ticks 0 and tick 11 and became gradual after 11 ticks (Figure 4.8-D). The abrupt change is attributed to the “spatial filtering” effect of the neighborhood rules applied (Moore and von Neumann) wherein individual and isolated pixels are filtered (salt and pepper effect in remote sensing image). As an effect, the resulting modelled land uses (Figure 4.8-C) appeared to be visually ‘smooth’. The modelled output was able to capture the same land use patterns in observed 2017 LULC.

This is attributed to the markov chain matrix model since we multiplied the markov matrix to the initial state where the values are derived from the reference images. The spatial transition however was realistically handled by the cell neighborhood rules which are effective for discrete land uses. Since CA is a self replicating system, this will generate a dynamic land use and land cover allocation with respect to the markov chain even probability model. However, there is a limit in terms of the change allocation since a threshold will only allow for a sensible and realistic result. This realistic result according to Gibbs *et al.* (2009) should follow a ‘typical’land use and land cover transition pattern

(Figure 4.9) wherein forests are typically degraded into shrubland before being transforming into the lowest form of vegetation community which is agriculture. However, this pattern is not observed in mangrove forest since mangrove can directly be converted to built-up, aquaculture or water because of its proximity to urban area. This is the reason this study developed a mangrove model to support this theory.

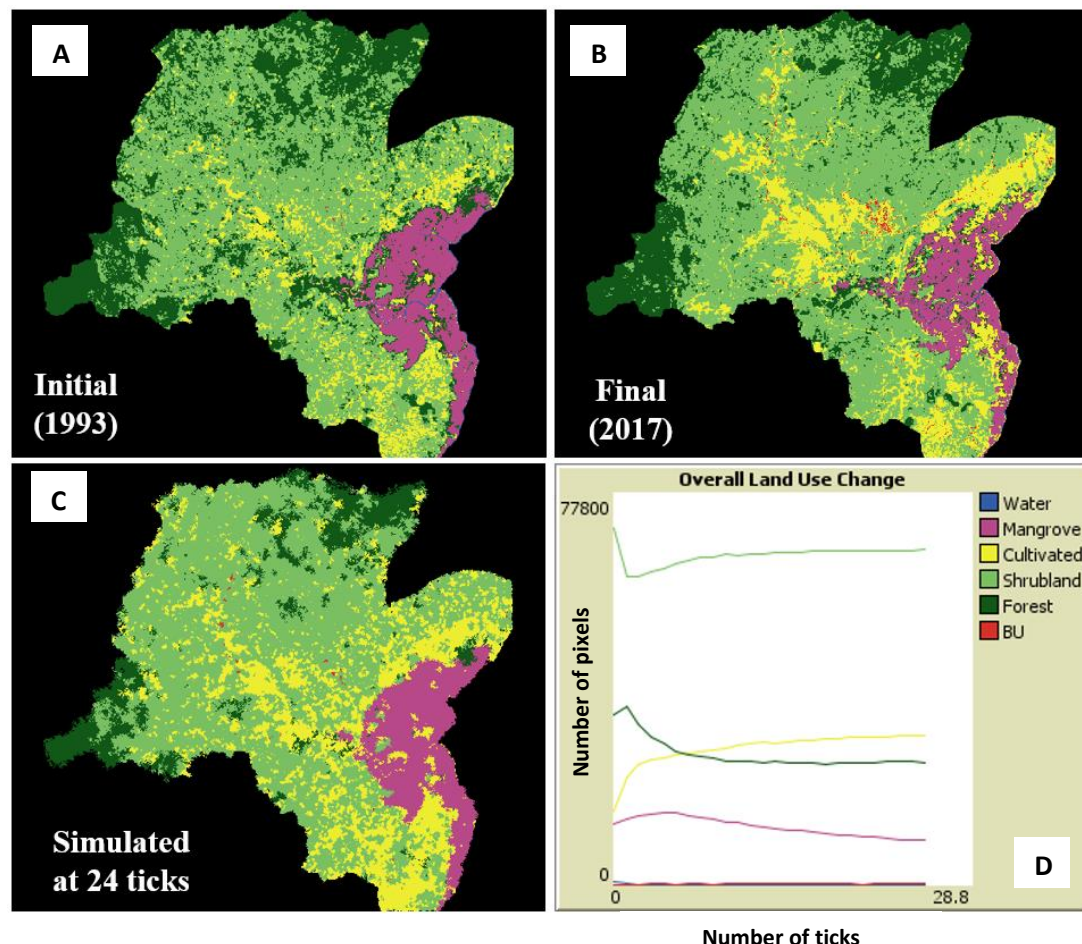


Figure 4.8 Reference images (A and B) corresponding to two different time periods (1993 and 2017). The resulting dynamic simulation model (C) and the graph (D) of land use and land cover exchange

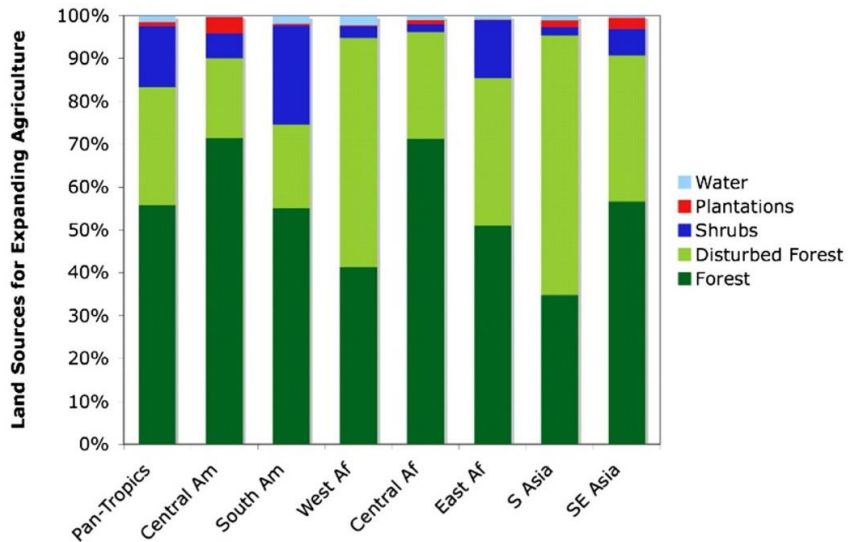


Figure 4.9 Typical land use and land cover transitions and exchange for major regions of the world (Gibbs *et al.*, 2009).

The background processes of the cellular automata implementation involve huge memory and computing resource. For each time step (ticks), individual cell of each class calculates the weighted sum of probabilities of surrounding neighbourhood cells and assigns the ‘new’ value to the central cell. The computed value is saved in the memory until all the cells/pixels have been computed. This repetitive procedure requires very heavy computing and memory resources especially when the modelled region consists of multiple classes and large area since computation is done in a simultaneously fashion. The model interface allows the user to define the number of time steps to achieve the desired ‘state’ at a given specific Markov weight as a probability matrix.

This study focused on testing *mangrove* class for multiple use case scenario modelling by raising the class matrix to a markov chain matrix multiplier. The information in Table 4.5 and Figure 4.10 lists the land transition probabilities for *mangrove* class with respect to all other class. Since the study can generate multiple Markov events (Figure 4.10), a general trend was observed wherein mangroves is projected to decrease dramatically in the future when other land use/cover are favoured within the watershed and coastal ecosystem. These dislocation, reallocation patterns are possible “what if” models/scenarios based on the previous state conditions. If in the future, innervations will be applied to alter land use and land cover dynamics which is also dependent on complex human activity, separate parameters and considerations are required to calibrate the cellular automata model. When such models integrates dynamic diverse human behavioural patterns, Agent Based Model (ABM) approach will be more appropriate. The CA-Markov model in this study can be utilized in re-creating scenarios within the Bataraza watershed especially for future conditions simulation and planning purposes on upland and coastal environments within Bataraza municipality. However, extending and expounding the applications of geosimulation on scenario-based modelling is beyond the scope of this study but would be a good to have as a recommendation for future studies.

Table 4.5 Markov chain models and resulting transition probability models for *mangrove* class allocation (in **bold**) versus all other classes within the Iwahig watershed

| Markov Chain | | | | | | | |
|---------------------|--------|---------------|------------|--------|-----------|--------|--|
| Events | Water | Mangrove | Cultivated | Built | Shrubland | Forest | |
| 1 | 0.0008 | 0.7373 | 0.1691 | 0.0000 | 0.0036 | 0.0891 | |
| 5 | 0.0010 | 0.2410 | 0.2185 | 0.0154 | 0.3999 | 0.1241 | |
| 10 | 0.0005 | 0.0804 | 0.2067 | 0.0473 | 0.5425 | 0.1225 | |
| 20 | 0.0003 | 0.0361 | 0.1906 | 0.1155 | 0.5431 | 0.1143 | |
| 40 | 0.0003 | 0.0293 | 0.1638 | 0.2396 | 0.4687 | 0.0983 | |

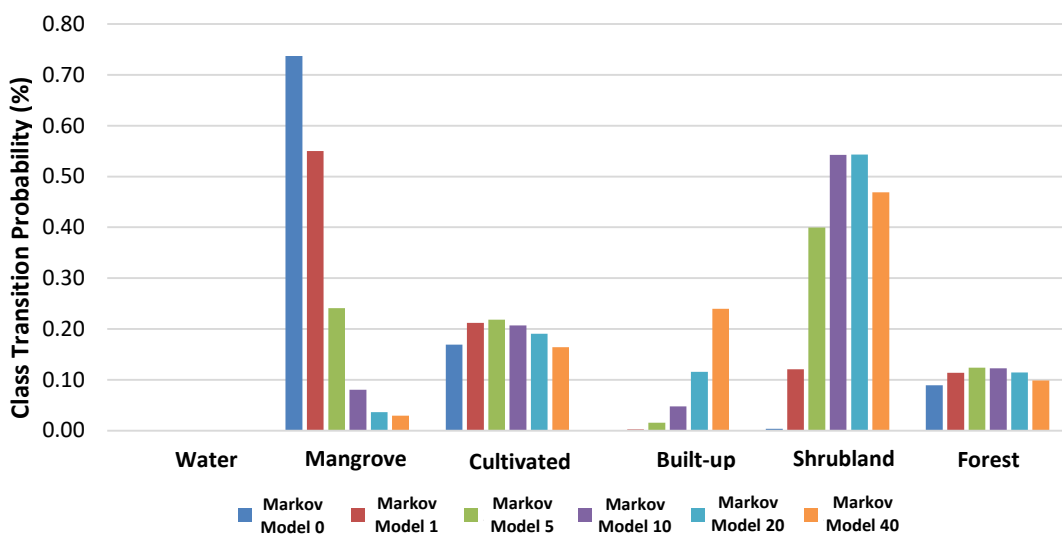


Figure 4.10 Multiple Markov chain events and corresponding projected *mangrove* class re-allocation with respect to all other classes. Model number corresponds to different Markov chain events used to exaggerate re-allocation probabilities within the watershed. Model 0 is close to 2017 condition while Model 1 to Model 40 are from ideal to worst case scenarios. All percentage values are sum total of the area of the Iwahig watershed.

Separate simulation exercises were performed for *cultivated* and *mangrove* classes. These models were designed so that user can modify the transition probability for these classes. To demonstrate the response and sensitivity of other land uses when a class probability is altered, a 15% probability of (0.15) was tested for *cultivated* class. Results showed an abrupt increase in area allocation for cultivated (and built-up) that resulted to a decrease in shrubland area (Figure 4.11 top left and top right). The same was done for *mangrove* class and results showed a significant decrease in *mangrove* where majority of the observed re-allocated class exchange was with *cultivated* area (Figure 4.11 bottom left and right).

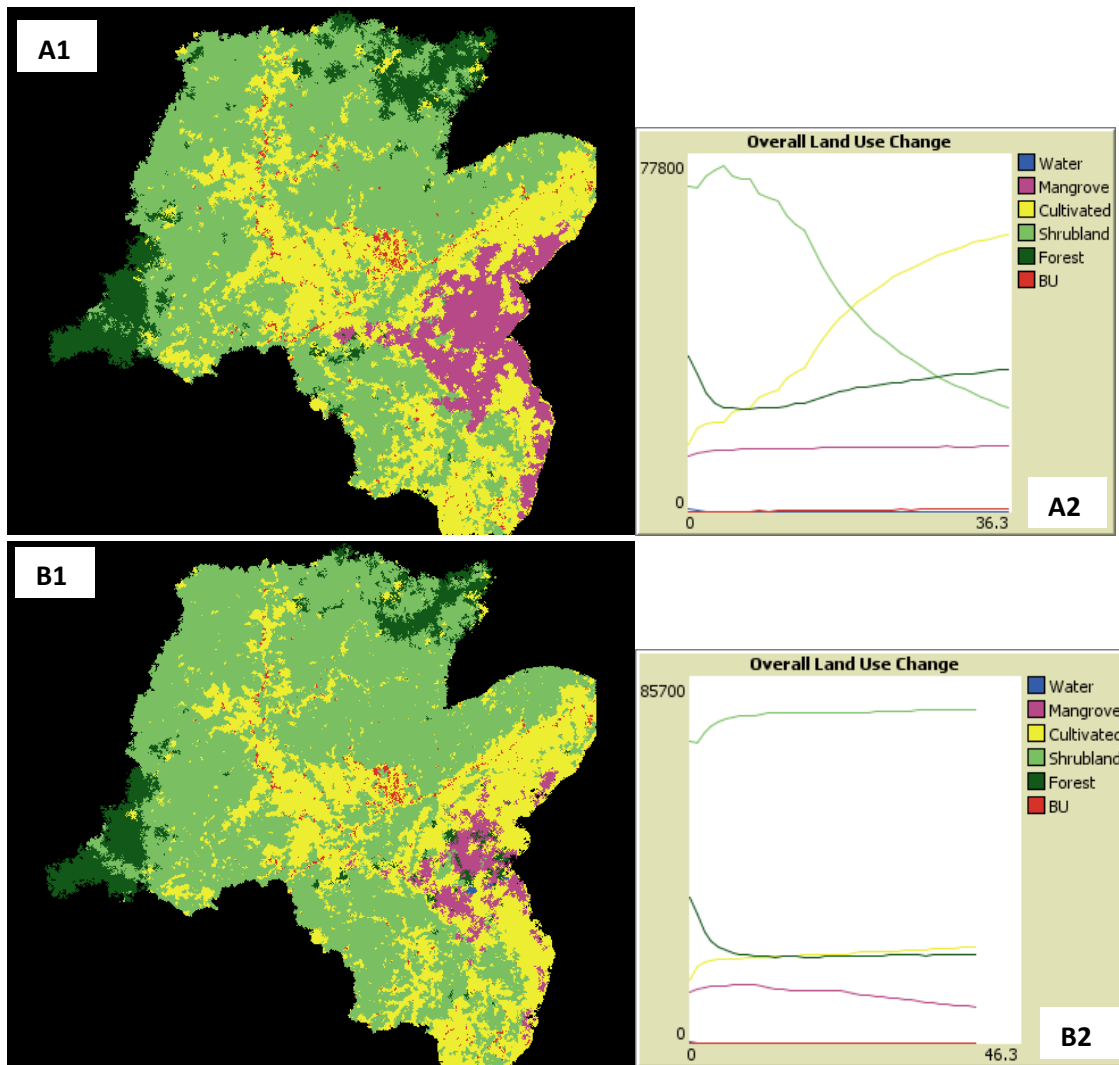


Figure 4.11 Simulated LULC by modifying *cultivated* class the probability (A1) and resulting class allocation on *built-up* class (A2) and modified *mangrove* class (B1) and resulting *mangrove* area trend (B2)

Figure 4.10 describes that Markov chain generates transition probabilities that always sums to 1. Clarke (1997) has noted that this probabilities can vary randomly,

systematically or chaotically because when the Markov matrix is increased to a large power, it forcibly generates a “static equilibrium state” and should therefore be interpreted with caution. It is therefore more reliable to use multiple set of images in developing markov models for a more reliable markov models. This is evident in graph as described in Figure 4.10 where the land use matrix was raised to a markov matrix power 40. It can be noticed that the equilibrium state (model 0 – 5) started to be “illogical” after raising the class probability matrix to 10 going to 40. The graph showed that transition probabilities of mangrove, cultivated, shrubland and forest classes decreased altogether while built up have increased abruptly which is an unusual scenario. A typical increase in built-up area usually results in an increase in cultivated area followed by degradation of forest to shrubland.

The LULC classes identified in this study were limited to 6 types. One limitation of Markov chain model is that it will not be able to capture new classes that are not present at the reference images and the model also assumes uniform transition probability rates (Kumar *et al.*, 2014). If for instance, a different land use (e.g. aquaculture) was identified in the in one of the reference image but is absent in the other, then Markov model will not be able to compute the transition probabilities and transition potential for that class. Thus, the number and type of classes must be identical for both the reference images. However, if we use Agent Based Models (ABM), this limitation

can be addressed to some degree because ABM has more flexibility of data objects in space and time because the level of data abstraction is more complex compared with that of cellular automata.

4.3.2 Simulation of mangrove mortality

This chapter discusses temporal mangrove cover changes by fragmentation analysis. The study referred to the work of Gonzales *et al.* (2015) on mangrove use survey for the entire Bataraza municipality. Gonzales' report suggested that cutting and utilization of mangroves in Bataraza municipality is preferential to *Rhizophora* species based on 600 respondents. This was supported by Walters (2005) who did a national study on mangrove utilization. Walters identified that *Rhizophora* species are the usual choice for fuel wood consumption and construction material for housing of majority of coastal communities in the Philippines that are living below poverty threshold. A time series mangrove classification was done to identify if small scale preferential cutting is one of the contributing factors to mangrove forest fragmentation in Iwahig watershed.

Temporal mangrove cover classification using moderate resolution remote sensing data revealed an increasing pattern of fragmentation of Iwahig mangrove from

1985 to 2010. Core area index which is the ratio of edge-to-interior (McGarigal, 2012) decreased from 1986 to 2015 together with the decrease in mangrove area. Perimeter area ratio (which is a measure of shape complexity) on the other hand increases with decrease in area as a result of increased number of small patches at the interior of the mangrove patch (Figure 4.12). These complex patterns of fragmentation have resulted in increased mangrove area accessibility along with urbanization in Bataraza and improved local accessibility by road.

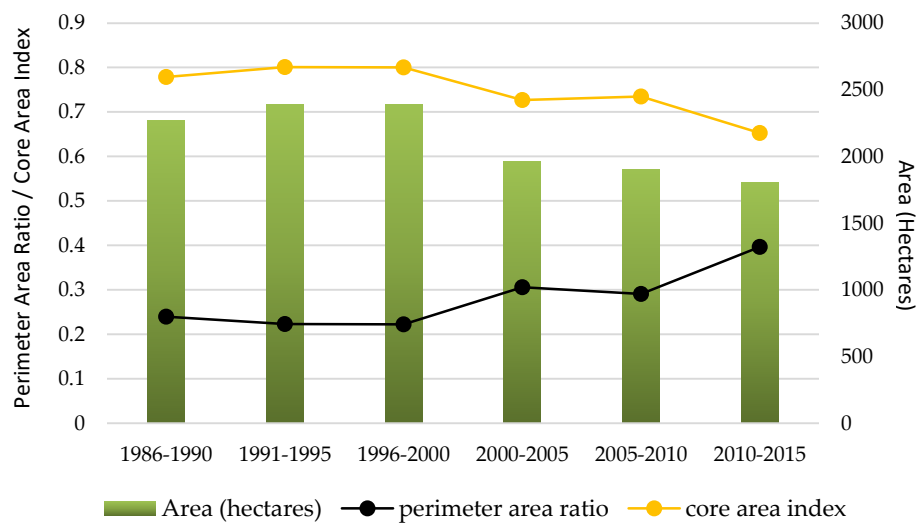


Figure 4.12 Temporal fragmentation trend of Iwahig mangrove forest from 1986 to 2015 using perimeter area ratio and core area index parameter

The resulting Principal Component Analysis (PCA) information was used to refer to the three mangrove zonation based on tidal positions. The center points of each

fragmented area/spot were assigned as ‘core’ influence where negative influence on mangrove patch increases as distance to core increased. For the simulation procedure, *core* parameter was set to an initial 150 meters radius of influence which is the computed average diameter of fragmented patches. Results showed that seaward mangroves have decreased by 1.24%, midstream mangroves by 24.8% and landward mangroves increased by 2.05% (Figure 4.13-B) after 30 iterations. These exchanges are attributed to increased area of existing fragmented mangroves and a birth of new fragmented regions for aquaculture (Figure 4.13-B). The simulation scenario in this model has enabled to create one possible future scenario of mangrove mortality based on a single parameter modification.

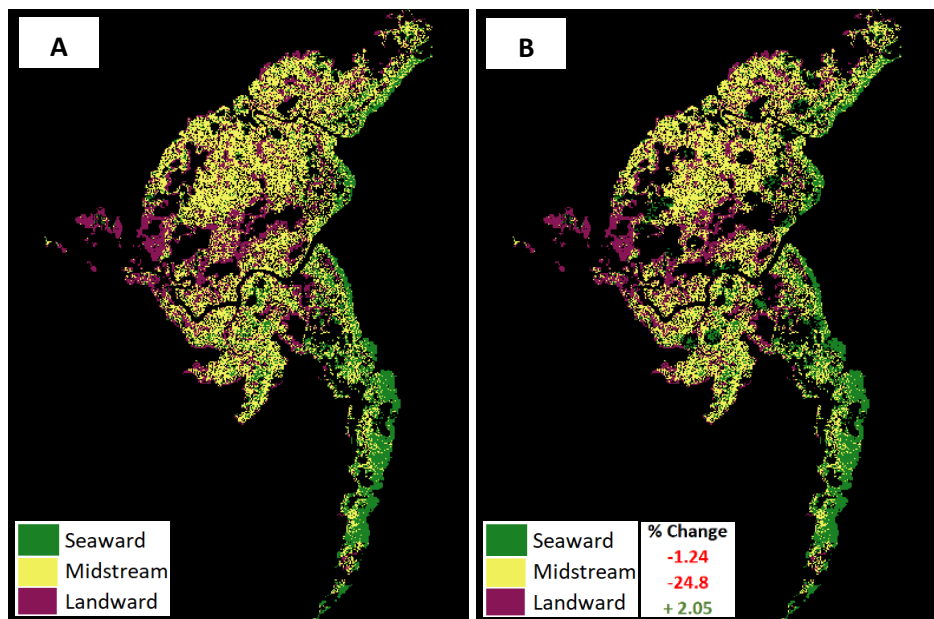


Figure 4.13 Actual (A) vs. simulated (B) mangrove fragmentation of different mangrove groups. Core distance influence used is 150 meters

High resolution Google Earth Image was used to verify the actual land use of the fragmented areas mapped in 2017 using Sentinel satellite data. Figure 4.14 illustrates that fragmented areas appeared to be ‘land preparation’ for aquaculture development. Visual inspection suggest that although these areas are not yet on its ‘operational’ stage during the time of this study, there is a high chance that these areas (Figures 4.14-A, B, C, and D) will develop into an aquaculture production if no interventions were made or the conditions were left unchanged. It is notable that after simulation, new patches are and exiting patches (fragmented area) became larger. It has been recorded that the historical trend of mangrove forest fragmentation is increasing (referring to Figure 4.12), and thus, the likelihood of the modeled future fragmentation condition (Figure 4.13-B) is high.

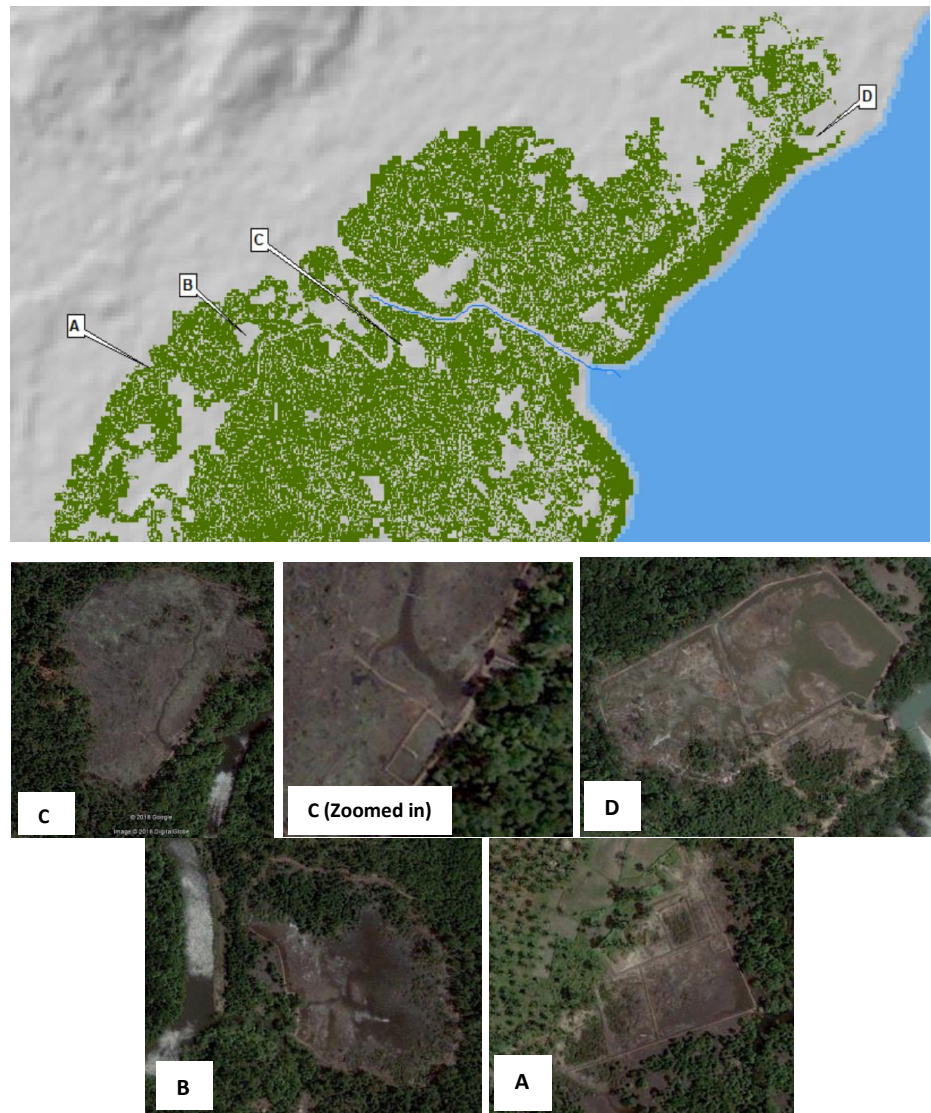


Figure 4.14 High resolution Google Earth images showing existing patches (2018) of preparatory coastal development within fragmented mangrove areas at selected mangrove locations within the study area

Bataraza municipality population has 69.7 % of its household with income below poverty threshold (PCSD INRMP 2015). The municipality alone has a 3.24 % growth

rate with projected 1.3 million population in 2020. PCSD reported that a number of Indonesian companies are leasing and buying lands further south of Palawan for oil palm and cacao plantations and this will cause drastic alteration in land use and land cover. With this scenario in place, in combination with the dynamic processes of land use and cover trasformation at the watershed scale as found in this study, environmental, climatological and social threats to mangrove will continue to affect mangroves in Bataraza, Palawan.

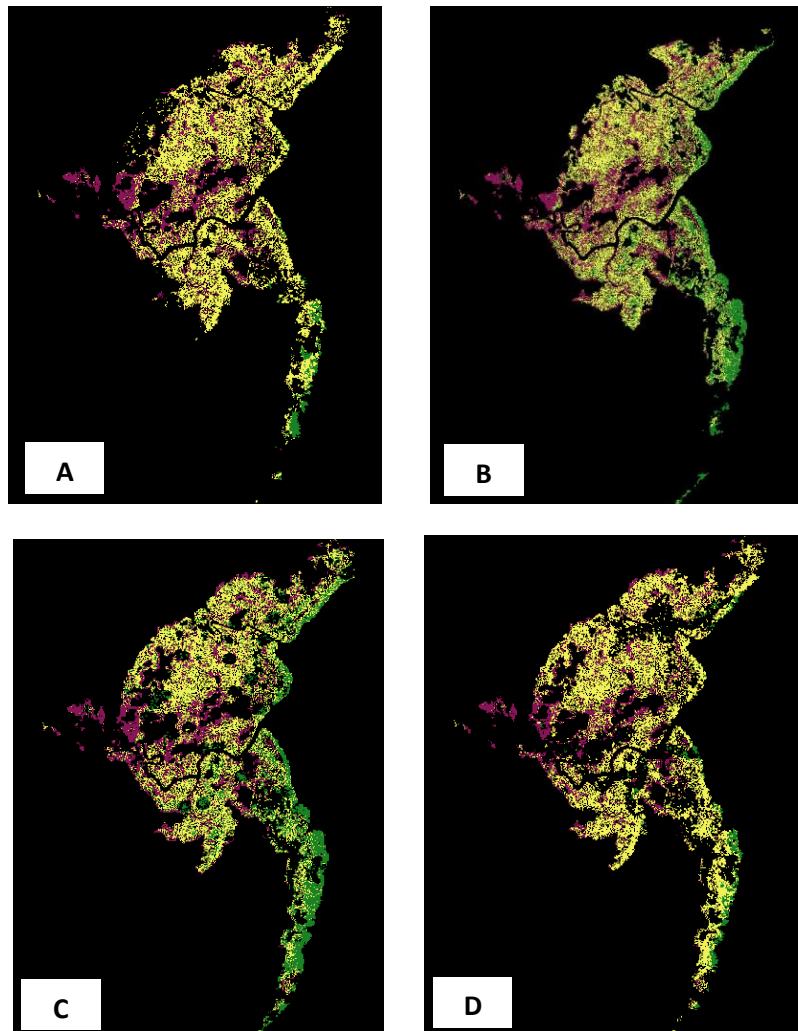


Figure 4.15 Simulated mangrove mortality scenarios with varying accessibility and proximity distances to built-up area (A), road network (B), fragmented core area (C) and river network (D).

Across the globe, mangrove species found primarily in the high intertidal and upstream estuarine zones, which often have specific freshwater requirements and patchy distributions, are the most threatened because they are often the first cleared

for development of aquaculture and agriculture (Polidoro *et al.*, 2010). Study suggest that although human interventions directly affect the mangrove species at the land edges—those established in the final successional stage, the effects of sea-level rise threatens the mangrove species at the water edges—those established in the pioneer stage. However, those mangrove species establishing in the later stages are more vulnerable to sea-level rise than are mangrove species that are established at earlier stages because the later-stage mangroves grow slower, have greater difficulty with dispersal, and reproduce slower than do the mangrove species at earlier stages, such as *Sonneratia* and *Avicennia* species (Polidoro *et al.*, 2010).

The primary threats to all mangrove species are habitat destruction and removal of mangrove areas for conversion to aquaculture, agriculture, urban and coastal development, and overexploitation. Of these, clear-felling, aquaculture and over-exploitation of fisheries in mangroves are expected to be the greatest threats to mangrove species over the next 10–15 years (Alongi, 2002). A study by Albers *et al.* (2015) suggested that floodplain restoration (close to its original state) promotes pre-conditions for mangrove rehabilitation. This ecological restoration has proved that conditions within the floodplain has been the ultimate best condition for natural mangrove recruitment. Previous works (Spalding *et al.*, 2010, Polidoro *et al.*, 2010, Primavera *et al.*, 2004, and Kjerfve, 1990) cited that middle to upper intertidal regions

of the floodplain that is not inundated 30% of the time are the best sites for planting mangroves.

The CA model can exaggerate parameter threshold to visualize how changing cell and class transition probability affects changes in mangrove zonation patterns. As an application, CA model can be used in creating and recreating scenarios to identify areas that might need interventions to prevent future problems or issues.

4.3.3 Simulation of Mangrove Gap Closure

Mangrove growth simulation was implemented with a number of assumptions. Since no field data were collected and due to time constraint in the conduct of study, individual species-based growth model is not possible. The research took inspiration on the work of Salmo & Juanico (2015) growth model for *Rhizophora mucronata*. Table 3.5 by PCSD has identified species of *Rhizophora mucronata* in the study area but individual trees were not recorded. The mangrove growth model will be implemented using the concept of Field of Neighborhood (FON) and Zone of Influence (ZOI) developed by Berger & Hildenbrandt (2000) approach which corresponds to seedling recruitment and species competition for space, light, and nutrients. Duke (2009) illustrates several stages of a general mangrove gap development. This research simulation model aims to simulate the recovery gap

recruitment, growth, and closure (Figure 4.16 image d, e and f) using various neighborhood parameters and plant densities in a cellular automata environment.

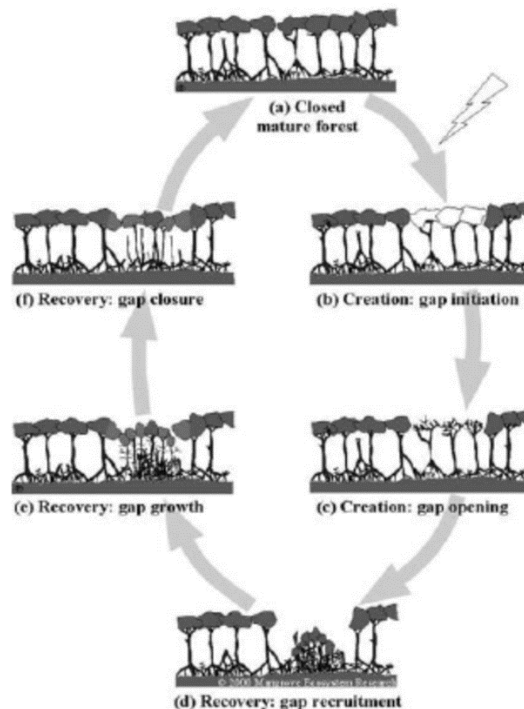


Figure 4.16 Different phases of mangrove forest light gap and recovery cycle.
Adapted from Duke, N. (2009).

There were at least ten (10) species of mangroves present in Bataraza municipality based on 2015 PCSD data. Since different species of mangrove will have varying responses to environmental stresses and conditions, the gap recruitment and closure model in this study was built on several assumptions. First, this study will use the term ‘gap’ to refer to mangrove opening and/or mangrove clearing as a result of coastal

development which are anthropogenic in nature as described in the previous section of this report (proximity-based mangrove mortality simulation). Second, species response to different condition in terms of nutrient and light requirement is assumed to be constant for all species in Iwahig watershed. Lastly, the FON and ZOI concept were used to simulate individual based species competition for space.

Available space for mangrove gap filling were modeled using the FON and ZOI developed by Berger & Hildenbrandt (2000) as implemented by Höfener, *et al.* (2009). Figure 4.17 below describes an illustration of the FOI of an individual tree as a function of the sum of neighboring FONs of surrounding trees that is in competition with itself at a given spatial distance. The greater the diameter at breast height (dbh), the larger the FON or “age dependent radius” which decreases from center of the tree outwards (Berger & Hildenbrandt (2000) as cited by Höfener, *et al.* (2009)). Zone of Influence (ZOI) concept tells us that plants with overlapping ZOI are actually neighbors. The FON increases with plant age (dbh) while the ZOI increases with closely spaced plants or trees.

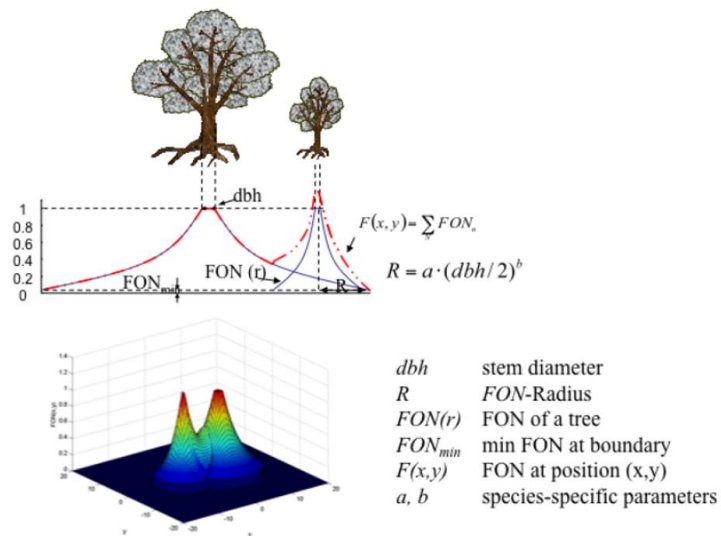


Figure 4.17 Hypothetical Field Of Neighborhood (FON) model adapted from (Höfener, *et al.*, 2009).

The cellular automata-based mangrove gap filling model implemented in this study can model several scenarios by being able to generate multiple initial trees that are distributed randomly. This random tree assignment can actually mimic a hypothetical seed dispersal or natural regeneration process in any mangrove ecosystem. Figure 4.18 shows a competition of trees at two different time scales where tree positions are randomly placed. The simulation by Höfener et. al (2009) describes different patterns of neighborhood competition using the FON and ZOI at different times.

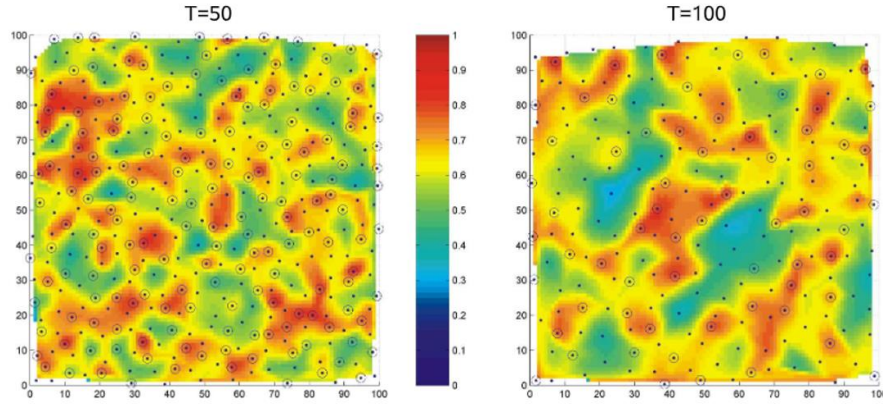


Figure 4.18 Model of mangrove tree competition adapted from Höfener *et al.* (2009) showing ZOI in red where strong plant-to-plant competition exist. Thus, the more suitable site goes from red to blue.

The cellular automata simulation carried in this exercise were also implemented in NetLogo. There were two general parameters that the user needs to set before running the simulation. First was the initial number of trees in the modelling grid. These initial trees are set randomly within the simulation area. The second parameter was the number of neighbors that each tree will search. Figure 4.19-Group A shows the initial model set-up where trees were placed randomly. Figure 4.19-Group B and Figure 4.19 Group C illustrates the mangrove growth models with FON = 36 cells and FON = 24 cells at 2000 iterations respectively. The simulation is computationally expensive because each individual cell runs a neighborhood cell search for every iteration. This means that computational requirement is exponential as more cells are considered at each iteration. Once the ZOI of each cell overlaps (at any given FON radius), the cell

will not be assigned a value because this means non-optimal condition since competition for sunlight, nutrient, and space is high. Thus, the black area in figure 4.19 represents a high ZOI. However, the FON concept is more spatially explicit model as found by Höfener *et al.* (2009).

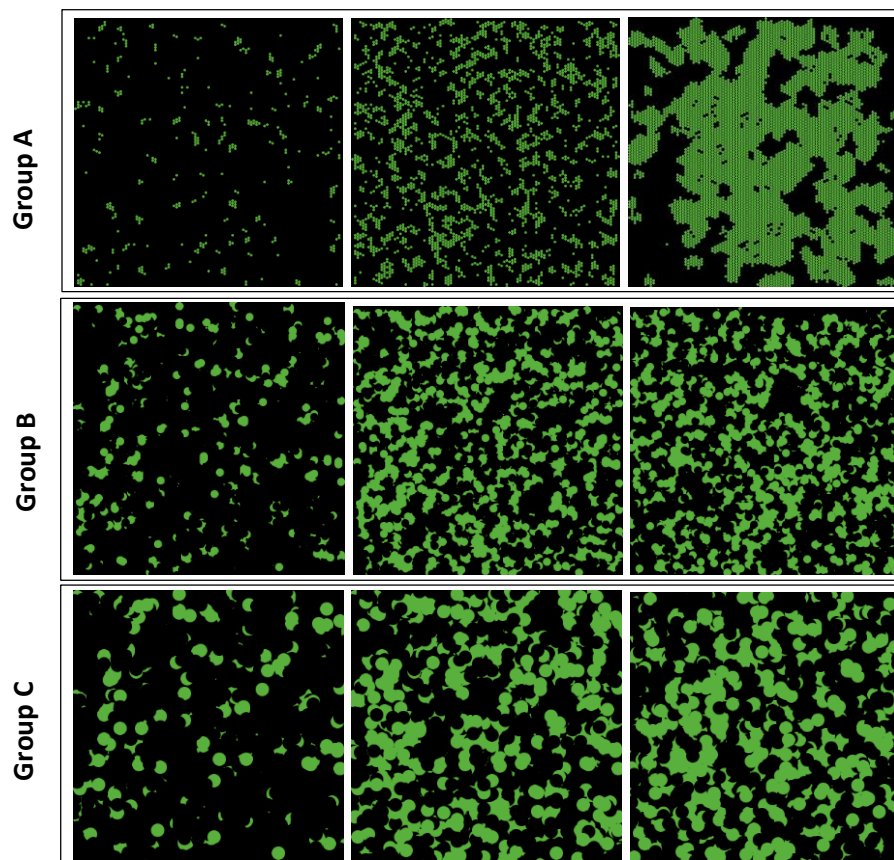


Figure 4.19 Mangrove gap filling models with fixed tree diameter configurations where tree positions are placed randomly. Group A (tree diameter @ 1 pixel), Group B (tree diameter @ 3 pixels) and Group C (tree diameter @ 5 pixels) and three iteration models (Left: 1000 iterations, Center: 2000 iterations, and Right: 3000 iterations). This model typical for an even aged forest (more or less same diameter) or plantation type. However, gap closure is static since the diameter at initial condition **does not** change or grow at every iteration.

Results showed that as the diameter of tree increases, the ZOI also increases. Since the ZOI or the competition area is higher at larger diameter trees, newly established plant will have to compete with larger trees for nutrient, space and sunlight. Simulation results showed that it is more favorable for mangrove if there are less matured trees which has large and overlapping FON. The case would be especially different with varying configurations of surrounding neighbors. If a patch is circular, the zone of influence will be exponential from the center of the patch to its boundary than if it were one sided or semi-circular (Figure 4.20). The simulation model results showed that mangrove gap filling is highly competitive at larger diameter trees where FON is high. Natural recruitment would allow understanding how these complex FON and mangrove gap filling apply in the field. It can be observed that the larger the diameter of the tree, the lesser is Zone of Influence (black region) which Höfener (2009) referred to as the competition area.

A natural forest typically is uneven aged where diameter of trees are mixed. Since the Iwahig watershed is a natural mangrove forest, a separate model was created wherein multiple tree diameter of random trees were assigned. This model (Figure 4.20-A) considers allows user to assign as many different diameter combinations and tree densities as possible which can generate thousands of dynamic and complex tree diameter and tree density combinations which can model thousands of overlapping FON scenarios. Simulation results in Figure 4.20-C showed that gap closure were

more realistic and has closed more area than non-dynamic single diameter model as seen in Figure 4.20-C. The computation time is 5 times (5X) longer because of the dynamic computation of multiple FON and overlapping ZOI at each iterations.

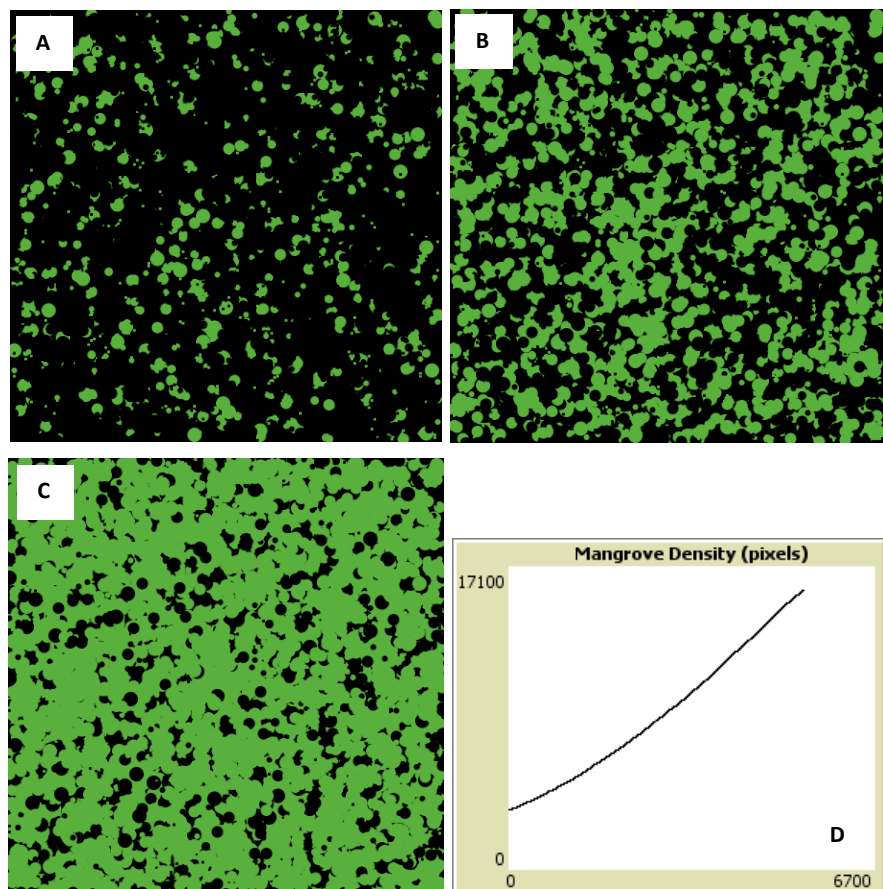


Figure 4.20 Hypothetical natural mangrove setting with mixed diameter setting. Each green dots (small, medium and large) in Figure A are individual mangrove trees. Dots that are not completely circle are overlapping in terms of diameter FON. The FON and mangrove diameter changes dynamically at each iterations which mimics the actual mangrove growth cycle. Dynamic FON and tree diameter allows incremental growth and gap closure.

While the model in Figure 4.20 better represents the Iwahig mangrove condition, the same procedure cannot be implemented in the Iwahig mangrove simulation model since the mangrove model uses a fixed cell 10 meter squared grid and cannot be dynamically set to be ‘random’ in size using Netlogo due to data format limitation. However, the same principle of FON were applied to model mangrove growth and rehabilitation as described in Figure 4.21 (B-D).

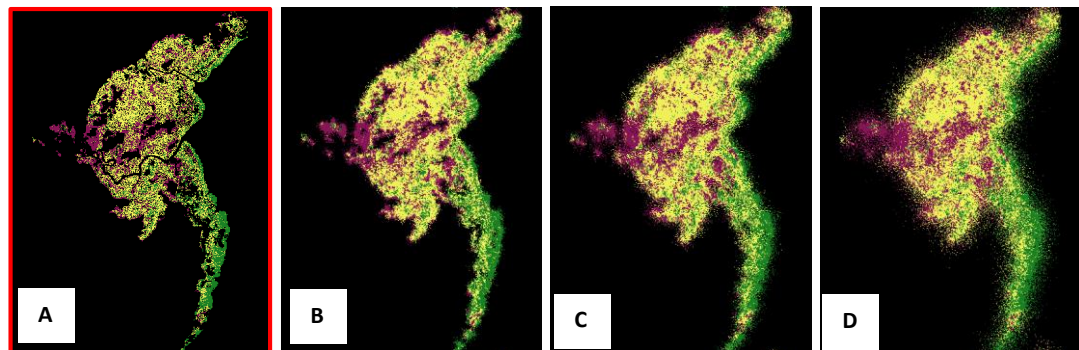


Figure 4.21 Simulated rehabilitated conditions for canopy gap closure using FON influence of 4, 8 and 16 neighbors for image B,C and D respectively. Image A is the 2017 actual mangrove condition.

At a landscape level, this study projected that more areas (upland and even lowland) will be considered for conversion from mangrove area to aquaculture, cultivated and built-up due to inevitable socio-economic pressures in the coastal resources and expanding population. As an effect, upland forest, shrubland and downstream mangrove will be re- allocated to cultivated area based on multiple

markov model scenarios. Simulation model projected that mangroves will be more fragmented due to local physical and social pressures (increasing urbanization, improved infrastructure for development, and demand for aquaculture derived products). On the contrary, simulation model for mangrove re-growth showed that fragmented and disturbed mangroves will occupy the same areas that are previously mangroves. Also, the model shows that mangrove at rehabilitated condition could potentially revert back to its original condition naturally.

4.4 Model Sensitivity

Iwahig Watershed Model

Quantity, exchange and shift metrics is a method to compare two contingency tables to derived class quantity disagreement and allocation disagreement (Pontius & Sta. Cruz 2014). Figure 43 show the illustration by Pontius and Sta. Cruz (2014) on how these parameters are measured and quantified. These metrics were used to compare the simulated and actual land use using a square contingency table comparison. It was observed that shrubland had the highest exchanged pixels with forest and cultivated class and the exchanged pixels in cultivated class are majority with shrubland. These observed self-replicating cell transitions is a very unique

characteristic of Cellular Automata. Mangrove interestingly has decreased as cultivated area increases which is actually the observed pattern in the 2017 LULC. An actual land use and land cover simulation model was generated as a result of spatial and temporal data abstraction to mimic land cover change patterns and transitions within a watershed. The total quantity, exchange and shift pixels is illustrated in Figures 4.23 and 4.24.

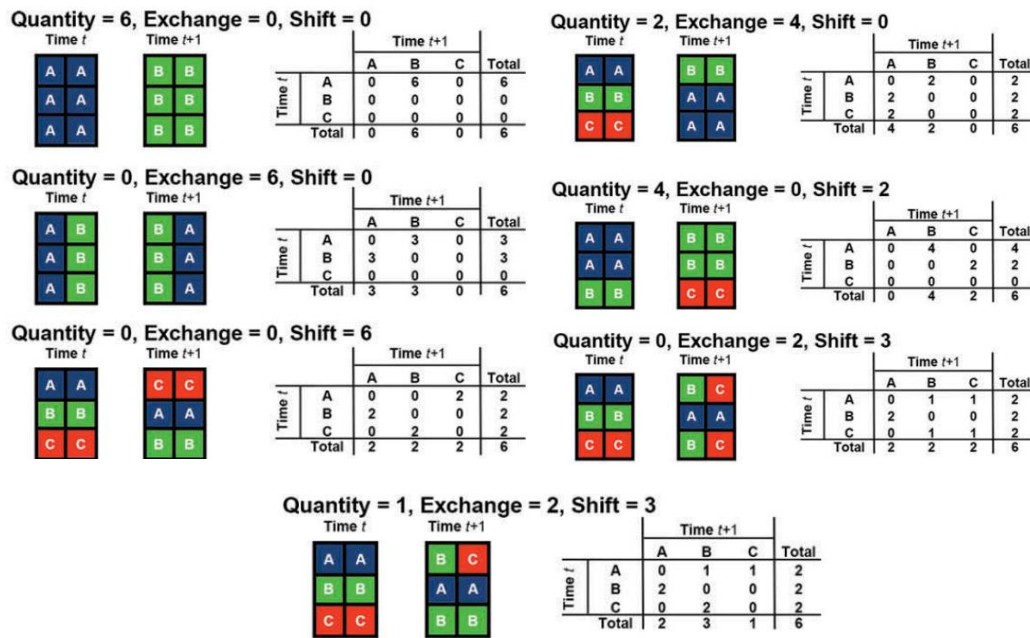


Figure 4.22 Quantity, Shift and Exchange metrics illustration by Pontius & Sta Cruz (2014). Original image from DOI: 10.1080/2150704X.2014.969814 page 7545

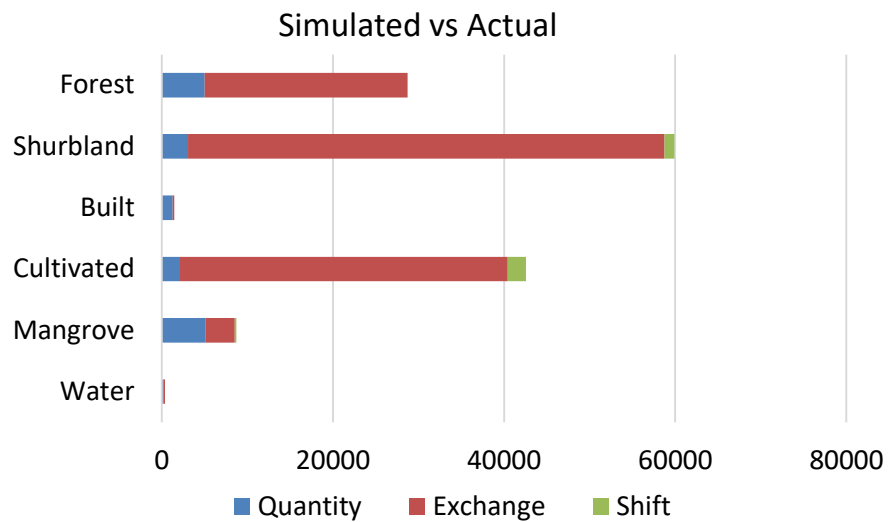


Figure 4.23 Quantity, exchange and shift contingency matrix (Pontius *et al.*, 2014) for 1993 LULC and simulated LULC after 24 iterations

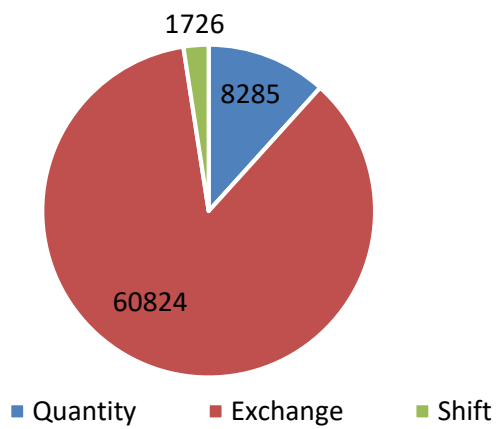


Figure 4.24 Overall Quantity, Exchange, and shift pixels from actual and simulated land use and land cover classes

5. SUMMARY AND CONCLUSIONS

Random forest regression is an effective statistical method for ecological data where the assumption of data normalization, homoskedasticity, and linearity of independent variables are usually violated. The variable importance in random forest provides a robust variable ranking which was used to find best correlation between mangrove and environmental variables. This study identified that area of tidally inundated plain, width of the main channel of a riverine mangrove, channel length, and presence of neighboring mangroves are significant conditions/settings which correlates to more than 67 percent of the variation in observed mangrove extents on a regional scale based on 30 selected parameters. The size and configuration of the watershed also plays an important role in the landscape processes including local geomorphologic setting, sedimentation, bioclimate, hydrology and land use and cover compositions which has dynamic and non linear interactions at a landscape level.

The conceptual diagram presented in this research supported and provided context in the cellular automata geosimulation model in understanding of physical processes that directly and indirectly affect land change transitions. This conceptual model provided context in the simulation process to guide the limitations in the simulation model that goes beyond the spatial and temporal bounds of the cellular automata Markov models.

This study has implemented a Cellular Automata model to simulate spatial behavior of six (6) types of land use and landcover at the watershed landscape level. Temporal dynamics of was modeled using Markov chain model to capture land use and land cover spatial allocation within the Iwahig waterhsed. These spatial and temporal data abstraction models enabled this research to explore and examine cenarios and event based models to recreate dynamical ‘what if’ conditions using simple rules. Cellular Automata and Markov chain based approach was able to produce a self-replicating land use and land cover change which produced dynamic allocations of land use and land cover. These land transition patterns derived from simplified rules were used to see how the mangrove will respond if the same pattern is observed or alteration of the pattern is introduced. The Iwahig watershed is projected to have an increase in cultivated area and expansion of built-up region. Mangrove is projected to be more fragmented at the core towards the upstream direction as urbanization and demand for agriculture and aquaculture and coastal development is inevitable. However, if there would be stricter implementation of local and regional environmental policies and more attention is put on conservation and rehabilitation, the Iwahig mangroves would recover naturally even without human intervention because mangroves will restore itself through natural recruitement process.

Finally, this study proved that combination of statistics, conceptual and contextual modelling, and spatially explicit cellular automata geosimulation are effective tools in understanding landscape and local processes on riverine mangrove ecosystems. While simulation models rely on the input and parameters that are used to understand the result, it is equally important to conduct statistical analysis to bridge the gap between model result interpretability, model parameterization, context, and data abstraction limitations..

6. RECOMMENDATIONS FOR FUTURE WORK

This study recommends the following for the improvement of this research:

- Implement a statistical regression model that considers all hydrologic classifications of mangrove (riverine, basin, fringing) to capture interactions between coastal and land processes comprehensively;
- Expand the geosimulation models developed in this study by integration of CA-ABM-Agent Based Model (ABM) that includes simulation of societal conditions influencing human behaviour toward perceptions of mangrove as a function of resource utilization; and
- Extend the mangrove growth and mortality model developed in this study in a more robust methodology in a species specific application.

REFERENCES

- Adhikari, S., Southworth, J., (2012). Simulating forest cover changes of Bannerghatta National Park based on a CA-Markov model: a remote sensing approach. *Remote Sens.* 4 (10), 3215–3243.
- Akin, A., Sunar, F., Berberoglu, S., (2015). Urban change analysis and future growth of Istanbul. *Environ. Monit. Assess.* 187 (8), p. 1–15.
- Alongi DM (2002) Present state and future of the world's mangrove forests. *Environ Conserv* 29: 331–349.
- Albers, T. & Schmitt, K. *Wetlands Ecol Manage* (2015) 23: 991.
<https://doi.org/10.1007/s11273-015-9441-3>
- Alkheder, S., Wang, J., Shan, J., (2006). May. Change detection-Cellular automata method for urban growth modeling. In *Proceedings of International Society of Photogrammetry and Remote Sensing Mid-term Symposium* (Vol. 7, p. 5).
- Allen, JA, Ewel, KC, & Jack, J (2001). Patterns of natural and anthropogenic disturbance of the mangroves on the Pacific Island of Kosrae. *Wetlands Ecology and Management* 9: 279–289, 2001
- Al-sharif, A.A., Pradhan, B., (2014). Monitoring and predicting land use change in Tripoli Metropolitan City using an integrated Markov chain and cellular automata models in GIS. *Arab. J. Geosci.* 7 (10), 4291–4301.
- Ambastha, K.R., Hussain, S.A., Badola, R. *et al.* (2010). Spatial Analysis of Anthropogenic Disturbances in Mangrove forest of Bhitarkanika Conservation Area J Indian Soc Remote Sens (2010) 38: 67
- Amir A., Duke N., (2009). A forever young ecosystem: light gap creation and turnover of subtropical mangrove forests in Moreton Bay, southeast Queensland, Australia
- Arsanjani, J.J., Kainz, W., Mousivand, A.J., (2011). Tracking dynamic land-use change using spatially explicit Markov Chain based on cellular automata: The case of Tehran. *Int. J. Image Data Fusion* 2 (4), 329–345.

- Barredo, J.I., Kasanko, M., McCormick, N., Lavalle, C., (2003). Modelling dynamic spatial processes: simulation of urban future scenarios through cellular automata. *Landsc. Urban Plan.* 64 (3), 145–160
- Berger, U. & Hildenbrandt, H., (2000) A new approach to spatially explicit modelling of forest dynamics: Spacing, ageing and neighbourhood competition of mangrove trees. *Eco-logical Modelling*, 132(3):287–302
- Bendicenti E., Di Gregorio S., Falbo F.M., Iezzi A., (2002). Simulations of forest fires by Cellular Automata modelling – in “Emergence in Complex, Cognitive, Social and Biological Systems”, pp 31-40. Kluwer Academic P.
- Blanco-Libreros, JF & Estrada-Urrea, EA. (2015) Mangroves on the Edge: Anthrome-Dependent Fragmentation Influences Ecological Condition (Turbo, Colombia, Southern Caribbean). *Diversity* 2015, 7, 206-228; doi:10.3390/d7030206
- Bone, C., Dragicevic, S., Roberts, A., (2006). A fuzzy-constrained cellular automata model of forest insect infestations. *Ecol. Model.* 192 (1), 107–125.
- Breiman, L., J. Friedman, R. Olshen, and C. Stone, (1984): Classification and regression trees. Wadsworth Books, 358.
- Breiman, Leo (2001). "Random Forests". *Machine Learning* 45 (1): 5–32. doi:10.1023/A:1010933404324
- Cabral, P.; Zamyatin, A. Markov Processes in Modeling Land Use and Land Cover Changes in Sintra-Cascais, Portugal. *Dyna* 2009, 191–198.
- Camacho, O.M.T.; Pontius, R.G., Jr.; Paegelow, M.; Mas, J.F. Comparison of simulation models in terms of quantity and allocation of land chance. *Environ. Model. Softw.* 2015, 69, 214–221.
- Chen, J., Gong, P., He, C., Luo, W., Tamura, M., Shi, P., (2002). Assessment of the urban development plan of Beijing by using a CA-based urban growth model. *Photogramm. Eng. Remote Sens.* 68 (10), 1063–1072.
- Cintron, G. & Novelli, YS. (1984) Methods for studying mangrove structure. In: Snedaker, C. and Snedaker, G. (eds) *The Mangrove Ecosystem: Research Methods*. UNESCO, Paris, France.

- Clarke, K., (2014). Cellular Automata and Agent Based Models. Handbook of Regional Science, DOI 10.1007/978-3-642-23430-9_63, # Springer-Verlag Berlin Heidelberg 2014
- Clarke, K.C., Gaydos, L.J., (1998). Loose-coupling a cellular automaton model and GIS: long-term urban growth prediction for San Francisco and Washington/Baltimore. *Int. J. Geogr. Inf. Sci.* 12 (7), 699–714.
- Couclelis, H., (1997). From cellular automata to urban models: new principles for model development and implementation. *Environ. Plan. B* 24, 165–174. Deep, S., Saklani, A., 2014. Urban sprawl modeling using cellular automata. *Egypt. J. Remote Sens. Space Sci.* 17 (2), 179–187.
- Cutler, D.R., T.C. Edwards, K.H. Beard, A. Cutler, K.T Hess, J.C. Gibson and J.J. Lawler. (2007). Random forests for classification in ecology. *Ecology* 88(11):2783-2792.
- David, L. (2010, October 29). Re: E-ZPass is a life-saver (literally) [Blog comment]. Retrieved from <http://freakonomics.com/2010/10/29/e-zpass-is-a-life-saver-literally/#comment-109178>
- De Almeida, C.M., Batty, M., Monteiro, A.M.V., Câmara, G., Soares-Filho, B.S., Cerqueira, G.C., Pennachin, C.L., (2003). Stochastic cellular automata modeling of urban land use dynamics: empirical development and estimation. *Comput. Environ. Urban Syst.* 27 (5), 481–509.
- DelSole, T. (1999). A Fundamental Limitations of Markov Models. *J. Atmospheric Sciences*. Vol. 57. pp. 2159-2169
- Department of Environment and Natural Resources. Palawan Integrated Natural Resources Management Report. (Undated)
- Duarte, C., *et al.* (1998). Relationship between sediment conditions and mangrove Rhizophora apiculata seedling growth and nutrient status. *Marine Ecology Progress Series*. Vol 175: 277-283
- Duke N., Ball M., & Ellison J., (1998) Factors influencing in mangroves biodiversity and distributional gradients. *Global Ecology and Biogeography Letters* (1998), 7, 27-47

- Duke, N. C., (1992). Mangrove floristics and biogeography, pp. 63–100. In Robertson, A. I., and Alongi, D. M. (eds.), Tropical Mangrove Ecosystems. Washington, D.C.: Coastal and Estuarine Studies Series, American Geophysical Union, 329 pp
- Duke, N.C., Lawn, P., Roelfsema, C.M., Phinn, S., Zahmel, K.N., Pedersen, D., Harris, C., Steggles , N., Tack C., (2003). Assessing historical change in coastal environments. Port Curtis, Fitzroy River Estuary and Moreton Bay regions. Final Report to the CRC for Coastal Zone Estuary & Waterway Management. Historical Coastlines Project, Marine Botany Group, Centre for Marine Studies, The University of Queensland, Brisbane. 258 pp.
- Dunca, C., Primavera J., Pettorelli N., Thompson J., Loma R., Koldewey H., (2016). Rehabilitating mangrove ecosystem services: A case study on the relative benefits of abandoned pond reversion from Panay Island, Philippines. *Marine Pollution Bulletin*. <http://dx.doi.org/10.1016/j.marpolbul.2016.05.049>
- Eslami-Andargoli L., Dale P., Sipe N. & Chaseling J. (2010) Local and watershed effects on spatial patterns of mangrove forest during wetter and drier periods: Moreton Bay,Southeast Queensland, Australia.
- Evans, J., Murphy, M., Holden Z., Cushman S., (2011). Modeling Species Distribution and Change Using Random Forest. pp-143. C.A. Drew *et al.* (eds.), Predictive Species and Habitat Modeling in Watershed Ecology: 139 Concepts and Applications, DOI 10.1007/978-1-4419-7390-0_8, © Springer Science+Business Media, LLC 2011
- FAO, (2007) The World's Mangroves 1980–2005, FAO Forestry Paper 153. Rome: Forest Resources Division, FAO, 77 pp.
- Fick, S.E. and R.J. Hijmans, (2017). Worldclim 2: New 1-km spatial resolution climate surfaces for global land areas. *International Journal of Climatology*
- Garcia K., Malabriga P., Gevaña D. (2014) Philippines' Mangrove Ecosystem: Status, Threats and Conservation. In: Faridah-Hanum I., Latiff A., Hakeem K., Ozturk M. (eds) *Mangrove Ecosystems of Asia*. Springer, New York, NY
- Ghosh, P., et al. (2017) Application of Cellular automata and Markov-chain model in geospatial environmental modeling – A review. *Remote Sensing Applications: Society and Environment*. 64-77

- Gilman, E., Ellison, J., Coleman, R., (2007). Assessment of mangrove response to projected relative sea-level rise and recent historical reconstruction of shoreline position. *Environmental Monitoring and Assessment* 124, pp. 105130.
- Gilman, E.L., Ellison, J., Duke, N.C., Field, C., (2007). Threats to mangroves from climate change and adaptation options. *Aquat. Bot.* (2008). doi 10.1016/j.aquabot.2007.12.009
- GIZ (2016), Integrated Coastal Protection and Mangrove Belt Rehabilitation in the Mekong Delta. Pre-feasibility Study for investments in coastal protection along 480 kilometers in the Mekong Delta
- Glenn, D.C.; Lewin, R.K.; Peet, T.T.V. Plant Succession: Theory and Prediction; Chapman & Hall: London, UK, (1992). 35. Hu, Z.; Lo, C. Modeling urban growth in Atlanta using logistic regression. *Comput. Environ. Urban Syst.* 2007, 31, 667–688.
- Gong, W., Yuan, L., Fan, W., Stott, P., (2015). Analysis and simulation of land use spatial pattern in Harbin prefecture based on trajectories and cellular automata—Markov modelling. *Int. J. Appl. Earth Obs. Geoinf.* 34, 207–216.
- Gonzales, Benjamin & Ria, Syamsuriati & S. Montaño, Bernaldo. (2017). Social benefits and impacts of mangrove resource utilization in Rio Tuba. *Advances in Environmental Science BIOFLUX.* 9.
- Gorelick, N., Hancher, M., Dixon, M., Ilyushchenko, S., Thau, D., & Moore, R. (2017). Google Earth Engine: Planetary-scale geospatial analysis for everyone. *Remote Sensing of Environment.*
- Guan, D., Li, H., Inohae, T., Su, W., Nagaie, T., Hokao, K., (2011). Modeling urban land use change by the integration of cellular automaton and Markov model. *Ecol. Model.* 222 (20), 3761–3772.
- Halmy, M.W.A., Gessler, P.E., Hicke, J.A., Salem, B.B., 2015. Land use/land cover change detection and prediction in the north-western coastal desert of Egypt using Markov-CA. *Appl. Geogr.* 63, 101–112.
- Hamilton S., & Casey D. (2016) Creation of a high spatio-temporal resolution global database of continuous mangrove forest cover for the 21st century (CGMFC-21). *Global Ecology and Biogeography, (Global Ecol. Biogeogr.)* (2016) 25, 729-738. John Wiley and Sons Ltd

- He, C., Okada, N., Zhang, Q., Shi, P., Li, J., (2008). Modelling dynamic urban expansion processes incorporating a potential model with cellular automata. *Landsc. Urban Plan.* 86 (1), 79–91.
- Hegde, NP *et al.* Study of cellular automata models for urban growth. *GIS Development, Map World Forum*
- Höfener, J., Rudolf, L., Berger, U., Gross T., Coarase graining of individual-based plant model. *Informatik 2009: Im Focus das Leben, Beiträge der 39. Jahrestagung der Gesellschaft für Informatik e.V. (GI), 28.9.-2.10.2009, Lübeck, Proceedings*
- Ho, T. (1995). Random decision forests. *Document Analysis and Recognition. 3rd International Conference on Document Analysis and Recognition.* IEEE. 10.1109/ICDAR.1995.598994
- Hogarth, P. J., (1999). *The Biology of Mangroves.* Oxford, New York: Oxford University Press
- Hollings T, Robinson A, van Andel M, Jewell C, Burgman M (2017) Species distribution models: A comparison of statistical approaches for livestock and disease epidemics. *PLoS ONE* 12(8): e0183626. <https://doi.org/10.1371/journal.pone.0183626>
- https://www.wildernesscommittee.org/sites/all/files/publications/Republic_20Act_207611_20IRR.pdf
- Huang, J., Wu, Y., Gao, T., Zhan, Y., Cui, W., (2015). An integrated approach based on Markov chain and cellular automata to simulation of urban land use changes. *Appl. Math.* 9 (2), 769–775.
- JH Primavera, WG Yap, JP Savaris, RJA Loma, ADE Moscoso, JD Coching, CL Montilijao, RP Poingan, ID Tayo (2013). Manual on Mangrove Reversion of Abandoned and Illegal Brackishwater Fishponds – Mangrove Manual Series No. 2. London, UK: ZSL. xii + 108 p.
- Kamusoko C, & Gamba J, (2015). Simulating Urban Growth using Random Forest-Cellular Automata (RF-CA) Model. *ISPRS Int. J. Geo-Inf.* 2015, 4, 447-470; doi: 10.3390/ijgi4020447

- Kamusoko, C., Aniya, M., Adi, B., Manjoro, M., (2009). Rural sustainability under threat in Zimbabwe—Simulation of future land use/cover changes in the Bindura district based on the Markov-cellular automata model. *Appl. Geogr.* 29 (3), 435–447.
- Karafyllidis, I., Thanailakis, A., (1997). A model for predicting forest fire spreading using cellular automata. *Ecol. Model.* 99 (1), 87–97.
- Kari J., (2005). Theory of Cellular Automata: A survey. *Theoretical Computer Science* 334 (2005) doi:10.1016/j.tcs.2004.11.021
- Kumar, S., Radhakrishnan, N., & Mathew, S., (2014) Land use change modelling using a Markov model and remote sensing, *Geomatics, Natural Hazards and Risk*, 5:2, 145-156, DOI: 10.1080/19475705.2013.795502
- Lepš, J. Mathematical modelling of ecological succession—A review. *Folia Geobot. Phytotax.* 1988, 23, 79–94.
- Liaw, Andy & Wiener, Matthew. (2001). Classification and Regression by Random forest. *Forest.* 23. Vol 2/3 ISSN 1609-3631
- Liu, Y. Modelling Urban Development with Geographical Information Systems and Cellular Automata; Taylor & Francis Group: New York, NY, USA, 2009; p. 177.
- Liu, Y., Phinn, S.R., 2003. Modelling urban development with cellular automata incorporating fuzzy-set approaches. *Comput. Environ. Urban Syst.* 27 (6), 637–658.
- Long J., Napton D., Giri C., Graesser J., (2013). A mapping and monitoring assessment of the Philippines' mangrove forests from 1990 to 2010. *J. Coastal Research.* DOI. 10.112/JCOASTRES-D-13.00057.1
- Long, J. B., & Giri, C. (2011). Mapping the Philippines' Mangrove Forests Using Landsat Imagery. *Sensors* (Basel, Switzerland), 11(3), 2972–2981. <http://doi.org/10.3390/s110302972>
- Louppe, G & W, Louis & Sutera, Antonio & Geurts, Pierre. (2013). Understanding variable importances in forests of randomized trees. *Advances in Neural Information Processing Systems* 26. ed., C. J. C. Burges and L. Bottou and M.

Welling and Z. Ghahramani and K. Q. Weinberger. pg 431-439., Curran Associates, Inc.

Lovelock, C.E., Ball, M.C., Martin, K.C., Feller, I.C., (2009). Nutrient enrichment increases mortality of mangroves. PLoS ONE 4, e5600.

Marceau, D., and Beneson, I., (2011). Challenges and Perspectives in Geosimulation. Advanced Geosimulation Models. 2011, 3-13

Masek, J.G., E.F. Vermote, N. Saleous, R. Wolfe, F.G. Hall, F. Huemmrich, F. Gao, J. Kutler, and T.K. Lim. (2013). LEDAPS Calibration, Reflectance, Atmospheric Correction Preprocessing Code, Version 2. ORNL DAAC, Oak Ridge, Tennessee, USA. <http://dx.doi.org/10.3334/ORNLDAA/1146>

Mazda Y., Wolanski E., Ridd PV (2007) Part I. Outline of the physical processes within mangrove systems. In: Mazda Y., Wolanski E., Ridd PV (eds) The role of physical processes in mangrove environments: manual for the preservation and utilization of mangrove ecosystems. Terrapub Publishers, Tokyo, pp 3-64

McGarigal, K., SA Cushman, and E Ene. (2012). FRAGSTATS v4: Spatial Pattern Analysis Program for Categorical and Continuous Maps. Computer software program produced by the authors at the University of Massachusetts, Amherst. Available at the following web site: <http://www.umass.edu/landeco/research/fragstats/fragstats.html>

McKee, K.L., Cahoon, D.R., Feller, I.C., (2007). Caribbean mangroves adjust to rising sea level through biotic controls on change in soil elevation. Global Ecology and Biogeography 16, pp. 545-556.

Memarian, H., Balasundram, S.K., Talib, J.B., Sung, C.T., Sood, A.M., Abbaspour, K., (2012). Validation of CA-Markov for simulation of land use and cover change in the Langat Basin, Malaysia.

Miller HJ (2009) Geocomputation. In: Fotheringham AS, Rogerson PA (eds) The SAGE handbook of spatial analysis. Sage, London

Mubea, K., Goetzke, R., Menz, G., (2014). Applying cellular automata for simulating and assessing urban growth scenario based in Nairobi, Kenya. Int. J. Adv. Comput. Sci. Appl. 5 (2), 1–13.

- Nadoushan, M.A., Soffianian, A., Alebrahim, A., (2015). Modeling Land Use/Cover Changes by the Combination of Markov Chain and Cellular Automata Markov (CAMarkov) Models. *J. Earth Environ. Health Sci.* 1 (1), 16.
- Opperman J., Lohse K., Brooks C., Kelly N. & Merenlender A. (2005) Influence of land use on fine sediment in salmonid spawning gravels within the Russian River Basin, California. *Can.J.Fish.Aquat.Sci.* 62, 2740–51.
- Palis, H.G., S.A. Pascolan and C.I. Villamor, (eds.). (2014). Proceedings of the 1st ASEAN Congress on Mangrove Research and Development, 3-7 December 2012, Manila, Philippines. Department of Environment and Natural Resources - Ecosystems Research and Development Bureau (DENR-ERDB), Philippines
- Pan, Y., Roth, A., Yu, Z., Doluschitz, R., (2010). The impact of variation in scale on the behavior of a cellular automata used for land use change modeling. *Comput. Environ. Urban Syst.* 34 (5), 400–408.
- PCSDS. (2015). Palawan Biosphere Reserve, Progress Report
- PCSDS. (2012): Coastal Resource Monitoring : Municipality of Bataraza, Province of Palawan. Palawan Council for Sustainable Development Staff. Puerto Princesa City, Philippines.
- PCSDS. (2005). The State of the Environment (2004), Province of Palawan, Philippines. Palawan Council for Sustainable Development, Puerto Princesa City, Philippines.
- Polidoro BA, Carpenter KE, Collins L, Duke NC, Ellison AM, *et al.* (2010) The Loss of Species: Mangrove Extinction Risk and Geographic Areas of Global Concern+B94n. *PLoS ONE* 5(4): e10095. doi:10.1371/journal.pone.0010095
- Pontius R. & Santacruz A., (2014). Quantity, exchange, and shift components of difference in a square contingency table. *International Journal of Remote Sensing.* Vol 35. No. 21. Pp 7543-7554. Taylor & Francis. Doi: 10.1080/2150704X.2014.969814
- Primavera J., & Esteban J., (2008) Review of mangrove rehabilitation in the Philippines: successes, failures and future prospects. *Wetlands Ecological Management.* DOI 10.1007/s11273-008-9101-y

Primavera J., (2000). Development and conservation of Philippine mangroves: institutional issues Ecological Economics 35 (2000) 91–106

Primavera, JH, Yap,WG., Savaris, JP., Loma, RJA., Moscoso, ADE., Coching, JD., Montilijao, CL, Poongan, RP., Tayo, ID., (2013). Manual on Mangrove Reversion of Abandoned and Illegal Brackishwater Fishponds – Mangrove Manual Series No. 2. London, UK: ZSL. xii + 108 p.

Proclamation No. 2152, series of (1981). Declaring the entire province of Palawan and certain parcels of the public domain and/or parts of the country as mangrove swamp forest reserves. Available at: <http://www.gov.ph/1981/12/29/proclamation-no-2152-s-1981>

Protected Areas and Wildlife Bureau—Department of Environment and Natural Resources. (2013). The National Wetlands Action Plan for the Philippines 2011-2016

R Core Team (2013). R: A language and environment for statistical computing. R Foundation for Statistical Computing, Vienna, Austria. URL <http://www.R-project.org/>.

Record, Sydne, N. D. Charney, R. M. Zakaria, and Aaron M. Ellison. (2013). “Projecting Global Mangrove Species and Community Distributions under Climate Change.” Ecosphere 4 (3) (March): art34. doi:10.1890/es12-00296.1. <http://dx.doi.org/10.1890/ES12-00296.1>.

Richmond, R., Rongo, T., Golbuu, Y., Victor, S., Idechong, N., Davis, G., Kostka, W., Neth, L., Hamnett, M., Wolanski, E., (2007) Watersheds and Coral Reefs: Conservation Science, Policy, and Implementation, BioScience, Volume 57, Issue 7, Pages 598–607, <https://doi.org/10.1641/B570710>

Rogers, K., Wilton, K.M., Saintilan, N., (2006). Vegetation change and surface elevation dynamics in estuarine wetlands of southeast Australia. Estuarine Coastal and Shelf Science 66, pp. 559-569.

Saenger, P., (2002). Mangrove Ecology, Silviculture and Conservation. Dordrecht: Kluwer Academic Publishers, 360 pp.

Salmo, S., Torio, D., & Esteban, JM., (2007). Evaluation of Rehabilitation Strategies and Management Schemes for the Improvement of Mangrove

Management Programs in Lingayen Gulf. Science Diliman (January-June 2007) 19:1, 24-34

Salmo S., & Juanico, D. (2015). An individual-based model of long-term forest growth and carbon sequestration in planted mangroves under salinity and inundation stresses. International Journal of Philippine Science and Technology, Vol. 08, No. 2, 2015

Sang, L., Zhang, C., Yang, J., Zhu, D., Yun, W., (2011). Simulation of land use spatial pattern of towns and villages based on CA-Markov model. Math. Comput. Model. 54 (3), 938–943.

Santibanez S.F., Kloft M.,and Lakes T., (2015). Performance Analysis of Machine Learning Algorithms for Regression of Spatial Variables. A Case Study in the Real Estate Industry. Geocomputations

Selvam V., & Karunagaran VN., (2017), Ecology and Biology of Mangroves

Semeniuk, V., (1994). Predicting the effect of sea-level rise on mangroves in north western Australia. Journal of Coastal Research 10, pp. 1050-1076.

Seto,K., & Fragkias, M. (2007). Mangrove conversion and aquaculture development in Vietnam: A remote sensing- based approach for evaluating the Ramsar Convention on Wetlands. Global Environmental Change 17 (2007) 486–500

Siemerink.M. (August 2011). Coastal Development through mangrove creek watersheds. p.20

Snedaker S. C. (1995) Mangroves and climate-change in the Florida and Caribbean region – scenarios and hypotheses. Hydrobiologia 295, 43–9

Spalding M, Blasco F and Field C (eds). (1997). World Mangrove Atlas. International Society for Mangrove Ecosystems, Okinawa, 178 p

Strayer D., Beighley R., Thompson L. *et al.* (2003) Effects of land cover on stream ecosystems: roles of empirical models and scaling issues. Ecosystems 6, 407–23.

- Thomas Houet, Laurence Hubert-Moy. Modeling and projecting land-use and land-cover changes with Cellular Automaton in considering landscape trajectories: An improvement for simulation of plausible future states. EARSeL eProceedings, European Association of Remote Sensing Laboratories, 2006, 5 (1), pp.63-76.
- Tomlinson, P. B., (1986). The Botany of Mangroves. Cambridge: Cambridge University Press, 413 pp.
- Tran, L. Fischer, A., (2017). Spatiotemporal Spatiotemporal changes and fragmentation of mangroves and its effects on fish diversity in Ca Mau Province (Vietnam). Journal of Coastal Conservation. DOI: 10.1007/s11852-017-0513-9
- Truong, S.H.; Ye, Q., and Stive, M.J.F., (2017). Estuarine mangrove squeeze in the Mekong Delta, Vietnam. Journal of Coastal Research, 33(4), 747–763. Coconut Creek (Florida), ISSN 0749-0208.
- Valiela, I., Bartholomew, M., Giblin, A. *et al.* Watershed Deforestation and Down-Estuary Transformations Alter Sources, Transport, and Export of Suspended Particles in Panamanian Mangrove Estuaries. Ecosystems (2014) 17: 96. <https://doi.org/10.1007/s10021-013-9709-5>
- Vazquez-Quintero, G. *et al.* (2016). Detection and Projection of Forest change by using the Markov Chain model and Cellular Automata. Sustainability 2016, 8, 236: doi:10.3390/su8030236
- Walsh ES, Kreakie BJ, Cantwell MG, Nacci D (2017) A Random Forest approach to predict the spatial distribution of sediment pollution in an estuarine system. PLOS ONE 12(7): e0179473. <https://doi.org/10.1371/journal.pone.0179473>
- Walters B, (2005). Patterns of local wood use and cutting of Philippine Mangrove Forests. Econ Bot (2005) 59: 66. [https://doi.org/10.1663/0013-0001\(2005\)059\[0066:POLWUA\]2.0.CO;2](https://doi.org/10.1663/0013-0001(2005)059[0066:POLWUA]2.0.CO;2)
- Walters B.,(2005) Ecological effects of small-scale cutting of Philippine mangrove forests. Forest Ecology and Management 206 (2005). 331-348

- Wilensky, U. & Stroup, W., (1999). HubNet. <http://ccl.northwestern.edu/netlogo/hubnet.html>. Center for Connected Learning and Computer-Based Modeling, Northwestern University. Evanston, IL.
- Wilensky, U. (1999). NetLogo. <http://ccl.northwestern.edu/netlogo/>. Center for Connected Learning and Computer-Based Modeling, Northwestern University. Evanston, IL.
- Woodroffe CD. 1992. Mangrove sediments and geomorphology. In Tropical Mangrove Ecosystems, ed. AI Robertson, DM Alongi, pp. 7–41. Washington, DC: Am. Geophys. Union
- Yang, X., Zheng, X.Q., Chen, R., (2014). A land use change model: Integrating watershed pattern indexes and Markov-CA. *Ecol. Model.* 283, 1–7.
- Yang, X.; Zheng, X.-Q.; Lv, L.N. A spatiotemporal model of land use change based on ant colony optimization, Markov chain and cellular automata. *Ecol. Model.* 2012, 233, 11–19.
- Yeh, A.G.O., Li, X., (2002). A cellular automata model to simulate development density for urban planning. *Environ. Plan. B* 29 (3), 431–450.
- Yimnang Golbuu, Eric Wolanski, Peter Harrison, Robert H. Richmond, Steven Victor, and Katharina E. Fabricius, (2011). Effects of Land-Use Change on Characteristics and Dynamics of Watershed Discharges in Babeldaob, Palau, Micronesia. *Journal of Marine Biology*, vol. 2011, Article ID 981273, 17 pages, 2011. doi:10.1155/2011/981273
- Zhao, Y. & Murayama, Y. A New Model to Model Neighborhood Interaction in Cellular Automata-Based Urban Geosimulation. *ICCS 2007, Part II, LNCS 4488*, pp. 550–557, 2007

APPENDICES

Appendix 1

Random Forest Regression (Coded in R)

```

library("caret")
library("randomForest")
library("pls")
library("party")
library("spdep")
library("corrplot")
library("ggplot2")
library("parallel")
library("dplyr")
library("RColorBrewer")
library("rfUtilities")
library("VSURF")

set.seed(123)
rm(list=ls())
setwd("D:/Data/")
filename = "table.txt"
data <- read.delim(filename, header = TRUE, sep = "\t")
form = Y ~ .
names(data)

#Correlation Plots
corrplot(cor(data),order = "hclust")

#Random forest control parameters
set.seed(123)
control <- trainControl(method='repeatedcv',number=10,repeats=10)
mtry <- sqrt(ncol(data))

#RandomForest Implementation
RF <- train(form,data=data,
            method = "rf",trControl=control,
            importance = TRUE, ntree = 1000)
plot(varImp(RF, useModel = TRUE), top=15)
RF
RF$finalModel
RF$results

#Random Forest with cross validation
RF2 <- randomForest(form,data=data, method = "rf",trControl=control,
                     importance = TRUE, ntree = 1000)
RF2
a <- rf.crossValidation(RF2, data, p = 0.1, n = 99, seed = NULL,
                        normalize = TRUE)
a
plot(RF2, type = "cv", stat = "producers.accuracy")
plot(RF2, imp = "sel")
rf.class.sensitivity(RF2, data, d = "1", p = 0.05, nperm = 999,
                      plot = TRUE, seed = NULL)

## Variable Selection Using Random Forest - VSURF
vsurf <- VSURF(form,data=data, mtry = 100, parallel = TRUE,
                ncores = 1, clusterType = "FORK")

```

Appendix 2

Land Use and Land Cover Change Comparison (Coded in R)

```

rm(list=ls())
gc(TRUE)
library(diffeR)
library(composite)
library(raster)
library(ggplot2)
library(vcd)
ref <- raster("D:/Data/final.tif")
comp <- raster("D:/Data/initial.tif")
composite(comp, ref, factor=2)
a<-crosstabm(comp, ref, percent=FALSE)
a
memb.ref <- memberships(comp, fact=2)
plot(memb.ref)
plot(comp)
plot(ref)
barplot(comp)

#Plots results
ctmatCompRef <- crosstabm(comp, ref)
diffTablej(ctmatCompRef)
overallAllocD(ctmatCompRef) #calculates overall allocation disagreement
overallDiff(ctmatCompRef) #calculates overall difference between from a square contingency table
overallDiffCatj(ctmatCompRef) #calculates overall difference at the category level from a square
contingency table
overallExchangeD(ctmatCompRef) #calculates overall exchange difference from a square contingency
table
overallQtyD(ctmatCompRef) #calculates overall quantity disagreement
overallShiftD(ctmatCompRef) #calculates overall shift difference from a square contingency table
quantityDj(ctmatCompRef) #calculates quantity difference at the category level from a square
contingency table
differenceMR(comp, ref, eval="original") #calculates difference metrics between a reference map and a
comparison map
overallComponentsPlot(comp, ref)#Plots the shift, exchange and quantity
#differenceMR(comp, ref, eval="multiple", fact=2)
#write.csv(exchangeDij(ctmatCompRef), "C:/Users/Michael/Desktop/sample.txt")
MAD(comp,ref, eval="multiple")

```

Appendix 3

Species Distribution Modelling (SDM) and Fragmentation Analysis (Coded in R)

```
#SDM TOOLS FOR Fragmentation analysis
rm(list=ls())
library("raster")
library("rgdal")
library("sp")
library("dplyr")
library("igraph")
library("SDMTools")
library("ggplot2")

y1<- raster("D:/Data/raster.tif")
patch = PatchStat(y1)
patch

plot(y1)
summary(y1)
structure(y1)
ppstat<- ClassStat(y1, cellsize = 30)
dplyr::tbl_df(ppstat)
hist(pps)

tmat = { matrix(c( 0,0,0,1,0,0,1,1,0,1,
                  0,0,1,0,1,0,0,0,0,0,
                  0,1,NA,1,0,1,0,0,0,1,
                  1,0,1,1,1,0,1,0,0,1,
                  0,1,0,1,0,1,0,0,0,1,
                  0,0,1,0,1,0,0,1,1,0,
                  1,0,0,1,0,0,1,0,0,1,
                  0,1,0,0,0,1,0,0,0,1,
                  0,0,1,1,1,0,0,0,0,1,
                  1,1,1,0,0,0,0,0,0,1),nr=10,byrow=TRUE) }

ggplot(tmat)

#calculate the patch statistics
plot(pps.data$core.area)
```

Appendix 4

Markov Chain Model (Coded in R)

```

library("markovchain")
library(diagram)
library(pracma)

data = "C:/Data.txt"

tmatrix<- as.matrix(read.table(data, header=TRUE, sep = "\t",
                               row.names = 1,
                               as.is=TRUE))
tmatrix
states = c("W", "M", "C", "BU", "S", "F")

mc <-new("markovchain",
         transitionMatrix = tmatrix,
         byrow=T,
         states = states,
         name = "Name")

plot(mc)
mc
tmatrix
plotmat(tpm,pos = c(1,5),
         lwd = 1, box.lwd = 2,
         cex.txt = 0.8,
         box.size = 0.1,
         box.type = "circle",
         box.prop = 0.5,
         box.col = "light yellow",
         arr.length=.1,
         arr.width=.1,
         self.cex = .4,
         self.shifty = -.01,
         self.shiftx = .13,
         main = ""))
a <- mc^50
plot(mc)
summary(a)

```

Appendix 5A

Iwahig Watershed Landscape Model (Coded in NetLogo)

```

globals [raster elev forest]
extensions [gis]
patches-own[lu slope floss a_c na_c a_s na_s a_w na_w a_m na_m a_b na_b a_f na_f]

to setup
  ca
  load-i
  reset-ticks
  set elev gis:load-dataset "C:\\slope.asc"
  gis:apply-raster elev slope
  gis:set-world-envelope (gis:envelope-of raster)
  set forest gis:load-dataset "C:\\ floss.asc"
  gis:apply-raster forest floss
  gis:set-world-envelope (gis:envelope-of raster)

end

to load-i
  set raster gis:load-dataset "C:\\lulc1993.asc"
  gis:set-world-envelope (gis:envelope-of raster)
  gis:apply-raster raster lu
  ask patches with [lu = 1] [set pcolor 105] ;WATER
  ask patches with [lu = 2] [set pcolor 126] ;MANGROVE
  ask patches with [lu = 3] [set pcolor 45] ;CULTIVATED
  ask patches with [lu = 4] [set pcolor 15] ;BUILT ;use ask patch-at 1 0 #this goes to the east of the patch
  ask patches with [lu = 5] [set pcolor 56] ;SHRUBLAND
  ask patches with [lu = 6] [set pcolor 62] ;FOREST
end

;neighbors - 8 surrounding pathes
;neighbors4 - 4 surrounding patches

to go2 ;revision
  ;CULTIVATED
  ask patches with [lu = 3] [set a_c 0.4779] ;CULTIVATED
  ask patches [set na_c ((a_c + sum [a_c] of neighbors) / 6)] ;vonn neuman
  ask patches with [lu = 3] [ set a_c na_c
    if a_c < threshold * cultivated_t and slope <= 8
    [set pcolor [pcolor] of one-of neighbors]]

```

Appendix 5B

Iwahig Watershed Landscape Model (Coded in NetLogo) continuation..

```

;SHRUBLAND
ask patches with [lu = 5] [set a_s 0.7439] ;SHRUBLAND
ask patches [set na_s ((a_s + sum [a_s] of neighbors) / 6)] ;vonn neuman
ask patches with [lu = 5] [ set a_s na_s
  if a_s < threshold + cultivated_t ;and slope >= 18
  [set pcolor [pcolor] of one-of neighbors]]
;WATER
ask patches with [lu = 1] [set a_w 0.5483] ;WATER
ask patches [set na_w ((a_w + sum [a_w] of neighbors) / 6)] ;vonn neuman
ask patches with [lu = 1] [ set a_w na_w
  if a_w < threshold ;and slope >= 18
  [set pcolor [pcolor] of one-of neighbors]]
;MANGROVE
ask patches with [lu = 2] [set a_m 0.7373] ;Mangrove
ask patches [set na_m ((a_m + sum [a_m] of neighbors) / 6)] ;vonn neuman
ask patches with [lu = 2] [ set a_m na_m
  if a_m < threshold + coastal_dev ;and slope >= 18
  [set pcolor [pcolor] of one-of neighbors]]
;BUILT-UP
ask patches with [lu = 4] [set a_b 0.0000] ;BUILT
ask patches [set na_b ((a_b + sum [a_b] of neighbors) / 6)] ;vonn neuman
ask patches with [lu = 4] [ set a_b na_b
  if a_b = threshold
  [set pcolor [pcolor] of one-of neighbors]]
;FOREST
ask patches with [lu = 6] [set a_f 0.4732] ;FOREST
ask patches [set na_f ((a_f + sum [a_f] of neighbors) / 6)] ;vonn neuman
ask patches with [lu = 6] [ set a_f na_f
  if a_f < threshold ;and slope >= 18
  [set pcolor [pcolor] of one-of neighbors]]

tick
if ticks = 50 [stop]
end
;; NOTE you can comment those that have high attraction

to export_data
let patches_out nobody
ask one-of patches
[set patches_out gis:patch-dataset pcolor]
gis:store-dataset patches_out "C:\\output.asc"
end

```

Appendix 6A

Mangrove Mortality and Growth Model (Coded in R)

```

extensions [gis]
globals [th raster sp raster0 raster1 raster2 raster3 raster4 raster5 threshold
]
patches-own [ alive dead grow mg core road stream built suit all
  a_s a_r na_s na_r a_l na_l a_m na_m suitability
]

to setup
  ca
  load-sp
  load-data
  reset-ticks
end

to load-sp
  set sp gis:load-dataset "C:\\\\Users\\\\Michael\\\\Documents\\\\data\\\\lu\\\\species.asc"
  gis:set-world-envelope gis:envelope-of sp
  gis:apply-raster sp mg
  ask patches with [mg = 1] [set pcolor 124] ;Landward
  ask patches with [mg = 2] [set pcolor 46] ; Midward
  ask patches with [mg = 3] [set pcolor 63] ;Seaward
  ask patches with [mg = 0] [set pcolor 0] ; No data
end

to load_orig
  set raster4 gis:load-dataset "C:\\\\Users\\\\Michael\\\\Documents\\\\data\\\\lu\\\\mg_suit.asc"
  gis:set-world-envelope gis:envelope-of raster4
  gis:apply-raster raster4 suit
  ask patches with [suit = 1] [set grow 1 set pcolor green]
  ask patches with [suit = 0] [set grow 0 set pcolor black]
end

```

Appendix 6B

Mangrove Mortality and Growth Model (Coded in R) continuation

```

to load-data
  set raster0 gis:load-dataset "C:\\\\Users\\\\Michael\\\\Documents\\\\data\\\\lu\\\\core.asc"
  gis:set-world-envelope gis:envelope-of sp
  gis:apply-raster raster0 core
  set raster1 gis:load-dataset "C:\\\\Users\\\\Michael\\\\Documents\\\\data\\\\lu\\\\road.asc"
  gis:set-world-envelope gis:envelope-of sp
  gis:apply-raster raster1 road
  set raster2 gis:load-dataset "C:\\\\Users\\\\Michael\\\\Documents\\\\data\\\\lu\\\\built.asc"
  gis:set-world-envelope gis:envelope-of sp
  gis:apply-raster raster2 built
  set raster3 gis:load-dataset "C:\\\\Users\\\\Michael\\\\Documents\\\\data\\\\lu\\\\streams.asc"
  gis:set-world-envelope gis:envelope-of sp
  gis:apply-raster raster3 stream
  set raster4 gis:load-dataset "C:\\\\Users\\\\Michael\\\\Documents\\\\data\\\\lu\\\\mg_suit.asc"
  gis:set-world-envelope gis:envelope-of sp
  gis:apply-raster raster4 suit
  ask patches with [suit = 1] [set suitability 1]
  ask patches with [suit = 0] [set suitability 0]
  set raster5 gis:load-dataset "C:\\\\Users\\\\Michael\\\\Documents\\\\data\\\\lu\\\\all.asc"
  gis:set-world-envelope gis:envelope-of sp
  gis:apply-raster raster5 all
end

to death
  road_i
  core_i
  stream_i
  built_i
;preference
;if ticks = 24 [stop]
end

to growth
  grow_l
end

to grow_l
  ask patches with [mg = 1] [set a_l 0.333] ;CULTIVATED
  ask patches [set na_l ((a_l + sum [a_l] of neighbors) / 9)] ;vonn neuman
  ask patches with [mg = 1] [ set na_l a_l
    if suitability = 1
      [set pcolor [pcolor] of one-of neighbors]]
  ask patches with [mg = 2] [set a_m 0.333] ;CULTIVATED

```

Appendix 6C

Mangrove Mortality and Growth Model (Coded in R) continuation

```

ask patches [set na_m ((a_m + sum [a_m] of neighbors) / 8)] ;vonn neuman
ask patches with [mg = 2] [ set na_m a_m
  if suitability = 1
    [set pcolor [pcolor] of one-of neighbors]]

ask patches with [mg = 3] [set a_s 0.333] ;CULTIVATED
ask patches [set na_s ((a_s + sum [a_s] of neighbors) / 8)] ;vonn neuman
ask patches with [mg = 3] [ set na_s a_s
  if suitability = 1
    [set pcolor [pcolor] of one-of neighbors]]
  tick
end
to setup2
  ca
  ;load-sp
  load_orig
  reset-ticks
end

to grow2
  load_orig
  set th 1 ;neighborhood threshold
  ask patches [
    set grow count neighbors with [pcolor = green]]
    ask patches[
      if grow >= th
        ;[set pcolor [pcolor] of one-of neighbors4]] ;OK
        [set pcolor [pcolor] of one-of patches in-radius 4]]
        ;[set pcolor (patches in-radius 8 with [ pcolor = green])]]
      tick
      if ticks = year [stop]
    end

  to road_i
    let t 1
    ask patches with [mg = 1] [ set a_s 0 set na_s 0]
    ask patches with [mg = 1]
    [ set a_s na_s
      if a_s = t or road <= road_t
        [set pcolor [pcolor] of one-of neighbors4]]
      ask patches with [mg = 2] [ set a_r 0 set na_s 0]
      ask patches with [mg = 2] [ set a_r na_r
        if a_s = t or road <= road_t

```

Appendix 6D

Mangrove Mortality and Growth Model (Coded in R) continuation

```

[set pcolor [pcolor] of one-of neighbors4]]
ask patches with [mg = 3] [ set a_r 0 set na_s 0]
ask patches with [mg = 3] [ set a_r na_r
  if a_s = t or road <= road_t
  [set pcolor [pcolor] of one-of neighbors4]]
  tick
  if ticks = 100 [stop]
end

to core_i
  let t 1
  ask patches with [mg = 1] [ set a_s 0 set na_s 0]
  ask patches with [mg = 1]
  [ set a_s na_s
    if a_s = t or core <= core_t or suit = 0
    [set pcolor [pcolor] of one-of neighbors4]]
    ask patches with [mg = 2] [ set a_r 0 set na_s 0]
    ask patches with [mg = 2] [ set a_r na_r
      if a_s = t or core <= core_t or suit = 0
      [set pcolor [pcolor] of one-of neighbors4]]
      ask patches with [mg = 3] [ set a_r 0 set na_s 0]
      ask patches with [mg = 3] [ set a_r na_r
        if a_s = t or core <= core_t or suit = 0
        [set pcolor [pcolor] of one-of neighbors4]]
        tick
        if ticks = 100 [stop]
      end

    to stream_i
      let t 1
      ask patches with [mg = 1] [ set a_s 0 set na_s 0]
      ask patches with [mg = 1]
      [ set a_s na_s
        if a_s = t or stream <= stream_t
        [set pcolor [pcolor] of one-of neighbors4]]
        ask patches with [mg = 2] [ set a_r 0 set na_s 0]
        ask patches with [mg = 2] [ set a_r na_r
          if a_s = t or stream <= stream_t
          [set pcolor [pcolor] of one-of neighbors4]]
          ask patches with [mg = 3] [ set a_r 0 set na_s 0]
          ask patches with [mg = 3] [ set a_r na_r
            if a_s = t or stream <= stream
            [set pcolor [pcolor] of one-of neighbors4]]
            tick

```

Appendix 6E

Mangrove Mortality and Growth Model (Coded in R) continuation

```

[set pcolor [pcolor] of one-of neighbors4]]
ask patches with [mg = 3] [ set a_r 0 set na_s 0]
ask patches with [mg = 3] [ set a_r na_r
  if a_s = t or road <= road_t
  [set pcolor [pcolor] of one-of neighbors4]]
  tick
  if ticks = 100 [stop]
end

to core_i
  let t 1
  ask patches with [mg = 1] [ set a_s 0 set na_s 0]
  ask patches with [mg = 1]
  [ set a_s na_s
    if a_s = t or core <= core_t or suit = 0
    [set pcolor [pcolor] of one-of neighbors4]]
    ask patches with [mg = 2] [ set a_r 0 set na_s 0]
    ask patches with [mg = 2] [ set a_r na_r
      if a_s = t or core <= core_t or suit = 0
      [set pcolor [pcolor] of one-of neighbors4]]
      ask patches with [mg = 3] [ set a_r 0 set na_s 0]
      ask patches with [mg = 3] [ set a_r na_r
        if a_s = t or core <= core_t or suit = 0
        [set pcolor [pcolor] of one-of neighbors4]]
        tick
        if ticks = 100 [stop]
      end

    to stream_i
      let t 1
      ask patches with [mg = 1] [ set a_s 0 set na_s 0]
      ask patches with [mg = 1]
      [ set a_s na_s
        if a_s = t or stream <= stream_t
        [set pcolor [pcolor] of one-of neighbors4]]
        ask patches with [mg = 2] [ set a_r 0 set na_s 0]
        ask patches with [mg = 2] [ set a_r na_r
          if a_s = t or stream <= stream_t
          [set pcolor [pcolor] of one-of neighbors4]]
          ask patches with [mg = 3] [ set a_r 0 set na_s 0]
          ask patches with [mg = 3] [ set a_r na_r
            if a_s = t or stream <= stream
            [set pcolor [pcolor] of one-of neighbors4]]
            tick

```

Appendix 6F

Mangrove Mortality and Growth Model (Coded in R) continuation

```

if ticks = 100 [stop]
end

to built_i
  let t 1
  ask patches with [mg = 1] [ set a_s 0 set na_s 0]
  ask patches with [mg = 1]
  [ set a_s na_s
    if a_s = t or built <= built_t
    [set pcolor [pcolor] of one-of neighbors4]]
  ask patches with [mg = 2] [ set a_r 0 set na_s 0]
  ask patches with [mg = 2] [ set a_r na_r
    if a_s = t or built <= built_t
    [set pcolor [pcolor] of one-of neighbors4]]
  ask patches with [mg = 3] [ set a_r 0 set na_s 0]
  ask patches with [mg = 3] [ set a_r na_r
    if a_s = t or built <= built_t
    [set pcolor [pcolor] of one-of neighbors4]]
  tick
  if ticks = 100 [stop]
end

to all_i
  let t 2.8
  ask patches with [mg = 1] [ set a_s 0 set na_s 0]
  ask patches with [mg = 1]
  [ set a_s na_s
    if a_s = t or all <= all_t or suit = 1
    [set pcolor [pcolor] of one-of neighbors4]]
  ask patches with [mg = 2] [ set a_r 0 set na_s 0]
  ask patches with [mg = 2] [ set a_r na_r
    if a_s = t or all <= all_t or suit = 1
    [set pcolor [pcolor] of one-of neighbors4]]
  ask patches with [mg = 3] [ set a_r 0 set na_s 0]
  ask patches with [mg = 3] [ set a_r na_r
    if a_s = t or all <= all_t or suit = 1
    [set pcolor [pcolor] of one-of neighbors4]]
  tick
  if ticks = 100 [stop]
end

to export_data
  let patches_out nobody
  ask one-of patches [
    set patches_out gis:patch-dataset pcolor
  ]
  gis:store-dataset patches_out "C:\\Users\\Michael\\Documents\\data\\lu\\export2.asc"
end

```

Appendix 7A

Mangrove Canopy Gap Growth Model (Coded in R)

```

globals [
  FON
  ;; This is a list of cells which are eligible to become alive.
  eligibles
]

breed [cells cell]

cells-own [
  hex-neighbors
  live-neighbor-count
  eligible?
]

to setup
  clear-all
  setup-grid
  read-FON
  ;; start with one live cell in the middle
  ask n-of density cells [become-alive]
  reset-ticks
end

to go
  random-seed 47822
  if empty? eligibles [ stop ]
  ask one-of eligibles [ become-alive ]
  if ticks = 100000 [stop]
  tick
end

to become-alive ;; cell procedure
  show-turtle
  set eligible? false
  set eligibles remove self eligibles
  ask hex-neighbors [
    set live-neighbor-count live-neighbor-count + 1
    if live-neighbor-count = 6 [ set color green ] set size random one-of [0.5 1.5 3 4.5 6] ;to set random
      dbh
      ;if live-neighbor-count = 6 [ set color green ] set size dbh ;to set based on diameter slider
      update-eligibility
  ]
end

```

Appendix 7B

Mangrove Canopy Gap Growth Model (Coded in R) continuation..

```

to update-eligibility ;; cell procedure
  ifelse eligible?
    ;; case 1: currently eligible
    [
      if not member? live-neighbor-count FON [
        set eligible? false
        set eligibles remove self eligibles
      ]
    ]
    ;; case 2: not currently eligible
    [
      ;; the check for hidden? ensures the cell isn't already alive
      if hidden? and member? live-neighbor-count FON [
        set eligible? true
        ;; The order of the list doesn't matter, but in NetLogo
        ;; (as in Logo and Lisp generally), FPUT is much much
        ;; faster than LPUT.
        set eligibles fput self eligibles
      ]
    ]
  end

  ;;; only allow the new alive cells to have number of neighbors as allowed by the FON
  to read-FON
    set FON []
    if one-neighbor? [ set FON lput 1 FON ]
    ;if two-neighbors? [ set FON lput 2 FON ]
    ;if three-neighbors? [ set FON lput 3 FON ]
    if four-neighbors? [ set FON lput 4 FON ]
    ;if five-neighbors? [ set FON lput 5 FON ]
    ;if six-neighbors? [ set FON lput 6 FON ]
    ;if eight-neighbors? [ set FON lput 8 FON ]
    ;if twelve-neighbors? [ set FON lput 12 FON ]
    ;if sixteen-neighbors? [ set FON lput 16 FON ]
    if twentyfive-neighbors? [ set FON lput 25 FON ]
    ;if thirtysix-neighbors? [ set FON lput 36 FON ]
    ask cells [
      set eligible? hidden? and member? live-neighbor-count FON
    ]
    set eligibles [self] of cells with [eligible?]
  end

  ;;; this was mostly taken from Hex Cells Example
  to setup-grid

```

Appendix 7C

Mangrove Canopy Gap Growth Model (Coded in R) continuation..

```

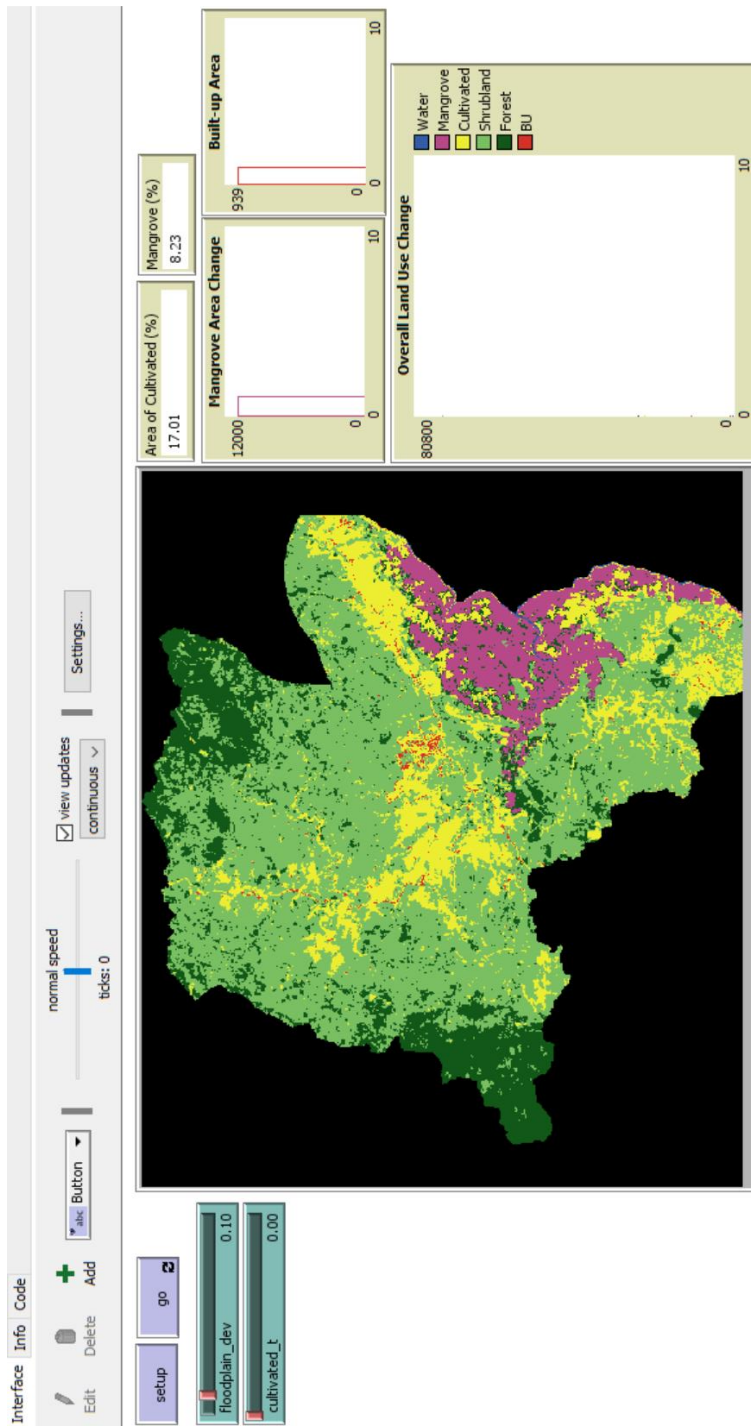
set-default-shape turtles "circle"
ask patches [
  sprout-cells 1 [
    hide-turtle
    set color 0
    set eligible? true ;default to false
    if pxcor mod 2 = 0 [
      set ycor ycor - 0.5
    ]
  ]
]

ask cells [
  ifelse pxcor mod 2 = 0 [
    set hex-neighbors cells-on patches at-points [[-1 -1] [0 -1] [1 -1]
                                              [-1 0] [0 0] [1 0]
                                              [-1 1] [0 1] [1 1]]
  ][
    set hex-neighbors cells-on patches at-points [[-1 -1] [0 -1] [1 -1]
                                              [-1 0] [0 0] [1 0]
                                              [-1 1] [0 1] [1 1]]
  ]
]
end

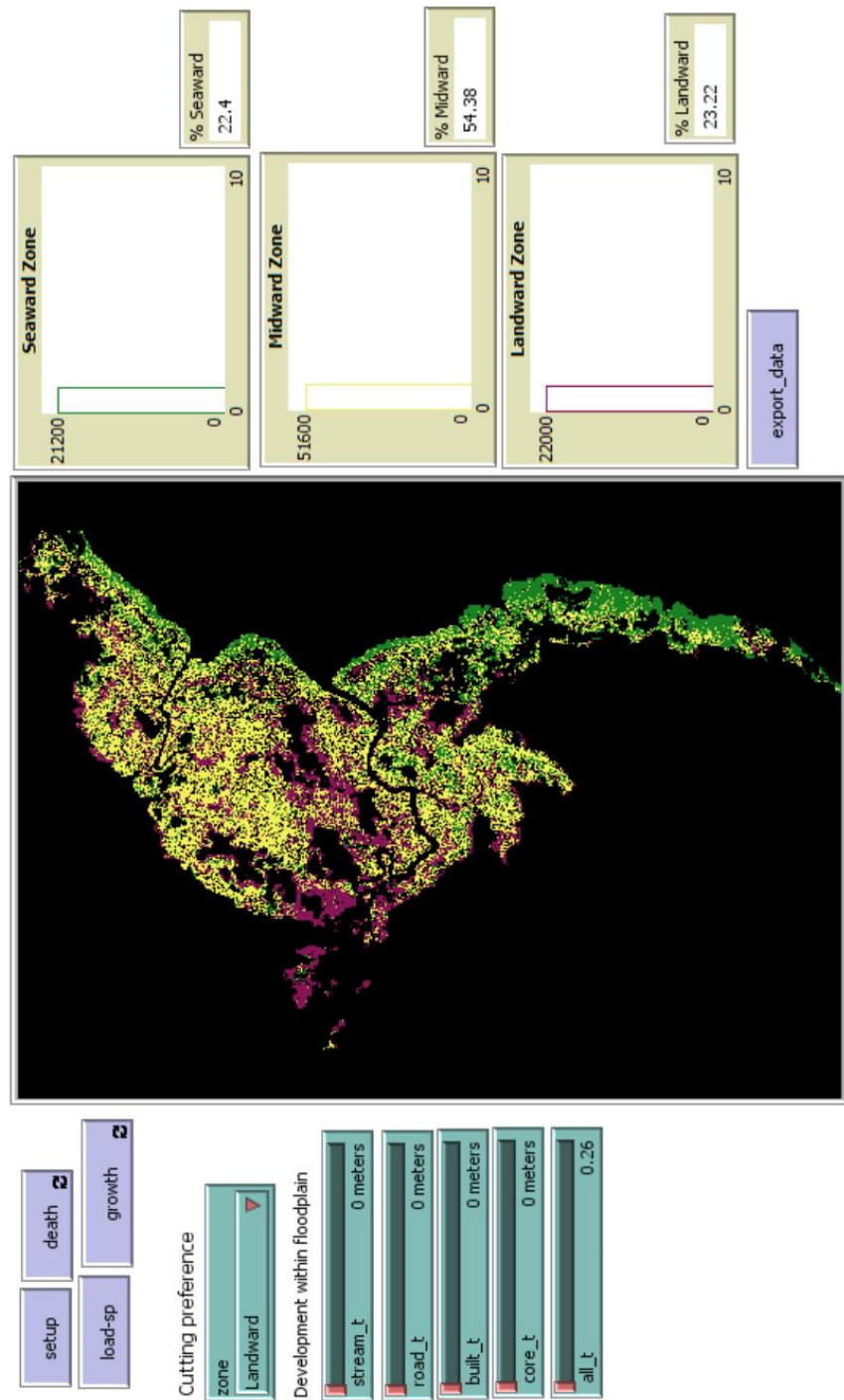
```

; Adapted and modified from Uri Wilensky (Copyright 2007)

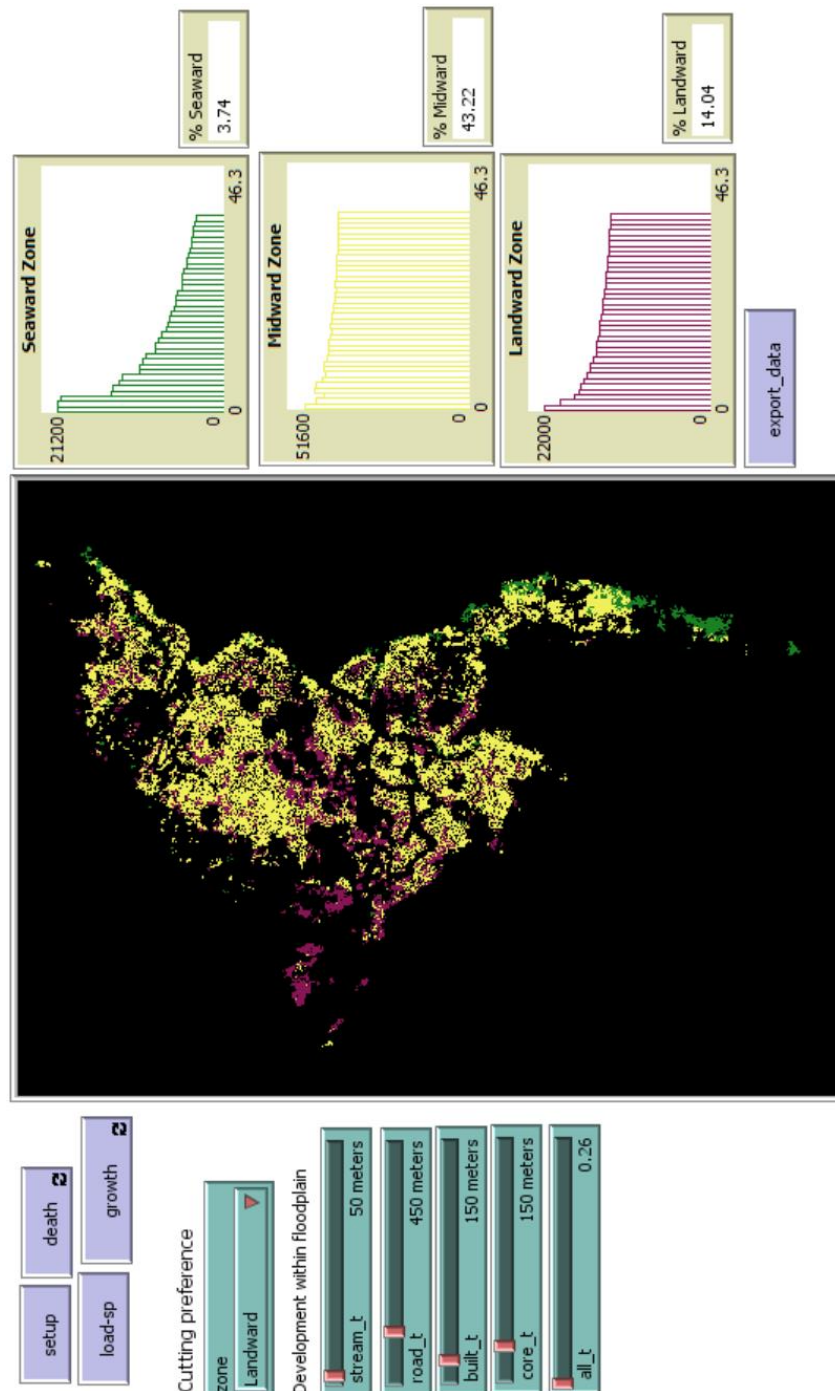
APPENDIX 8. Graphical User Interface (GUI) of NetLogo Landscape simulation model



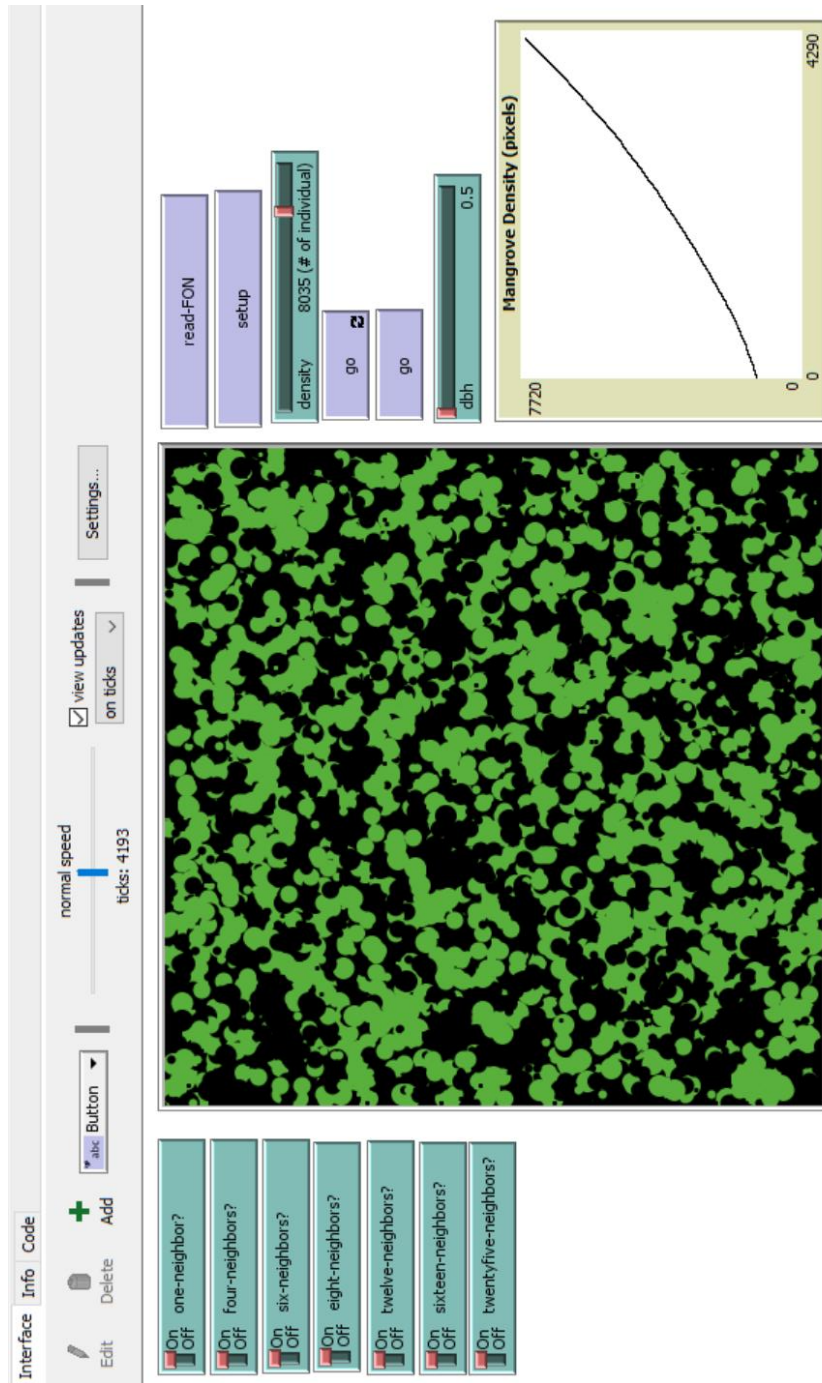
APPENDIX 9. Graphical User Interface (GUI) of NetLogo mangrove mortality model
(A)



APPENDIX 10. Graphical User Interface (GUI) of NetLogo mangrove mortality model
(B)



APPENDIX 11. Graphical User Interface of mangrove canopy gap growth model



APPENDIX 12. R-codes for Random Forest Model

```

#RandomForest Regression
library("caret")
library("randomForest")
library("pls")
library("party")
library("spdep")
library("corrplot")
library("ggplot2")
library("parallel")
library("dplyr")
library("RColorBrewer")
library("rfUtilities")
library("VSURF")
library("rpart")
library("rpart.plot")
library("randomForestExplainer")

set.seed(123)
rm(list=ls())
# data for mangrove devrease
setwd("D:/Data/01_Thesis/08_Regression_R")
filename = "III.txt"
data <-read.delim(filename, header = TRUE, sep = "\t")
form = Mg_Area ~ .
names(data)

#Correlation Plot
corrplot(cor(data),order = "hclust")

#Control
set.seed(123)
control <- trainControl(method='repeatedcv',number=10,repeats=10)
mtry <- sqrt(ncol(data))

#RandomForest
RF <- train(form,data=data,
            method = "rf",trControl=control,
            importance = TRUE, ntree = 1000)
plot(varImp(RF, useModel = TRUE), top=15)
RF$finalModel

```

```

RF$results

#Random Forest with cross validation
RF2 <- randomForest(form,data=data, method = "rf",trControl=control,
                     importance = TRUE, ntree = 1000)

RF2

#Explain RF plots
plot_importance_ggpairs(RF2)
plot_importance_ggpairs(importance_frame)
plot_multi_way_importance(RF2, x_measure = "mse_increase",
                           y_measure = "node_purity_increase",
                           size_measure = "p_value", no_of_labels = 5)
plot_min_depth_interactions(RF2)

#https://cran.rstudio.com/web/packages/randomForestExplainer/vignettes/randomForestExplainer.html

#CrossValidation
CV <- rf.crossValidation(RF2, data, p = 0.1, n = 99, seed = NULL,
                         normalize = TRUE)
CV
plot(RF2, type = "cv", stat = "producers.accuracy")
plot(RF2, imp = "sel")
rf.class.sensitivity(RF2, data, d = "1", p = 0.05, nperm = 999,
                      plot = TRUE, seed = NULL)

## Variable Selection Using Random Forest - VSURF
vsurf <- VSURF(form,data=data, mtry = 100, parallel = TRUE,
                ncores = 1, clusterType = "FORK")

summary(vsurf)
vsurf$viselect.interp
names(data)
plot(vsurf)

RF2 <- rpart(form,data=data)
rpart.plot(RF2)
plot(RF2$finalModel)
text(RF2$finalModel)

```

APPENDIX 13. R-codes for Markov Chain Model

```

library(markovchain)
library(magrittr)
library(Gmisc)

file = "C:/Users/Michael/Documents/R/tpm.txt"
tmatrix<- as.matrix(read.table(file, header=TRUE, sep = "\t",
                                row.names = 1,
                                as.is=TRUE))
#IMPORTANT: Returns the type of data
str(b)

tmatrix
b <- tmatrix^3
b
transitionPlot(tmatrix)

transitionPlot(tmatrix,
               fill_start_box = c("#0761f2","#d8863a","#e3e56b","#bf3422","#60a85c","#094f05"),
               type_of_arrow = "simple", #gradient
               box_label = c("Initial State", "Transition State"))
transition$render()
addTransitions(mtrx, label, txt, fill_clr, txt_clr)

transitions$title <- "Charnley class in relation to THR"
transitions$arrow_type <- "simple"
table(data$Charnley_class_1yr, data$Charnley_class_2yr, data$Sex) %>%
  transitions$addTransitions(label="2 years after")
library(grid)
transitions$max_lwd <- unit(.05, "npc")
transitions$render()

tdata = "C:/Users/Michael/Documents/tdata.xls"
tdata.head

data<- data.frame(source = c("A", "A", "A", "B", "B", "C", "C"),
                  target = c("A", "B", "C", "B", "C", "C", "C"))
data2 <- data.frame(source = c("D", "D", "E", "E", "E", "E", "F"),
                     target = c("D", "E", "D", "E", "F", "F", "F"))

```

```

transitions.1 <- getRefClass("Transition")$new(table(data.1$source, data.1$target), label =
c("Before", "After"))
transitions.2 <- getRefClass("Transition")$new(table(data.2$source, data.2$target), label =
c("Before", "After"))

# wish to render transition 1 and transition 2 next to each other
transitions.1$render()
transitions.2$render()

transitions <- table(data$Charnley_class, data2$Charnley_class_1yr, data) %>%
  getRefClass("Transition")$new(label=c("Before surgery", "1 year after"))
transitions$title <- "Charnley class in relation to THR"
transitions$arrow_type <- "simple"
table(data$Charnley_class_1yr, data$Charnley_class_2yr, data$Sex) %>%
  transitions$addTransitions(label="2 years after")
library(grid)
transitions$max_lwd <- unit(.05, "npc")
transitions$render()

#no_boxes = 5
#tm <- matrix(tmatrix, nrow=no_boxes, ncol=no_boxes)

transitionPlot(tmatrix,
  #fill_start_box = c("#65f442", "#428ab7"),
  type_of_arrow = "gradient",
  box_label = c("Initial State", "Transition State"),
  min_lwd = unit(0.2, "mm"), max_lwd = unit(5, "mm"))

```

APPENDIX 12. R-codes for Mangrove Fragmentation

```

#SDM / FragStat
#SDM TOOLS FOR Fragmentation analysis
rm(list=ls())
library("raster")
library("rgdal")
library("sp")
library("dplyr")
library("igraph")
library("SDMTools")
library("ggplot2")

y1<- raster("D:/Data/01_Thesis/01_Data/LULC/GEE/0005con.tif")
patch = PatchStat(y1)

```

```
patch

plot(y1)
summary(y1)
structure(y1)
ppstat<- ClassStat(y1, cellsize = 30)
dplyr::tbl_df(ppstat)
hist(pps)

tmat = { matrix(c( 0,0,0,1,0,0,1,1,0,1,
                  0,0,1,0,1,0,0,0,0,0,
                  0,1,NA,1,0,1,0,0,0,1,
                  1,0,1,1,1,0,1,0,0,1,
                  0,1,0,1,0,1,0,0,0,1,
                  0,0,1,0,1,0,0,1,1,0,
                  1,0,0,1,0,0,1,0,0,1,
                  0,1,0,0,0,1,0,0,0,1,
                  0,0,1,1,1,0,0,0,0,1,
                  1,1,1,0,0,0,0,0,0,1),nr=10,byrow=TRUE) }

ggplot(tmtat)

#do the connected component labelling
ccl.mat = ConnCompLabel(tmat)
ccl.mat
image(t(ccl.mat[10:1,]),col=c('grey',rainbow(length(unique(ccl.mat))-1)))

#calculate the patch statistics
plot(pps.data$core.area)
```

APPENDIX 14. R-codes for Fragmentation Model

```
#SDM TOOLS FOR Fragmentation analysis
rm(list=ls())
library("raster")
library("rgdal")
library("sp")
library("dplyr")
library("igraph")
library("SDMTools")
library("ggplot2")

y1<- raster("D:/Data/01_Thesis/01_Data/LULC/GEE/0005con.tif")
patch = PatchStat(y1)
patch

plot(y1)
summary(y1)
structure(y1)
ppstat<- ClassStat(y1, cellsize = 30)
dplyr::tbl_df(ppstat)
hist(pps)

tmat = { matrix(c( 0,0,0,1,0,0,1,1,0,1,
                  0,0,1,0,1,0,0,0,0,0,
                  0,1,0,1,0,1,0,0,0,1,
                  1,0,1,1,1,0,1,0,0,1,
                  0,1,0,1,0,1,0,0,0,1,
                  0,0,1,0,1,0,0,1,1,0,
                  1,0,0,1,0,0,1,0,0,1,
                  0,1,0,0,0,1,0,0,0,1,
                  0,0,1,1,1,0,0,0,0,1,
                  1,1,1,0,0,0,0,0,0,1),nr=10,byrow=TRUE) }

ggplot(tmat)

#do the connected component labelling
ccl.mat = ConnCompLabel(tmat)
ccl.mat
image(t(ccl.mat[10:1]),col=c('grey',rainbow(length(unique(ccl.mat))-1)))
#calculate the patch statistics
plot(pps.data$core.area)
```

